AD-A122 443 WINTER CONDITIONS IN THE BERING SEA(U) NAVAL POSTGRADUATE SCHOOL MONTEREY CA R H BOURKE ET AL. MAY 81 NPS-68-81-004 1/2

UNCLASSIFIED F/G 8/10 NL

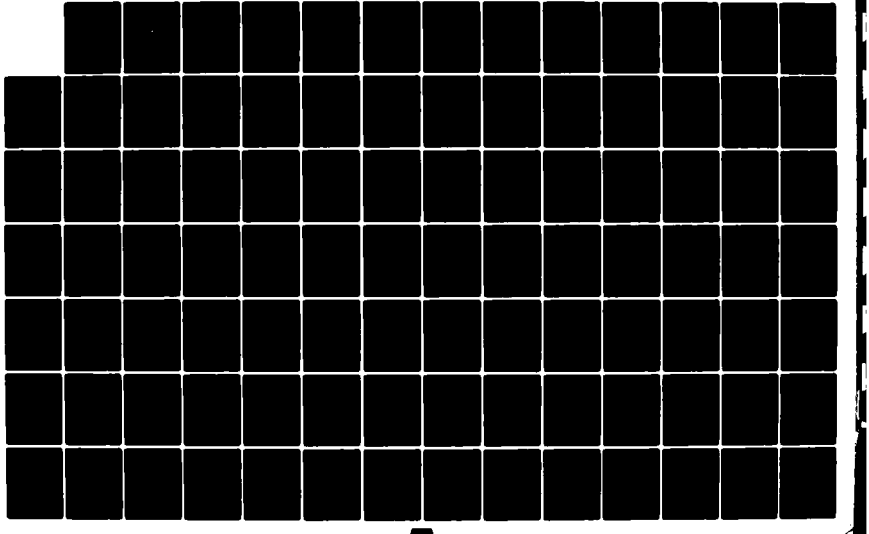

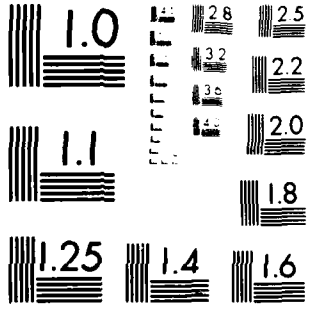

NPS 68-81-004

NAVAL POSTGRADUATE SCHOOL

Monterey, California

WINTER CONDITIONS IN THE BERING SEA

by

Robert H. Bourke and Robert G. Paquette

May 1981

Interim Report for Period 1 Oct 1979 - 1 May 1981

Approved for public release; distribution unlimited

Prepared for:
Director, Arctic Submarine Laboratory
Naval Ocean Systems Center
San Diego, CA 92152

NAVAL POSTGRADUATE SCHOOL
Monterey, California

Rear Admiral John J. Ekelund
Superintendent

David A. Schrady
Acting Provost

The work reported herein was supported in part by the Arctic Submarine Laboratory, Naval Ocean Systems Center, San Diego, California under Project Order Nos. 000007 and 00164.

This report was prepared by:

ROBERT G. PAQUETTE
Professor of Oceanography

ROBERT H. BOURKE
Associate Professor of Oceanography

Reviewed by:

CHRISTOPHER N. K. MOOERS, Chairman
Department of Oceanography

WILLIAM M. TOLLES
Dean of Research

Unclassified

SECURITY CLASSIFICATION OF THIS PAGE (When Data Entered)

REPORT DOCUMENTATION PAGE		READ INSTRUCTIONS BEFORE COMPLETING FORM
1. REPORT NUMBER NPS 68-81-004	2. GOVT ACCESSION NO. AD-A122443	3. RECIPIENT'S CATALOG NUMBER
4. TITLE (and Subtitle) Winter Conditions in the Bering Sea		5. TYPE OF REPORT & PERIOD COVERED Interim 1 Oct 1979 - 1 May 1981
		6. PERFORMING ORG. REPORT NUMBER NPS 68-81-004
7. AUTHOR(s) Robert H. Bourke and Robert G. Paquette		8. CONTRACT OR GRANT NUMBER(s) N 66001-80-P000007 N 66001-81-WR00164
9. PERFORMING ORGANIZATION NAME AND ADDRESS Naval Postgraduate School Monterey, CA 93940		10. PROGRAM ELEMENT, PROJECT, TASK AREA & WORK UNIT NUMBERS Element: 62759N Work:540-MR01 Project: ZF59-555 Task: ZF59-555-694
11. CONTROLLING OFFICE NAME AND ADDRESS Arctic Submarine Laboratory Code 54, Bldg 371, Naval Ocean Systems Center San Diego, CA 92152		12. REPORT DATE May 1981 13. NUMBER OF PAGES 102
14. MONITORING AGENCY NAME & ADDRESS(if different from Controlling Office)		15. SECURITY CLASS. (of this report) UNCLASS 15a. DECLASSIFICATION/DOWNGRADING SCHEDULE

16. DISTRIBUTION STATEMENT (of this Report)

Approved for public release; distribution unlimited

17. DISTRIBUTION STATEMENT (of the abstract entered in Block 20, if different from Report)

18. SUPPLEMENTARY NOTES

19. KEY WORDS (Continue on reverse side if necessary and identify by block number)

Bering Sea	Icebreaker	Freezing point
Sea Ice	Oceanography	POLAR STAR
Yukon River	CTD	

20. ABSTRACT (Continue on reverse side if necessary and identify by block number)

This report presents the results of the oceanographic cruise of the USCGC POLAR STAR to the ice-covered areas of the Bering Sea in February-April, 1980. The 83 stations made represent the most extensive set of under-ice observations in the area using modern, high precision conductivity-temperature-depth recordings and elucidate features not observable in the historical data. Two crossings of the ice margin were made, separated by 600 Km. These showed that cold, dilute water overlies warmer saltier water of Bering Sea origin. This

DD FORM 1 JAN 73 1473 EDITION OF 1 NOV 65 IS OBSOLETE
S/N 0102-014-6601 |

Unclassified

SECURITY CLASSIFICATION OF THIS PAGE (When Data Entered)

#20 - ABSTRACT - (CONTINUED)

latter water is present far back on the shelf, some 200 km behind the ice edge. Dilution and stratification due to river run off, especially from the Yukon River, was quite predominant along the north-eastern margin of the Bering Sea. A strong salinity front (2 ‰ over 60 km) separated oceanic water from the more dilute coastal water. Localized high salinity areas, indicative of rapid brine formation, were infrequently found. To some extent they were correlated with regions of ice divergence, especially north and south of St. Lawrence I. With the exception of the ice margin area and those obviously influenced by river run off, most of the waters were within 0.01° to 0.02°C of the equilibrium freezing point curve of Doherty and Kester (JMR(32),1974).

TABLE OF CONTENTS

List of Figures

WINTER CONDITIONS IN THE BERING SEA

BY

Robert H. Bourke and Robert G. Paquette

1. INTRODUCTION

This report presents the results of an oceanographic cruise of the USCGC POLAR STAR to the ice-covered areas of the Bering Sea in February-April, 1980 as part of the MIZPAC Project. This is a more detailed report than that of Newton and Anderson (1980) which also describes the results of this cruise. The ship left Sitka, Alaska on 25 February 1980 and took two stations in deep water northwest of Unimak Pass on 29 February. It then proceeded generally northward, taking stations across the shelf break and on into the ice at 57° N. The ship reached Nome on 13 March, then proceeded to circumnavigate St. Lawrence I. and exited through the ice margin on 2 April about 600 km northwest of the point of entry. Essentially all of the under-ice area was on the shallow shelf of the Bering Sea. Table 1 is a summary of significant information pertaining to the cruise. The cruise track and station distribution are shown in Fig. 1.

The scientific party concerned with oceanography consisted of four persons, see Table 1, amply assisted by the marine science technicians aboard. Three additional scientists came aboard at Nome to carry out an acoustic experiment south of St. Lawrence I. None of their work is reported herein, but the oceanographic observations supporting the acoustic experiment are reported.

The data obtained are the most extensive set of under-ice observations in the area using modern, high-precision conductivity-temperature-depth recordings. This was an unusual opportunity to observe mid-winter, under-ice

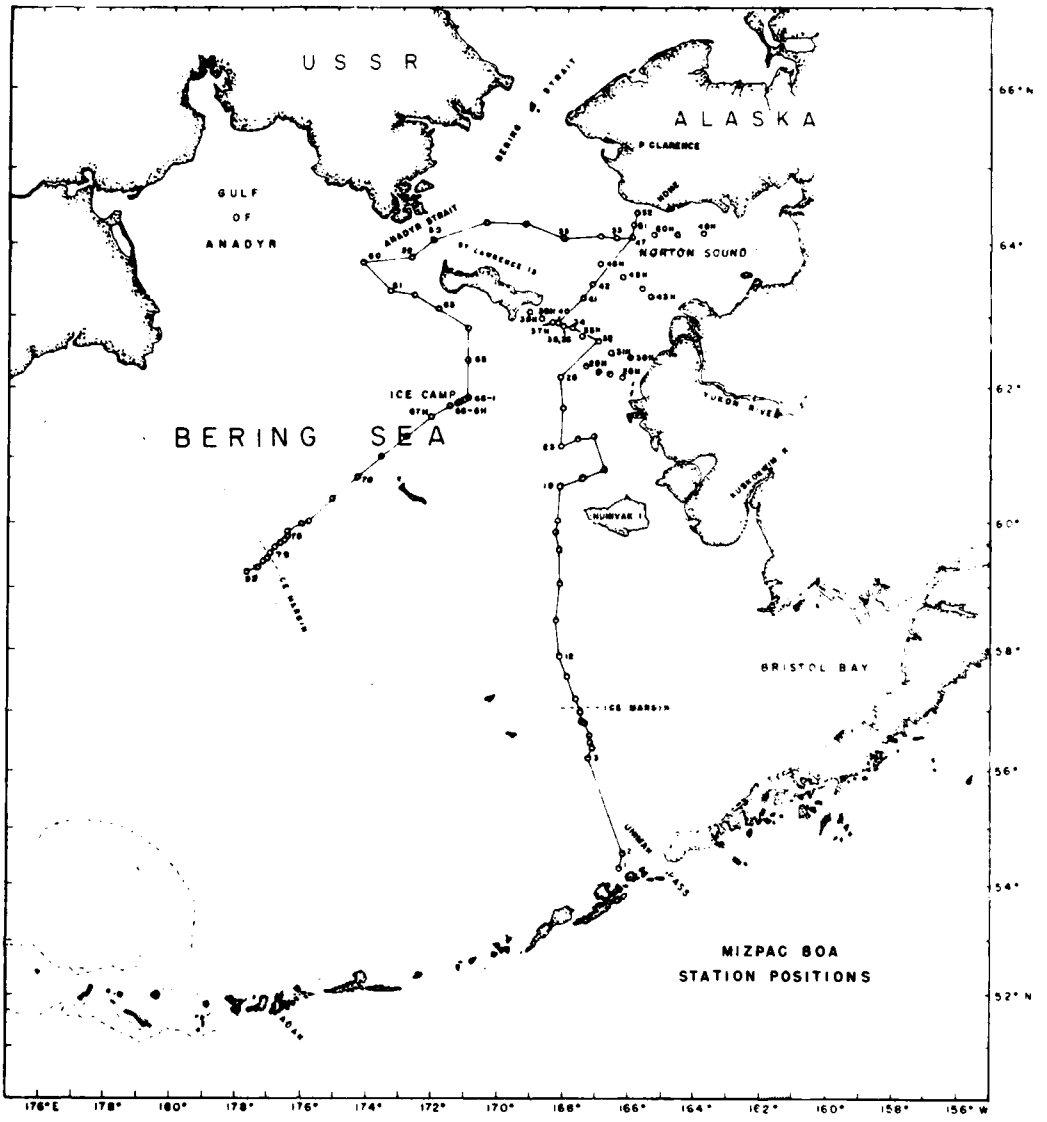

Fig. 1. Cruise track of USCGC POLAR STAR to the ice-covered Bering Sea in February-April 1980 illustrating the station distribution. Those taken from a hovering helicopter are indicated by the suffix "H".

Table 1

MIZPAC 80 CRUISE SUMMARY

EMBARKATION: 24 February 1980 at Sitka, Alaska

DISEMBARKATION: 4 April 1981 at Adak, Alaska

SHIP: USCGC POLAR STAR

INSTRUMENTS: Neil Brown Instrument Systems Mark III CTD,
Applied Physics Laboratory--Univ. of Washington
light-weight CTD,
Hewlett-Packard 9835 calculator and 9872A plotter

NAVIGATION SYSTEMS: SAT NAV, LORAN, OMEGA, RADAR, VISUAL

STATIONS OCCUPIED: By ship 67
By helicopter 16
Total 83

NANSEN CASTS: 21

SCIENTIFIC PARTY: Dr. M. Allan Beal, Arctic Submarine Laboratory, Chief Scientist
Dr. Robert G. Paquette, Naval Postgraduate School
Dr. Robert H. Bourke, Naval Postgraduate School
Dr. John L. Newton, Science Applications, Inc.
Mr. Birger G. Anderson, Science Applications, Inc.
Mr. Kim O. McCoy, Naval Postgraduate School

oceanographic conditions and processes in this dynamically active basin. Additionally it provided an opportunity to examine the marginal sea-ice zone of the winter Bering Sea. The scientific objectives of the cruise are described below.

Objectives

The cruise had the following objectives.

1. To describe the general oceanographic conditions near and under the ice.
2. To find any oceanographic phenomena near the ice edge which might be due to the presence of ice.
3. To characterize the brine convection process with respect to:
   a. Effect of latitude. Salinity ought to increase with latitude due to greater freezing rates towards the north.
   b. Effect of divergence of the ice in locations like Norton Sound and the south side of St. Lawrence I. High salinities might be expected in places where the heat-insulating ice cover diverges.
   c. Effect of fresh water inflow. Are the Yukon and Kuskokwim River influences notable? Do they cause stratification with the consequent effects on the depth of brine convection?
   d. Possible formation of high-salinity water in the shallows. In theory, this should occur. One wonders if the production of such water is rapid enough to cause a saline lower layer to flow into adjacent water columns.
   e. Layering of water of different salinities. This has reference to both b and d above. If high salinities are produced locally in the shallows or in areas of divergence, do these heavier waters run under adjacent water columns to cause layering?

4. Discover the direction of flow of low-salinity water resulting from the Yukon and Kuskokwim River discharges.

5. Discover the direction of outflow of cold, saline water from the Gulf of Anadyr, if such exists. Objectives 4 and 5 together, if achieved, might shed some light on the general winter flow through Bering Strait. Note that the Yukon definitely flows northward in summer. So does a water called "Anadyr Water" by Coachman, Aagaard and Tripp (hereinafter termed CAT, 1975, p. 27). Evidence for the northward flow of Anadyr Water in winter is weaker, if the two waters can be compared summer and winter (pp. 70-73).

6. Examine a theory by Pease (1980) that the ice edge in the Bering Sea is positioned by the balance between the flow of ice southward and melting by warm southern water. In essence, this implies that the ice margin is farther south than it would be if only atmospheric and radiational heat exchanges were doing the cooling. One should expect to find a low-salinity band near the ice edge.

Prior to a discussion of the cruise findings we first present the historical picture of what is known concerning the winter oceanography of the shallow Bering Sea. This is followed by a section on water circulation and one outlining sea-ice formation and brine-convected circulation for readers unfamiliar with these processes. A summary of sea-ice and meteorological conditions encountered during the cruise is presented next. The analysis of the cruise results has been divided into four sections which are both process oriented and geographically coherent: (1) crossings of the ice margin, (2) influence of the Yukon and Kuskokwim Rivers, (3) processes occurring around St. Lawrence Island, and (4) conditions near the freezing point. Appendix A contains a detailed report on instrument behavior and calibration and data editing procedures. Appendix B lists station position and climatological

information. Vertical profiles of temperature, salinity, sound speed, and density (sigma-t) for each station are shown in Appendix C.

2. PRIOR MEASUREMENTS AND ANALYSIS

This section catalogs the prior winter oceanographic measurements and lists the sources of the few recent partial discussions of general oceanographic conditions in winter. The winter circulation pattern over the Bering Sea shelf is discussed in the next section.

Measurements of salinity and temperature under ice in the Bering Sea have been nearly all made by Nansen bottles. Table 2 shows the statistics for the portions of those cruises which are in or near ice. The entire cruises may well have comprised more stations than are noted. Most of these were gleaned from National Oceanographic Data Center archives for the Bering Sea, using the initial test that the surface temperature be less than -1° C and the latitude less than 66°. Where these temperatures are mostly warmer than -1.6° C, it is concluded that the ship scarcely penetrated the ice margin and this condition is noted in the table.

The cruise tracks of these cruises are plotted by Lohrmann (1979). He presents a selected group of property cross-sections in the course of looking for frontal zones near and under the ice in winter and spring. However, his analysis is not extensive enough for the present purpose.

Coachman, Aagard and Tripp (1975) discuss the approach of water temperature to the freezing point, using STATEN ISLAND 1969 data (p. 46) and they discuss winter Anadyr Water and its alternating but presumed net northward flow through Anadyr Strait using the results of STATEN ISLAND 1969 and NORTHWIND 1968. In their discussion of freezing points they use Thompson's equation (Sverdrup, Johnson and Fleming, 1942) which gives freezing temperatures

Table 2

STATIONS IN AND NEAR ICE IN THE BERING SEA

Year	Ship	Dates	Stations	In/Near Ice	Location
1951	Burton Island	1/31-2/23	26	In	E, W, and N of St. Lawrence I.
1954	Burton Island	5/1 -5/27	20	Near	S, W, and N of St. Lawrence I. to Bering Str.
1955	Burton Island	4/26-5/19	12	In	E. Bering; W and NW of St. Lawrence
	Northwind	3/7 -4/18	42	In	E. Bering from Pribilofs to Nome
1960	Staten Island	1/26-2/23	20	In	S. Central Bering Sea
1961	Pervnets	3/29-4/21	11	Near	SE and Central ice margin
1968	Northwind	2/03-2/19	34	In	Gulf of Anadyr, Anadyr Str, S. of St. Lawrence
1969	Staten Island	2/14-4/25	67	In	W, NW and N of St. Lawrence to Bering Str.
1970	Northwind	1/31-2/17	25	In	Along most of ice margin; SW and S of St. Lawrence
	Fort Niagara	3/30-4/26	16	Near	Near Bristol Bay
1971	Glacier	3/27-4/20	32	In	Pribilofs to St. Matthew I. to Nome
1972	Burton Island	2/26-3/16	16	In	Pribilofs to Central Bering Sea to W and N of St. Lawrence

about 0.01° C higher than that of Doherty and Kester (1974) which is used in this report. Thus, they show more evidence of apparent supercooling than do the present data.

3. WATER CIRCULATION

Winter circulation in the Bering Sea is discussed by Hughes, Coachman and Aagaard (1974), although incompletely. They conclude that the Kamchatka Current intensifies during winter and, presumably, the northwesterly flow along the continental slope in the central Bering Sea either intensifies or at least is not decreased. There is an unsupported statement that "...the cyclonic gyre which dominates the deep basin in summer must encompass nearly the entire sea in winter" (p. 93). The winter circulation chart they suggest is confined to the deep-water areas outside the ice. Coachman, Aagaard and Tripp (1975) show evidence of Bering Sea Water entering the southeastern Gulf of Anadyr in winter, as in summer, but its rate of flow and course on exit from the Gulf of Anadyr (now as "Anadyr Water") are not known. Counter to the evidence of directly measured southerly flow by NORTHWIND 1968 (p. 71), they conclude that flow through Anadyr Strait is generally northerly. They base this conclusion on the need for a mechanism to supply high-salinity water to the region north of Anadyr Strait (p. 70). There is no need for advection of water from the south to account for the few moderately high salinities which have been observed. These salinities are likely generated in situ by brine rejection, as will be evident elsewhere in this report.

Some evidence for winter water flow can be deduced from the movement of ice. Muench and Ahlnäs (1976) tracked ice flows by means of satellite photographs in the months of March, April and May of 1974. Nearly all of their drift vectors are southwesterly, particularly from the latitude of St. Lawrence Island and southward. North of the island, the velocities were weaker and,

in a few cases, had northerly components. McNutt (1981) also shows ice drifts for parts of the months of February and March 1976 and March and April 1977. In March, nearly all the observed drifts were southerly. In February 1976, east of St. Lawrence I., the drift was mostly southerly during one 6-day period and mostly northerly in another 5-day period. Pease (1980) proposes that the general drift of ice is south-southwesterly under the influence of prevailing northeast winds and the evidence of the present report will agree with that conclusion.

It has been suggested that southerly drift of the ice does not preclude northerly flow of the underlying water. To argue the question clearly, it is necessary first to deal with continuity. If water is carried southward with the ice across the width of the Bering Sea, both ice and water flow would soon stop, in the absence of a counterflow, due to the resulting inclination of the sea surface. Therefore, water must be supplied to the northern Bering Sea. On the average, this water cannot come from Bering Strait because the flow there is presumed to be northerly even in winter (CAT, 1975) but probably with many southerly flow events (Bloom, 1964; CAT, p. 67; Coachman and Aagaard, 1981) which weakens its average flow in winter. Furthermore, if one postulates ice drift speeds of 0.25 ms^{-1} (Pease, 1980) across the width of the central Bering Sea, one is dealing with possible transports of water far greater than can reasonably be expected from Bering Strait.

The probable mechanism for replacement of most of the water is a northward compensating flow along the bottom. Evidence for such a flow will be seen in the discussion of the western ice-margin crossing where water from the southern Bering Sea is seen to intrude northward under the ice for over 200 km. Farther northward, the temperature and salinity signatures of the southern water have been destroyed by mixing and brine convection and, although northward flow along the bottom must continue, there is no way to tell whether it goes through Anadyr Strait or the strait east of St. Lawrence I., or both.

4. THEORETICAL CONSIDERATIONS

For readers unfamiliar with the freezing of sea ice and associated phenomena, the following elementary explanations are given. In freezing, seawater precipitates crystals of pure water ice which eventually become closely enough packed to grow into a massive structure. The salts in the seawater in part remain in the liquid brine, part of which convects downward and mixes with the upper part of the water column. Brine convection continues to reach deeper only if the mixture of brine and resident seawater remains denser than the water beneath. Thus, a sufficiently large density gradient will put a lower limit on the depth of convection. If the vertical density gradient is small, convection may continue to the bottom, leaving a well mixed uniform water column. This is especially notable in shallow seas and shelf areas.

Part of the brine remains behind, in trapped interstices between the ice crystals and, if the temperature subsequently becomes low enough, may deposit solid salts. New ice may have a bulk salinity of the order of 15 ‰, but the brine gradually drains until bulk values of salinity in thick ice near the end of the freezing season are more like 4 ‰.

If the water beneath the ice were not circulating, freezing could be expected to build up its salinity. Assuming the average ice temperature is -10° C, its salinity 7 ‰ and its density 0.93, one meter of ice rejects enough salt to raise the salinity 2.1 ‰ in a 10-m water column. The resultant salinity increase is inversely proportional to the length of water column so that shallow water is potentially capable of generating relatively high salinities. Other factors being equal, the greater the freezing impulses,

the more ice will be frozen and the more brine produced. Therefore, one expects higher salinities in the north where it is colder.

While one meter of ice is a reasonable thickness to expect under static conditions in the northern Bering Sea (Potocsky, 1965), the amount of ice generated and the salinity increase can be much greater if the ice is caused to diverge by wind action. Ice presents a thermal resistance to the passage of heat and heat is lost much more rapidly through thin ice or open water than through thick ice. From the results of Maykut (1976) we have estimated that the rate of freezing in open water in the northern Bering Sea in mid-winter is of the order of 30 times greater than under one meter of ice. Since the ice was diverging from the northern Bering Sea, as will be shown, potential salt enrichment much greater than 2.1 ‰ in 10 m are likely.

The rate of freezing in March is a matter of some doubt. During this month the ice is at its farthest southward extent and freezing and melting forces must be close to a balance, particularly south of latitude 60°N. North of this latitude frazil ice could be seen forming in the open leads, and from Maykut's Table 3 (1976, p. 60) we would conclude that heat was still being lost from an open sea surface at latitude 62.5°N in March. Yet, as will be seen, we will be forced to the conclusion that the net effect of open water at this latitude near the mouth of the Yukon was to cause the water to warm a few hundredths of a degree C. This may have been due to anomalously warm conditions during one or more previous weeks.

The brine sources may be localized, particularly along the downwind shore of the mainland or of an island. If a water column of high salinity is produced, the density forces are such as to exert a lateral pressure outward near bottom and an inward pressure from surrounding water near the surface. If the bottom slopes offshore, there would be a tendency for the high-salinity water to flow down along the bottom. Such tendencies to flow would quickly

come into balance with the Coriolis force and friction to yield a flow mostly normal to the lateral pressure gradient but with some cross-isobar flow. Thus, a column of high-salinity water over a flat bottom might be expected to be associated with anticyclonic rotation in its lower part and cyclonic rotation in its upper part. The base of the column should spread, but at an unknown rate, under adjacent water columns and might render two-layered a water column which would otherwise be uniformly stirred top-to-bottom by brine convection.

Flow of high-salinity water down a sloping bottom also would be modified from a simple downhill flow into one which is mostly parallel to the slope. Here, however, channelling of the flow downslope may occur if a sufficiently deep trough leads in that direction because flow parallel to the slope would be resisted by gravity acting on the dense water piled up against the right bank of the trough. A linear analog of this circular situation, but without friction, has been discussed by Stommel and Veronis (1980).

5. GENERAL CONDITIONS

The ice margin lay generally along the shelf break of the Bering Sea, except the southeastern end where it crossed into the shelf before reaching land near 55° N on the Alaska Peninsula. The southeastern margin was diffuse and consisted of large floes of thickness commonly 30 to 60 cm. In the central Bering Sea the margin consisted of bands of thin ice approximately 1 to 1.5 km apart. No banding was evident along the southeastern margin.

The ice became thicker toward the north, as much as 1 to 1.5 m thick in places when not rafted. There was also much thin young ice, new ice and open water, the latter particularly along the coast north of Nunivak I. and near the mouth of the Yukon River. In Norton Sound, the ice thicknesses were about 0.3 m, much thinner than the prediction of 1 m which would be derived from

the expected mean value of 1945 Celsius frost-degree days for Nome and Zubov's Equation (see Potocsky, 1965).

North of St. Lawrence I., thick, compact ice with a remarkably high ridge frequency was found. The average ridge height was probably greater than 2 m and ridges higher than 2 m were of the order of 50 m apart. South of St. Lawrence I., the ice was thin to moderate in thickness, the thicker, unrafted fields approximating 60 cm in thickness. The Naval Polar Oceanography Center ice maps showed young and new ice south of St. Lawrence I. before and during the cruise. Fig. 2 is an example of one map.

These behaviors point to a southward flow of ice from the northern Bering Sea under the influence of the prevailing northerly to northeasterly winds, shown in stick diagram form in Fig. 3. The pile-up of ice against the northern side of St. Lawrence I. is undoubtedly due to the southward pressure of ice acting against an obstacle.

During the early part of the cruise air temperatures were unusually high for this area and time of year, remaining above -3° C, and often slightly above freezing, until Station 36 was reached. Temperatures thereafter decreased rapidly with further northward progression finally reaching a low of -25° C near Station 55, northeast of St. Lawrence I. From Station 56 on, the air temperatures were generally between -10° and 0° C and they remained below 0° C even to the last station, Station 83.

6. CROSSINGS OF THE ICE MARGIN

Two crossings of the ice margin were made, an easterly one north of Unimak Pass, and a westerly one while exiting from the ice west of the canyon near 175°W in the central Bering Sea (Fig. 1). These crossings were

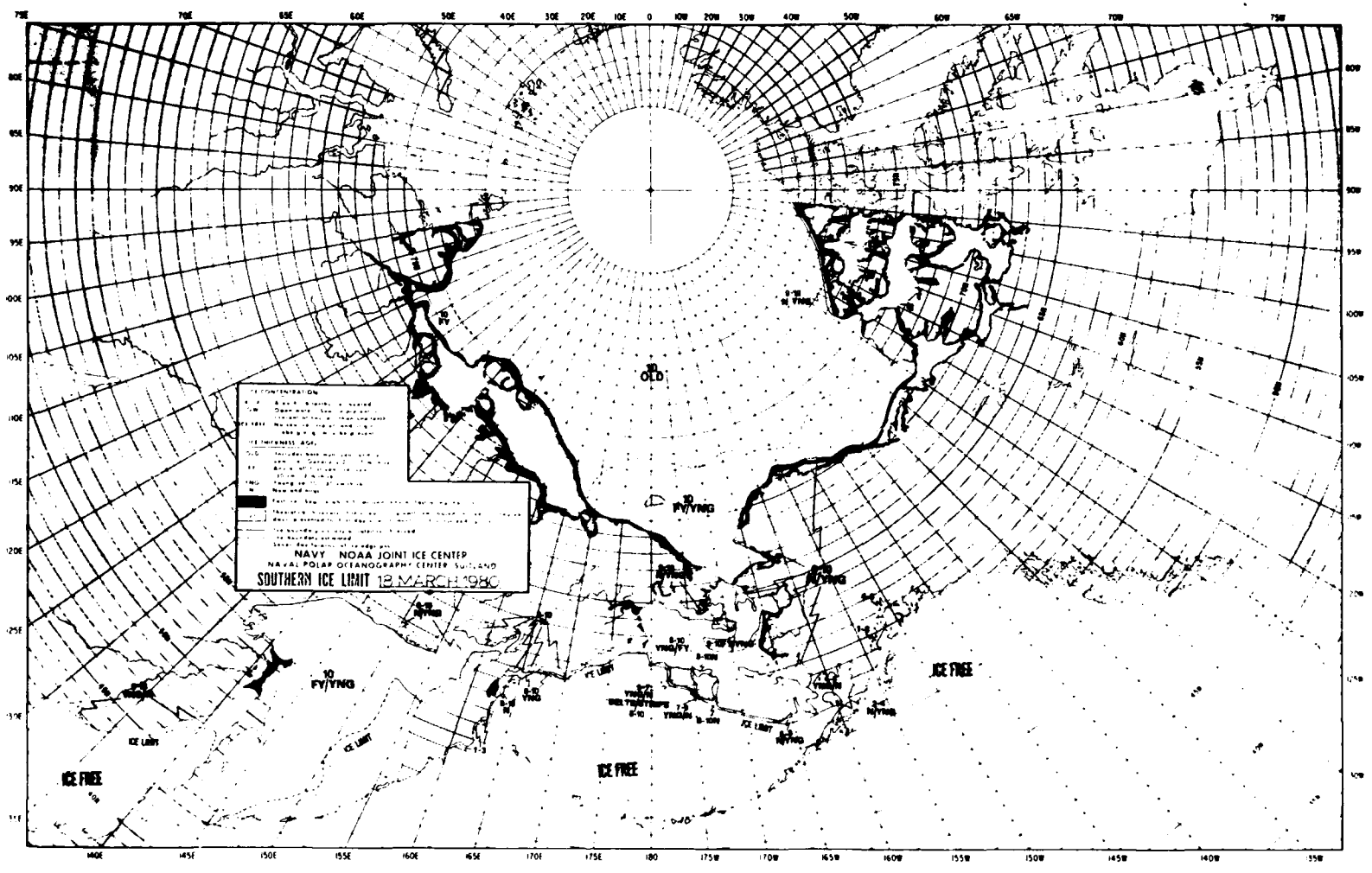

Fig. 2. Ice forecast map for 18 March 1980 issued by the Naval Polar Oceanography Center illustrating ice age, thickness and presence of polynyas.

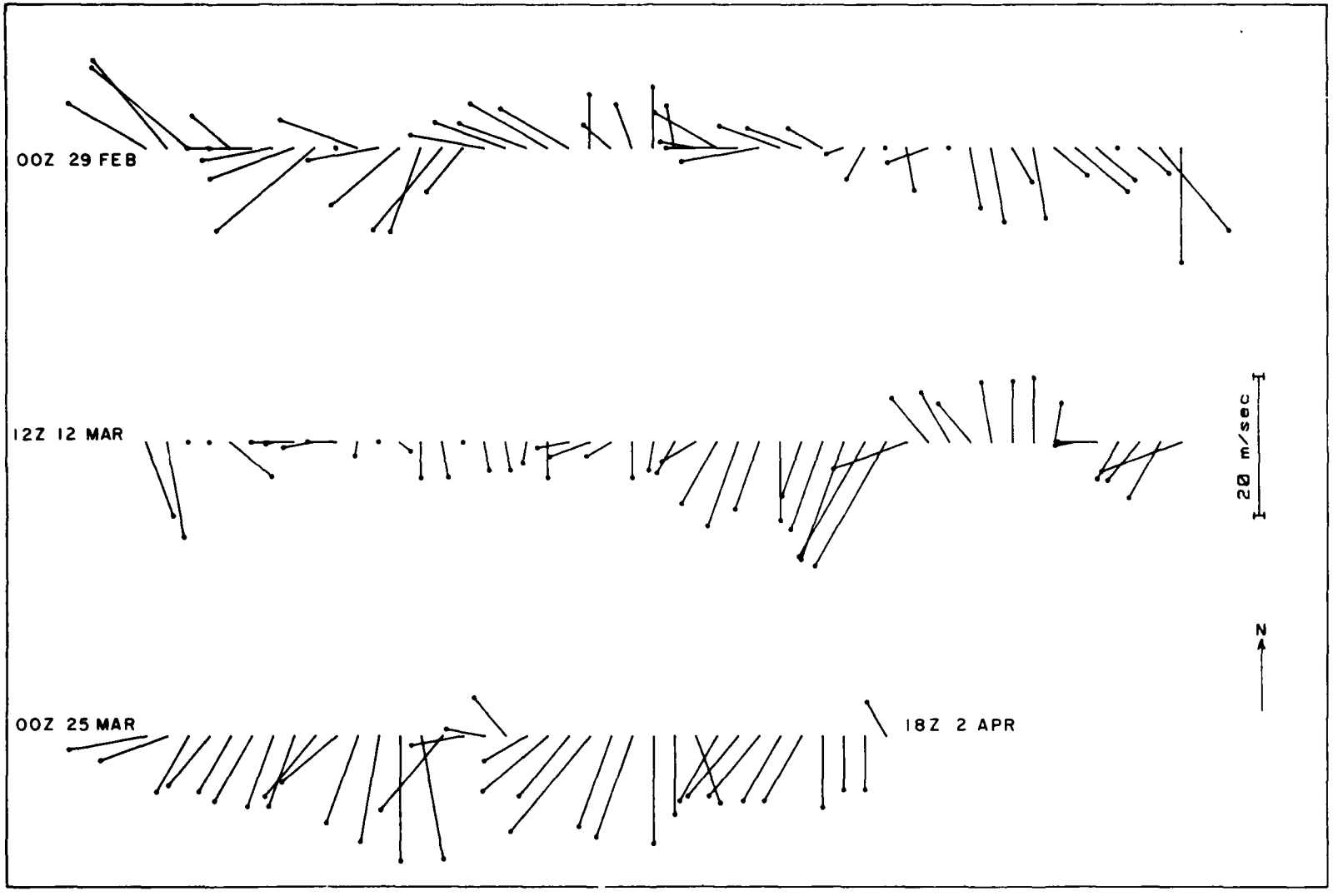

Fig. 3. Wind flow vectors at the ship position plotted every 6 hours. The dots are in lieu of arrow heads. There are no real zeros; dots without vectors indicate missing data. Time/date groups are in Greenwich (Z) time. Winds were predominantly from the north to northeast during the cruise.

about 600 km apart and, even at this distance, some similarities are present. Likewise, some notable dissimilarities are also present.

The Eastern Crossing

The characteristics of the waters on the slope and outer shelf in the eastern crossing are shown in Fig. 4, a temperature and salinity cross-section from Stations 3 through 17. Ice was first encountered at Station 9; 30 km northward, at Station 10, the ice concentration had increased to 10/10. The station spacing was approximately 25 km outside the ice, but increased to about 50 km within the ice pack.

Fig. 4 also shows that stratification of the water column is observed from Stations 3 to 10 whereafter the water column abruptly becomes almost perfectly vertically homogeneous. A cold, dilute upper layer extends some 140 km south of the ice. This upper layer is cold and relatively dilute because of a combination of three processes: 1) the melting of ice to the north and mixing of the melt water southward, aided by the prevailing northerly winds; 2) contributions of fresh water from the Kuskokwim and possibly the Yukon Rivers and 3) a certain amount of atmospheric cooling, possibly a weak effect because the air temperatures when the ship passed were somewhat above freezing (see Appendix B). However, the historical average temperature for February and March (Potocsky, 1975) is about -5° C and this may be a more realistic average during the preceding period when the water properties were generated. The cold, dilute layer overlies the warmer, saltier, more southerly Bering Sea water which has advected onto the shelf.

In Fig. 5, temperature-salinity correlations have been plotted separately for the surface and the bottom waters of the eastern and western crossings, the latter to be described later. Consecutive stations are connected by lines. The plot for the eastern crossing illustrates the bottom warmer and

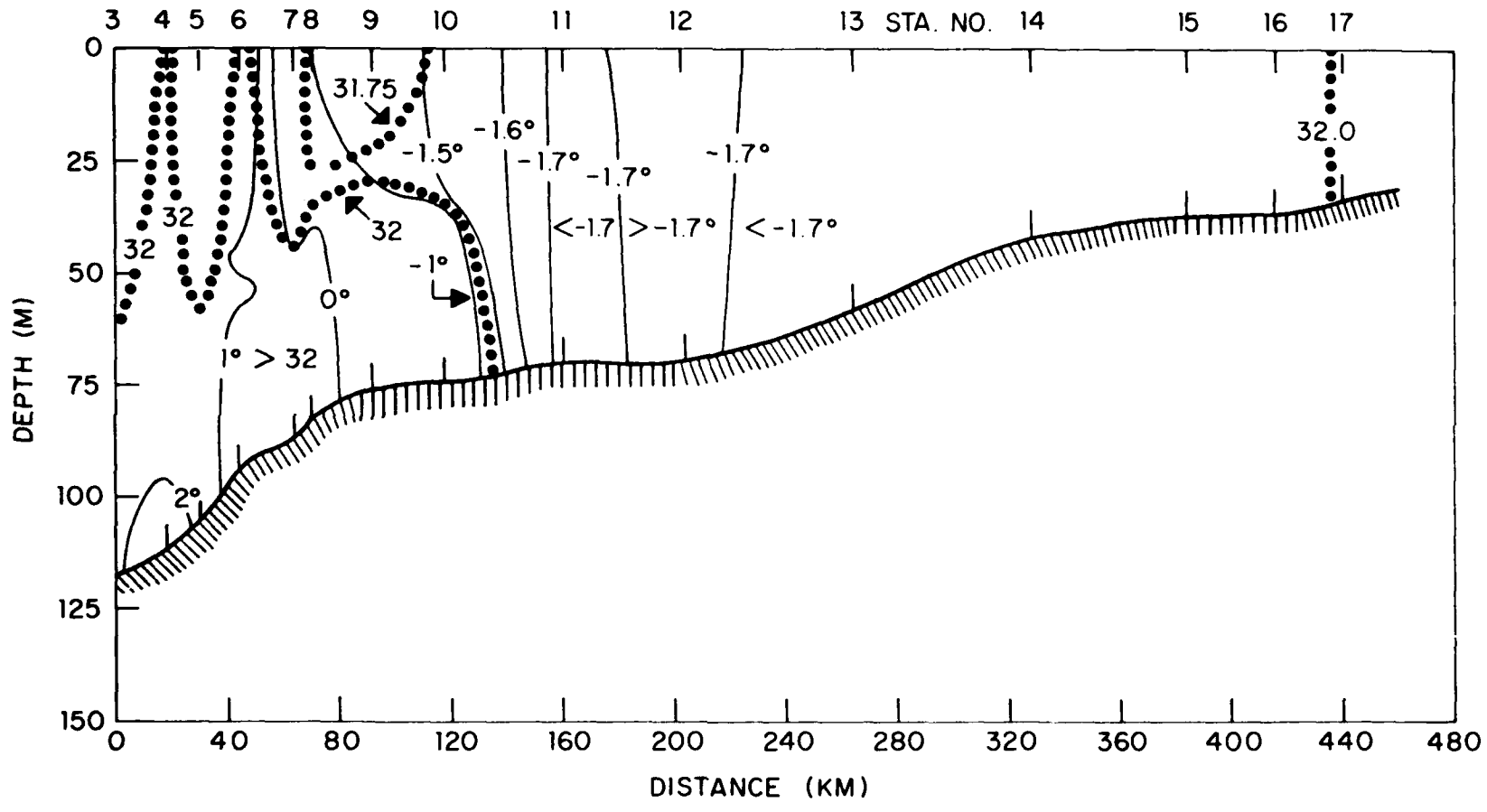

Fig. 4. Temperature and salinity cross-section along the eastern crossing of the ice margin, Stations 3-17. Note the rather abrupt transition near Station 10 from relatively warm southerly Bering Sea Water to cold, well-mixed underice water. Salinity contour interval is 0.25 ‰, temperature contour interval 1° C except for waters colder than -1.5° C where the interval is 0.1° C.

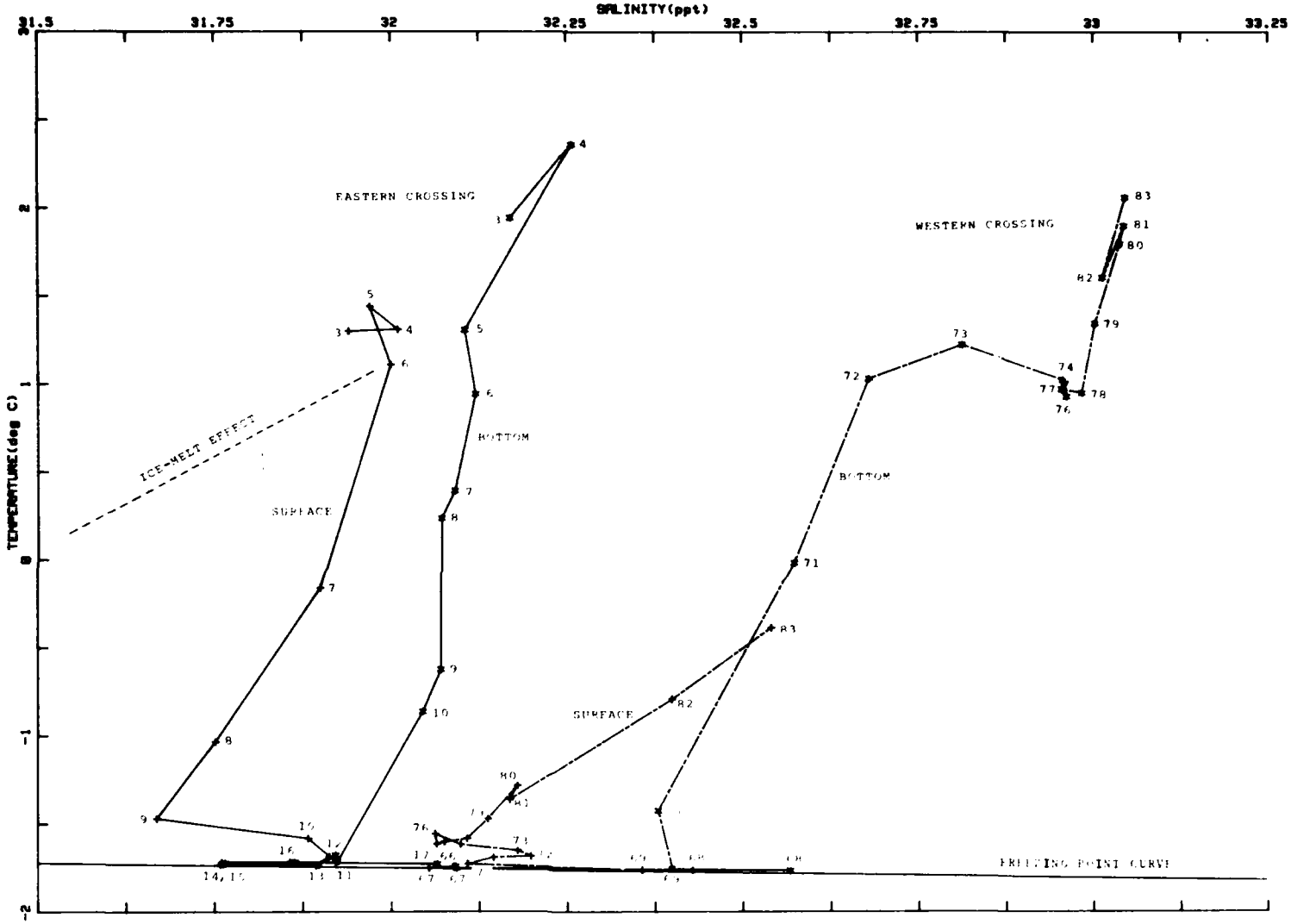

Fig. 5. Temperature-salinity pairs for the surface and bottom layers of both ice-margin crossings in relation to the Doherty and Kester (1974) freezing point curve. Note in the eastern crossing the relative freshness, the much smaller top-to-bottom difference in properties and the more rapid cooling than that due to ice melt alone. The T-S change due to ice melt alone is shown as a dashed line.

more saline than the surface at all stations prior to Station 11 except Stations 5 and 6. In these two, the bottom is colder than the surface. At Station 11 the top and bottom become essentially identical and remain so, although varying fairly widely in salinity, to Station 17. By most standards, the region between Stations 3 and 11 would be considered a frontal zone with maximum temperature change occurring just outside the ice between Stations 6-8.

The general cooling and dilution of both layers in the direction of the ice is indicative of the effect of melting ice. However, the observed dilution-to-cooling ratio is only half or less of that to be expected from the melting of ice (ca. 3/8 $‰ - °C^{-1}$), which indicates either that atmospheric cooling has played an important part or vertical mixing with the bottom layer is providing salt. That this latter process occurs is suggested by the general parallelism of the curves for surface and bottom layers. The substantial contribution of melt water to the surface layer continues as the ice edge is approached until, at Station 9, the abrupt change in slope indicates the preponderant effect of mixing with the water type of Station 11 behind the ice margin. Beyond Station 11 both surface and bottom salinities fluctuate, perhaps reflecting non-uniform brine generation or varying admixtures of river water.

The maximum effect of ice melt may be seen at Station 9. Farther north, vertical mixing due to thermal and brine convection, aided perhaps by other mixing processes such as tidal stirring, has finally overcome the stratification. The fact that the temperature at Station 11 and beyond is nearly at freezing argues for brine convection, not necessarily in situ, as the principal generating process. Slight warming above the freezing temperature in

the northern part of this section is part of a general slight, fluctuating elevation of the temperature above freezing which will be discussed later.

Stratification of the water column nearly completely disappears at Station 11. From here northward 100 km to Station 13 the temperature-salinity properties are quite similar. Temperatures at Stations 11 and 13 are within 0.02° C of the freezing point but those at Station 12 are somewhat elevated, to 0.06° C above freezing. Because of the relatively warm air temperatures present at this time (warmer than -3° C), and the decrease in salinity, this area can not be considered an active freezing zone.

Stations 14 and 15, and to some extent Stations 16 and 17, southwest of Nunivak I. are notably more dilute than those to the north or south. The water columns are well mixed and within 0.02° C of freezing, but have salinities of 31.76 ‰ (Fig. 5). This dilution may reflect the admixture of Kuskokwim River effluent. It is also possible that this localized dilution was caused by ice melt; these stations were taken in largely open-water areas (< 3/10 ice coverage) due to ice divergence in the lee of Nunivak I. at a time of relatively warm air temperatures, at or near freezing. It will be seen that there is a similar low-salinity area in the western crossing, which suggests some widespread phenomenon rather than the localized effect of river water as the cause.

Northward from Nunivak I. to the center of the strait east of St. Lawrence I. (Stations 17-35) the waters were uniformly cold and well mixed. Salinity slowly increased by 1 ‰ over this 320 km reach (Fig. 6) as the ice thickness gradually increased with its consequent increase in brine production. As will be seen in the following section, this transect lies seaward of the diluting effects of the Yukon River.

At this point the northward course of the description is interrupted to examine the western crossing in comparison with the eastern crossing.

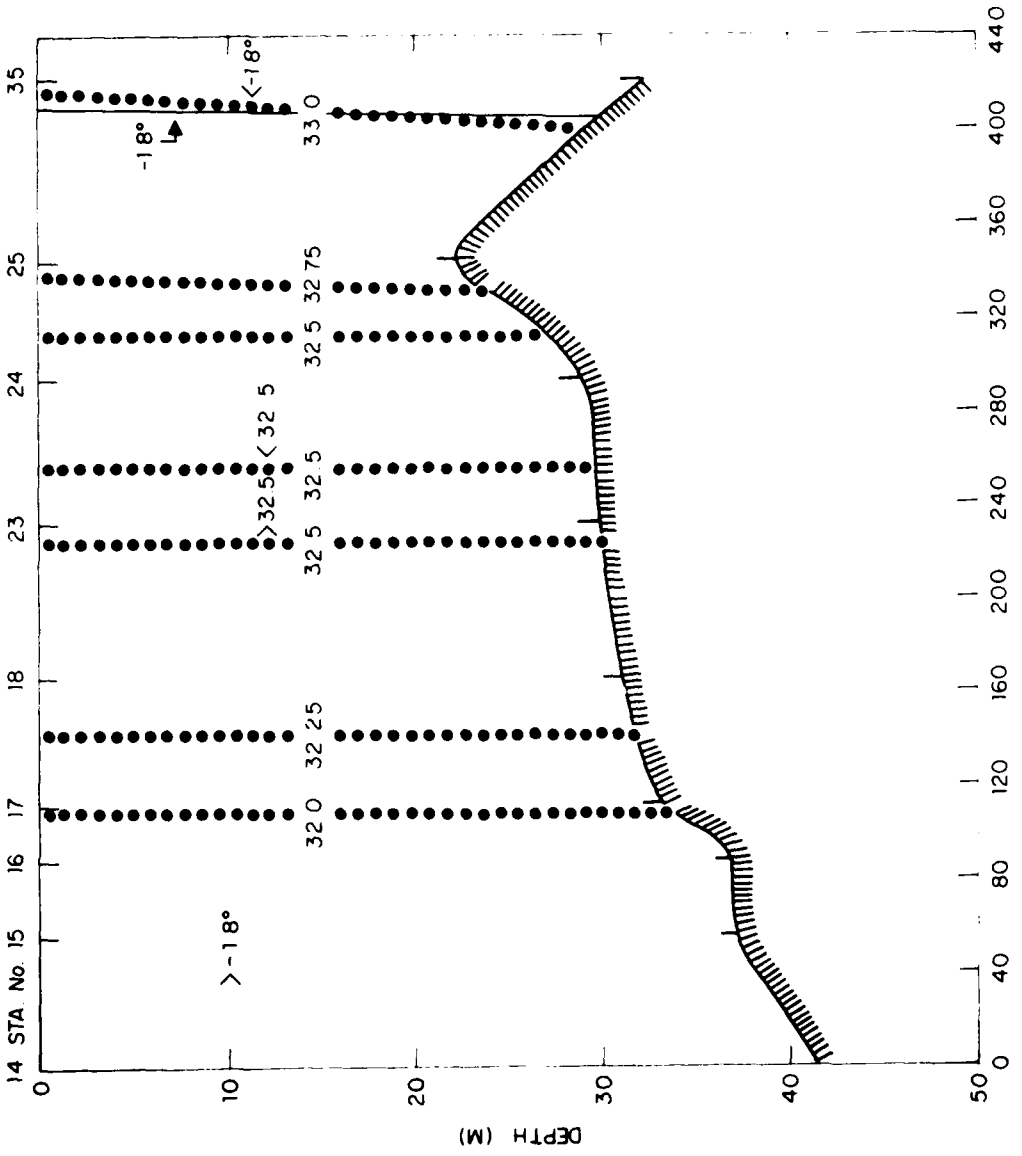

Fig. 6. Temperature and salinity cross-section along the track from west of Nunivak I. to the throat of the strait east of St. Lawrence I., Stations 14-35. Note the increase of salinity with increasing latitude.

The Western Crossing

Winter oceanographic conditions within the central Bering Sea were observed on the outbound crossing of the ice margin beginning with Station 66 and ending at Station 83, a traverse of 480 km. The geography may be seen in Fig. 1, the temperature and salinity cross-section in Fig. 7 and the T-S diagram again in Fig. 5. The ice edge was encountered at Station 79 near the edge of the shelf in 150 m of water. Unlike the eastern crossing where high ice concentrations were noted within 20 km of the ice edge, the western ice margin was comprised of a series of bands of relatively thin (< 0.3 m) ice. This condition extended some 100 km behind the ice edge to about Station 72.

The most notable difference between the two crossings is the extent to which warm, salty Bering Sea water underran the ice, some 200 km to beyond Station 70. Conversely, the pool of cool, dilute melt water (ca. -1.65° C and 32.1 ‰) occupying the upper half of the water column for some 240 km behind the ice edge is also notable. Rather than the abrupt transition between warm Bering Sea water and under-ice water observed in the easterly crossing, here one sees these waters separated by a sharp halocline/thermocline which shows a marked undulation of approximately 200 km wave length. The salinities of both layers of this crossing are 0.3 to 0.7 ‰ higher than in the eastern crossing.

Temperature finestructure is observed in the thermocline and upper portion of the lower layer beginning at Station 74, 50 km behind the ice edge and continuing southward beyond Station 83. This is in contrast to the eastern crossing wherein finestructure is only weakly observed at Stations 5 and 6. Mixing across the thermocline, aided by the strong northward advection of the lower-layer waters of the central Bering Sea, is more conducive to interleaving and finestructure formation here than to the southeast.

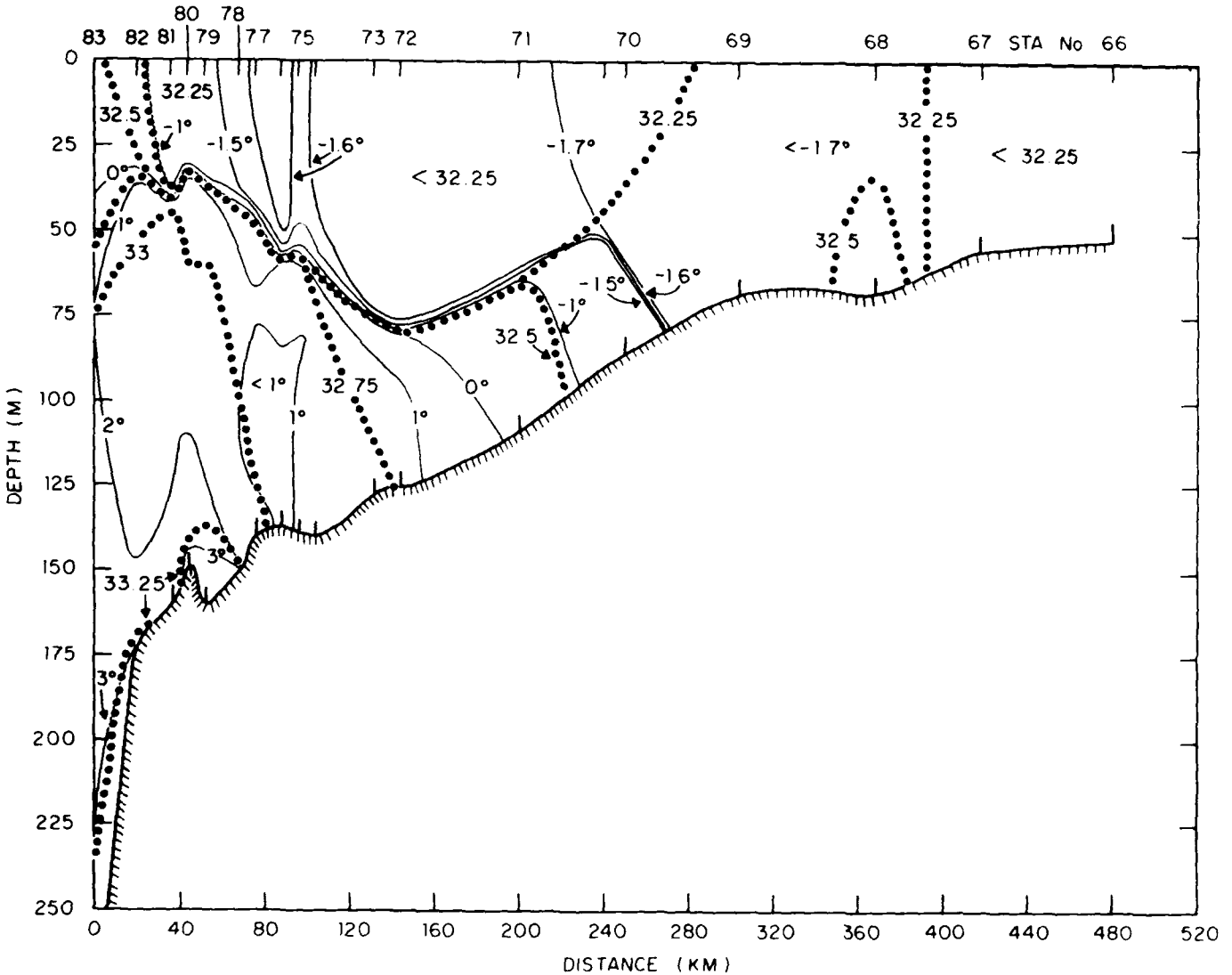

Fig. 7. Temperature and salinity cross-section along the western crossing of the ice margin, Stations 66-83. Contour interval as in Fig. 4. Note that relatively warm Bering Sea Water extends up on to the shelf some 200 km behind the ice edge (Station 79).

Fig. 7 indicates that near the shelf break a deeper, warmer Bering Sea water is present from Station 77, 20 km inside the ice, to beyond Station 83. The water of this layer is uniformly warm and salty (> 3° C, ~34.4 ‰) and confined to depths generally greater than 140 m. No distinct bottom layer was observed at Station 81. This water was omitted when plotting the temperature-salinity correlations of Fig. 5 as it is too deep to affect the waters above it or farther back on the shelf.

The temperature-salinity diagram is particularly interesting in comparison to the eastern crossing. Now, the slope of the curve for the surface layer between Stations 83 and 78 is almost exactly that which would be caused entirely by melting ice. This was generally a region of scattered ice floes, with the ice becoming reasonably compact north of Station 79. Adherence to the melting-diluting slope is indicative of a strong interaction of ice and warmer water caused either by a pronounced southward flow of ice or strong lateral mixing.

The salinity and temperature differences between the surface and bottom layers are much more marked than in the east. The bottom layer comes close to freezing at Station 69, 250 km from the ice edge; the surface remains more dilute until Station 66 is reached, 430 km from the ice edge. These phenomena are probably caused by a strong northerly component of the flow in the bottom layer. The fact that the salinity and temperature of the bottom layer continually approach those of the upper layer indicates that vertical mixing is going on enroute. Melting has nearly ceased in the upper layer north of Station 78. Signs of active brine generation, indicated by sharp upswings in salinity at the surface, are sporadic from Station 75 northward. Brine

convection does not penetrate to bottom until Station 66 is reached. Thus we see much of this 430 km wide underice section of shelf subject to freezing influences at the surface which are overcome by heat mixing upward from below.

As in the eastern crossing, an anomalous low-salinity band is observed in the central shelf region centered on Stations 67 and 66 (Fig. 5). Isohaline waters approximately 0.4 ‰ less than those to the north or south are present. The phenomenon does not appear to be caused by local melting. The waters here and on both sides have no surplus heat to cause melting. The phenomenon was found in BURTON ISLAND 1972 in March near Station 12 at 61°-21'N, 175°-03'W, about 100 km north of our Station 71 and again at Station 40 at 61°-26'N, 174°-24'W, 78 km north of our Station 70. In 1972 the central salinity was below 32 ‰. The origin of this low salinity water is not readily apparent but it most likely presents a patch of dilute water formed elsewhere at an earlier time and advected into this region.

7. INFLUENCE OF THE RIVERS

Two rivers can influence the oceanography of the area studied, the Yukon and the Kuskokwim. It will be shown that the Yukon has significant effects even though its flow rate in winter approximates 3 to 4% of its peak flow in June (CAT, p. 39; USGS, 1980). In summer, the Kuskokwim flows at 20 to 25% of the rate of the Yukon (CAT, p. 39). Its relative flow in winter is likely to be no larger, and probably smaller because of the increase of the ratio of cooling surface to volume as size decreases. We did not approach the Kukokwim closely enough to demonstrate its effects unequivocally and so will devote most of our attention to the Yukon.

The influence of Yukon River discharge on the water mass structure of Bering Sea water in summer is a well-documented feature of the summertime

circulation in the northern Bering Sea and Bering Strait regions (see, for instance, CAT, p. 37). However, the winter situation is relatively unknown. Figs. 8 and 9, which show the horizontal distribution of salinity near the surface and sea floor, indicate that Yukon River water is readily observed as a low-salinity contribution in Norton Sound and off the Yukon River delta.

Comparing Fig. 8 with the summer situation and using the 5 m salinities from the BROWN BEAR 1979 cruise as an easily accessible example (CAT, p. 37), we find the salinity pattern of the two seasons comparable in the northeast Bering Sea and outer Norton Sound, except that winter salinities are higher by roughly 3 ‰ in areas a little removed from the river mouth and perhaps 6 ‰ higher near the river mouth. Salinities near bottom are roughly 2 ‰ higher in winter. Comparison of the 5 m salinity fails to take into account the upper several meters of the water column which can have a dramatically lower salinity in summer, especially in Norton Sound.

Temperature-salinity cross sections, Figs. 10 and 11, indicate that south of the Yukon delta Yukon water remains near the coast, being well delineated by the 32.25 ‰ contour. The southern extent of Yukon water is not well-defined but Figs. 8 and 9 indicate that it does not extend far south of the delta, i.e., south of 62°N unless it is landward of Stations 20 and 21. Station 30H appears to be in the core of the water issuing from the southern branch of the delta. Here the surface-layer salinity is 30.85 ‰, 0.6 ‰ less than the bottom layer (Fig. 11). A transect along the axis of Norton Sound (Fig. 12) indicates that the waters become increasingly more dilute and stratified towards the head of the Sound. These low salinities must be due to Yukon water because the smaller rivers entering Norton Sound must be thoroughly frozen. Station 47 exhibits notable stratification: the salinity increases from 31.5 to 32.3 ‰ between 5 and 8 m depth.

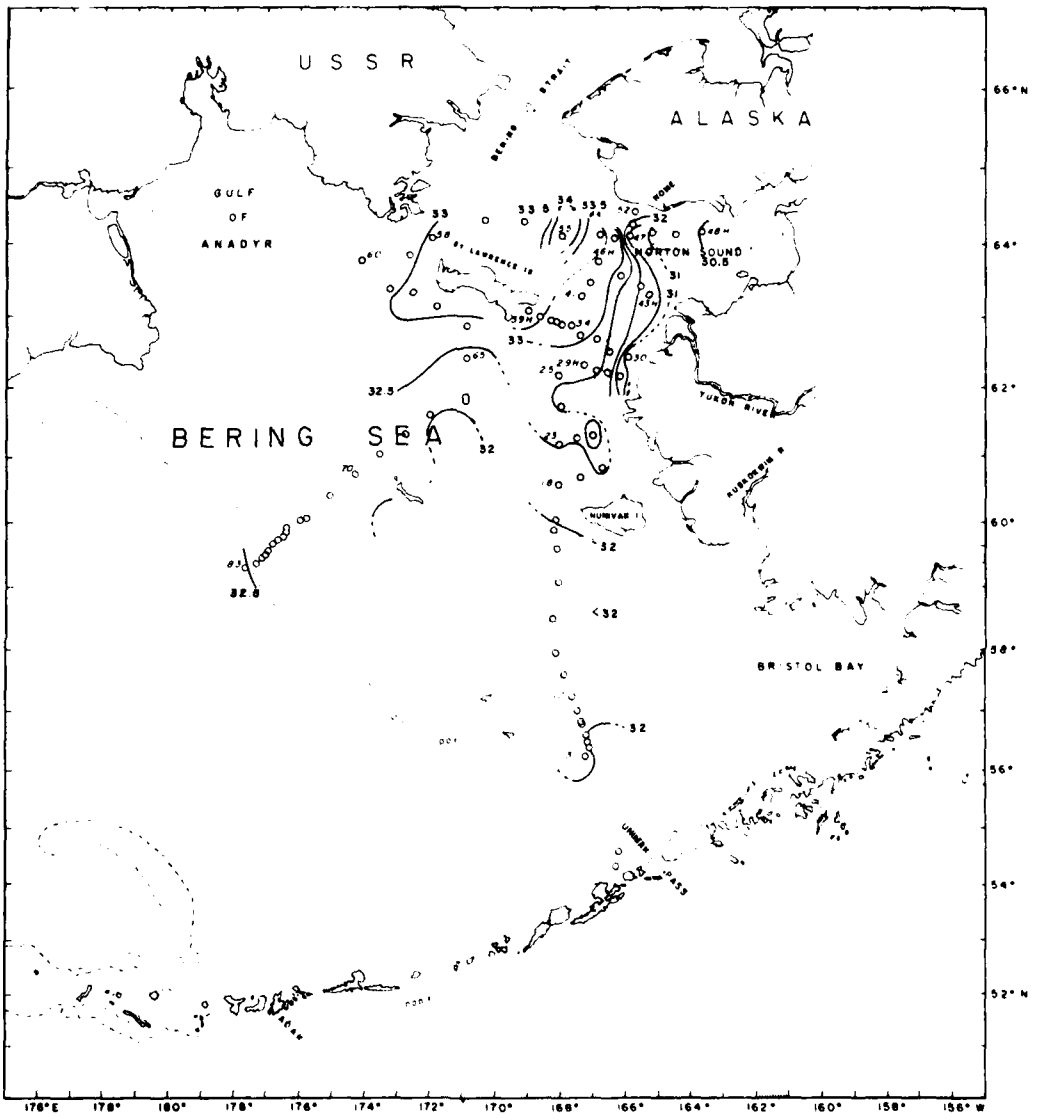

Fig. 8. Horizontal distribution of near-surface salinity. Contour interval is 0.5 ‰ .

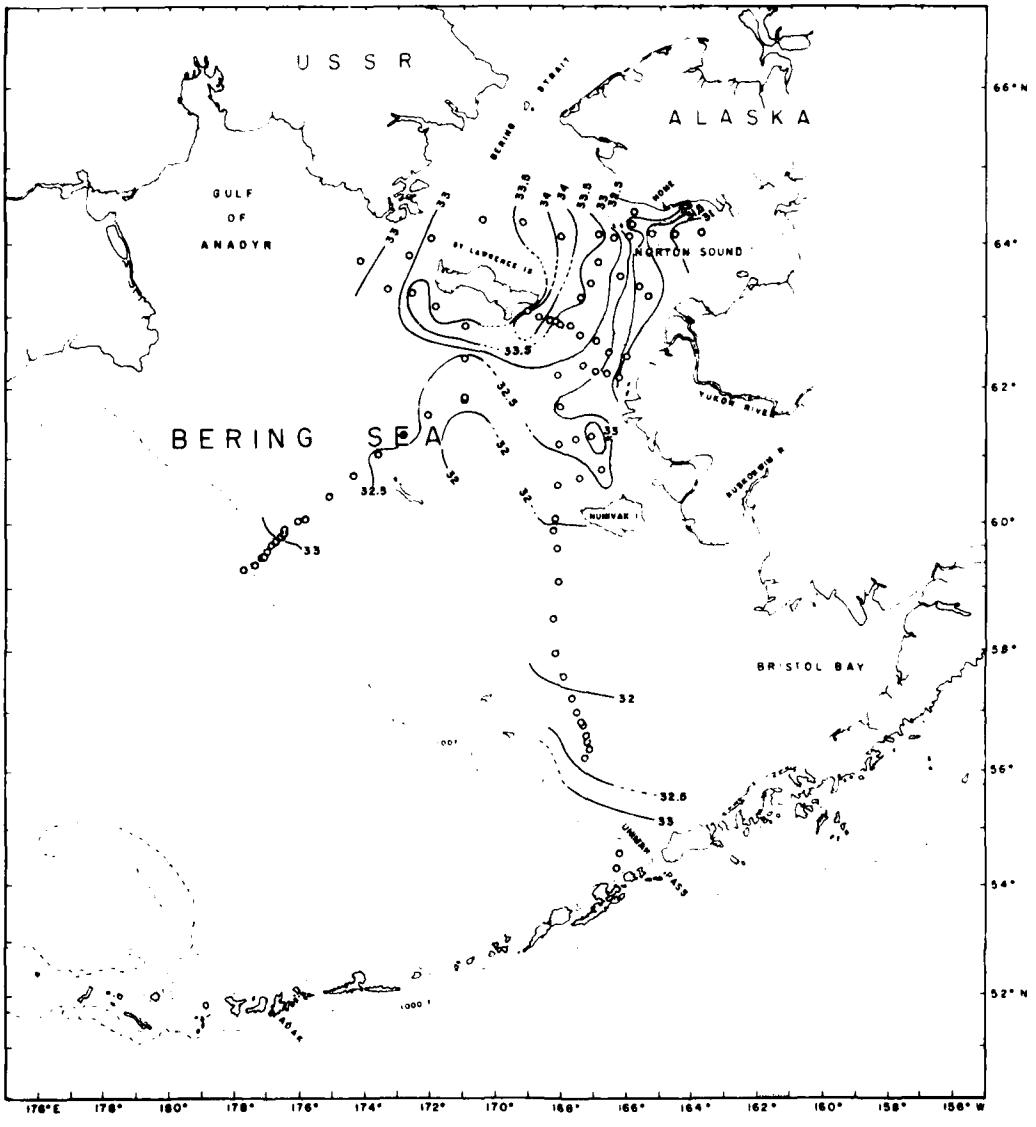

Fig. 9. Horizontal distribution of bottom salinity. Contour interval is 0.5 ‰.

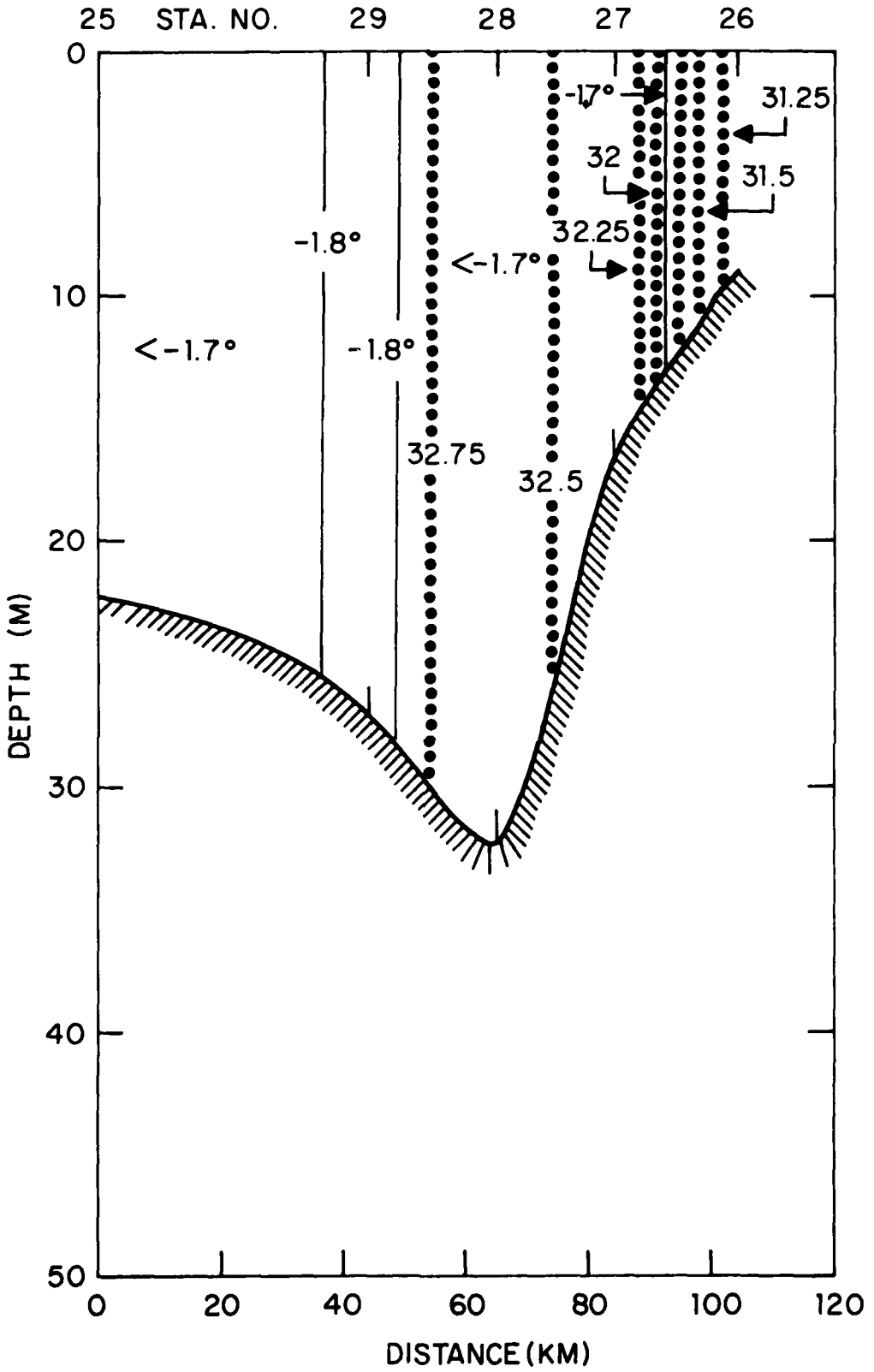

Fig. 10. Temperature and salinity cross-section from a line of stations (25-29) in shallow water south of the Yukon delta. Note the sharp horizontal salinity gradient which delineates the westward extent of Yukon water.

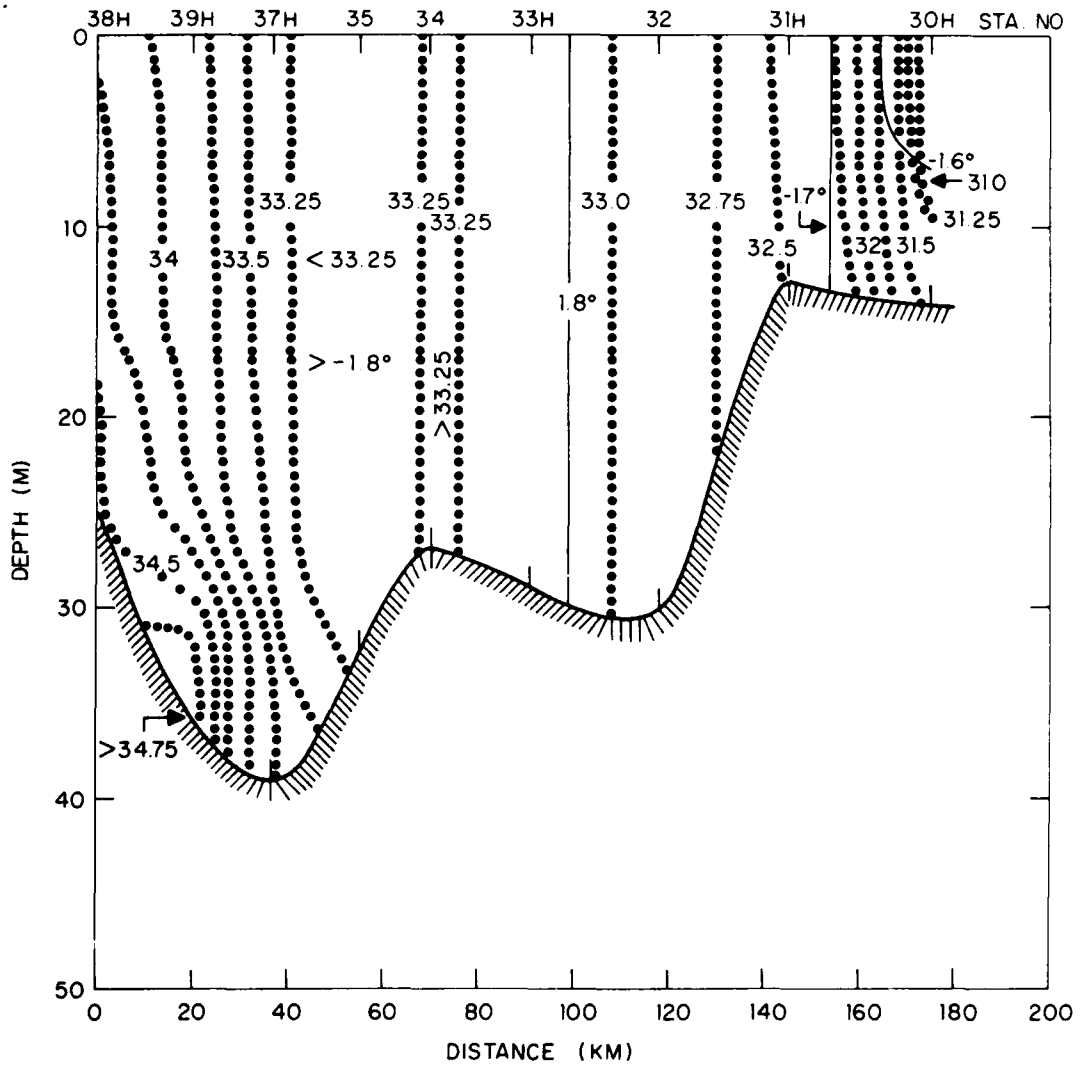

Fig. 11. Temperature and salinity cross-section from a line of stations (38H-30H) across the strait east of St. Lawrence I. A high-salinity band indicative of possible brine enrichment is observed just east of St. Lawrence I. while low-salinity Yukon River water is observed mainly shoreward of Station 31H.

The westward bulge of low salinity in Figs. 8 and 9, near Station 47 and Station 51 just to the north, suggests the possible exit route of low-salinity water from Norton Sound. The low-salinity signature disappears quickly between Stations 47 and 53, the site of the strongest salinity front found on the Bering Sea shelf, 2 ‰ over 60 km. It appears possible that the water follows its summer trajectory northwestward along the Alaskan coast.

The region south of Nome and in Norton Sound is a region of ice divergence. The ice there is usually thin, in spite of air temperatures in the vicinity of -20° C. This area would be expected to be an area of rapid brine generation because of the thin insulating ice cover. It appears as a low-salinity area here because of the effect of Yukon water. However, in comparison to summer, the surface salinities well into the Sound have risen about 10 ‰; farther to the west, the increase has been 2-3 ‰ except in the upper few meters, as stated above.

8. PROCESSES OCCURRING AROUND ST. LAWRENCE ISLAND

The surface salinity contours (Fig. 8) show that Yukon water is confined to the eastern margin of Bering Sea. To the west, once salinities have increased to 32.5 ‰, salinity stratification ceases (Fig. 12). By Station 53 all appearances of Yukon water have vanished. From there westward to Station 57 (Fig. 13) high salinity water (33.25-34.28 ‰) is present.

The presence of such high salinities in the coldest part of the Bering Sea is not necessarily surprising. In principle, this is what is to be expected, if the ice is continually being swept south and renewed as Pease (1980) proposes, and brine equivalent to 5 m of ice has been generated. What appears inconsistent at first is the fact that this region of high salinities, far from being an area of thin ice and thus rapid freezing, is the area with the

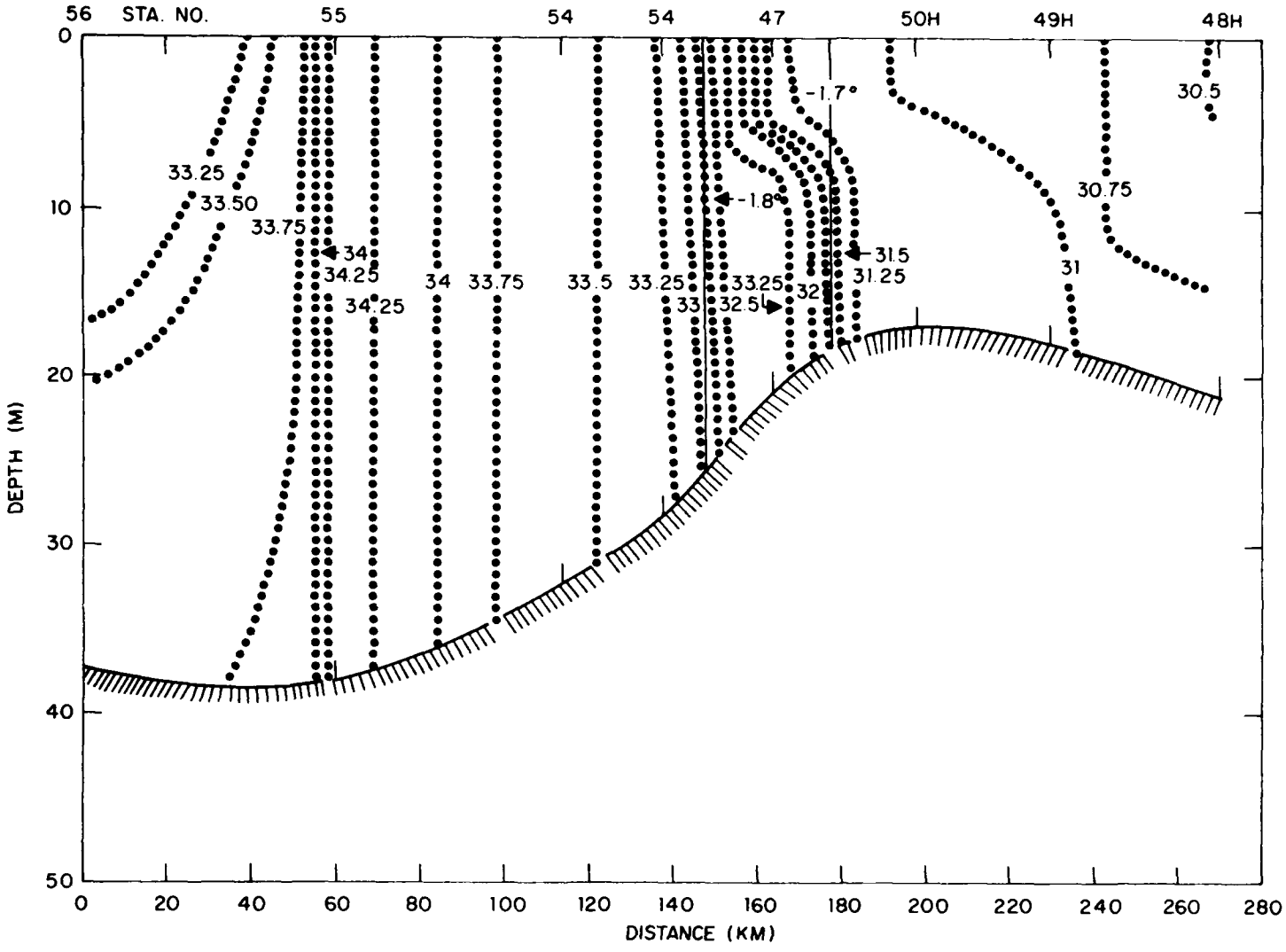

Fig. 12. Temperature and salinity cross-section from a transect along the axis of Norton Sound (48H-56). The salinity front between stations 47 and 53, delineating the western boundary of Yukon Water, is the strongest front found on the Bering Sea shelf, 2 ‰ over 60 km. Note the high salinity band between Stations 54 and 56.

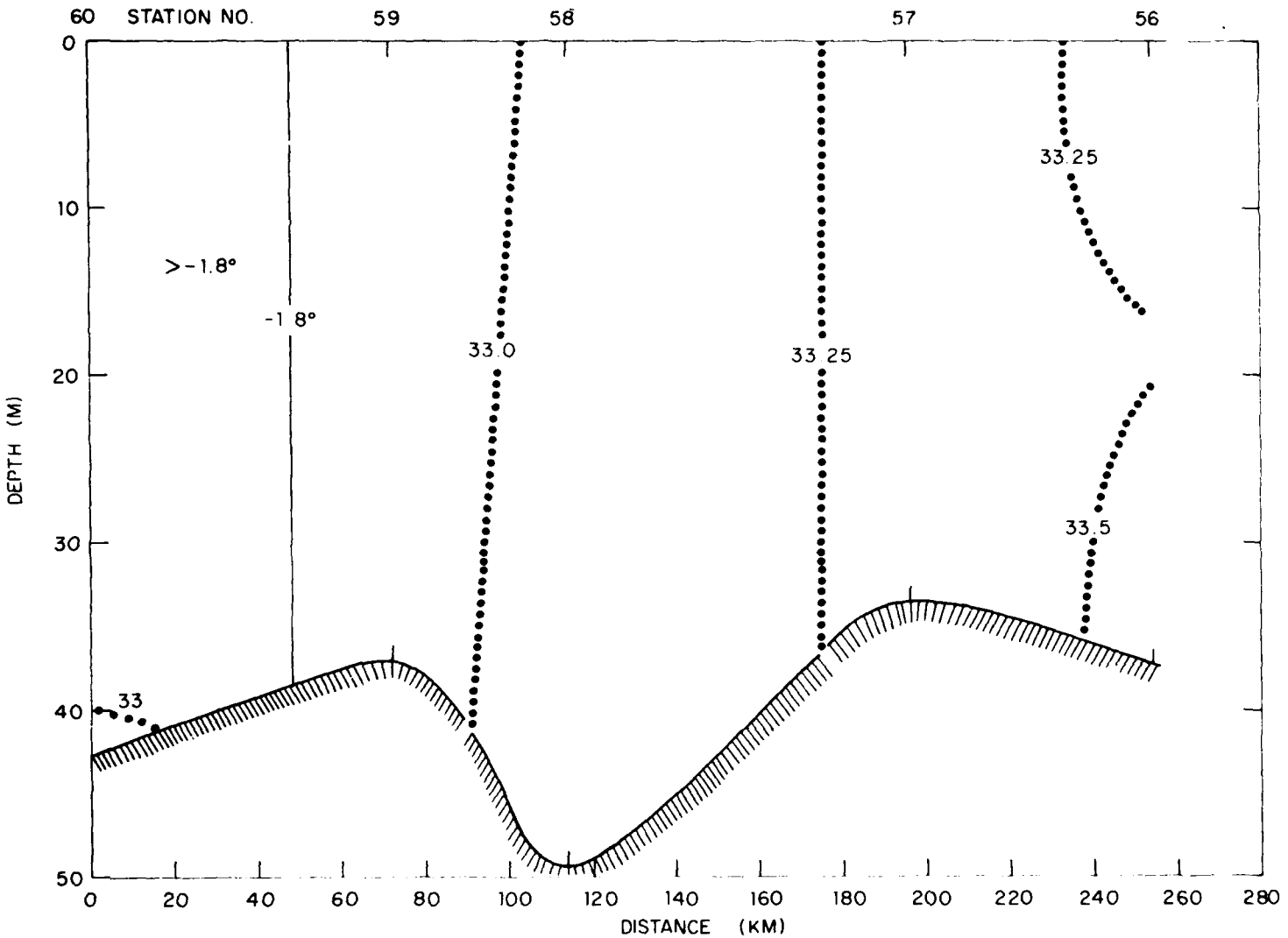

Fig. 13. Temperature and salinity cross-section from a line of stations (56-60) north of St. Lawrence I. showing uniformly high salinities.

thickest ice of the entire cruise. However, this may have been a local condition; helicopter observations showed thinner ice perhaps 15 km to the north. Further evidence of thin ice in the area is given by McNutt (1981) from a study of satellite images. She found frequent occurrences of a large tongue of thin ice extending in a direction between 150° T and 190° T for up to 250 km from the Port Clarence-Cape Prince of Wales area in February and March of 1976, 1977 and 1979 (Fig. 14). Such a tongue could have been a brine-generating area. It should be noted that brine accumulation and thin ice need not coincide at all times. The accumulation is likely to be the time integral of thin-ice effects over a period perhaps as great as several weeks.

Not excluded from consideration is the possibility that the high salinities have flowed southward from the Bering Strait area and possibly even the Chukchi Sea. The tongue of thin ice is a possible indicator of southward flow. Also, Coachman and Aagaard (1981) give evidence that there are a substantial number of strong southward-flow events in Bering Strait in the winter.

Two other facts are of interest in connection with the highest salinity observed, 34.28 ‰ at Station 55. Just to the south-southwest of this station, salinities above 34 ‰ were observed at Station 38H near the eastern tip of St. Lawrence I. (Figs. 8 and 11). This raises the possibility that the high salinities are in the form of a tongue extending more or less southward. Unfortunately, the salinities at Station 38H are not directly measured but are computed from the temperatures on the assumption that freezing equilibrium obtained. Water froze in the conductivity cell at this station. We believe the error in salinity due to temperature error is unlikely to exceed ±0.2 ‰ and the assumption of freezing equilibrium puts a lower limit on the salinity; it could be higher.

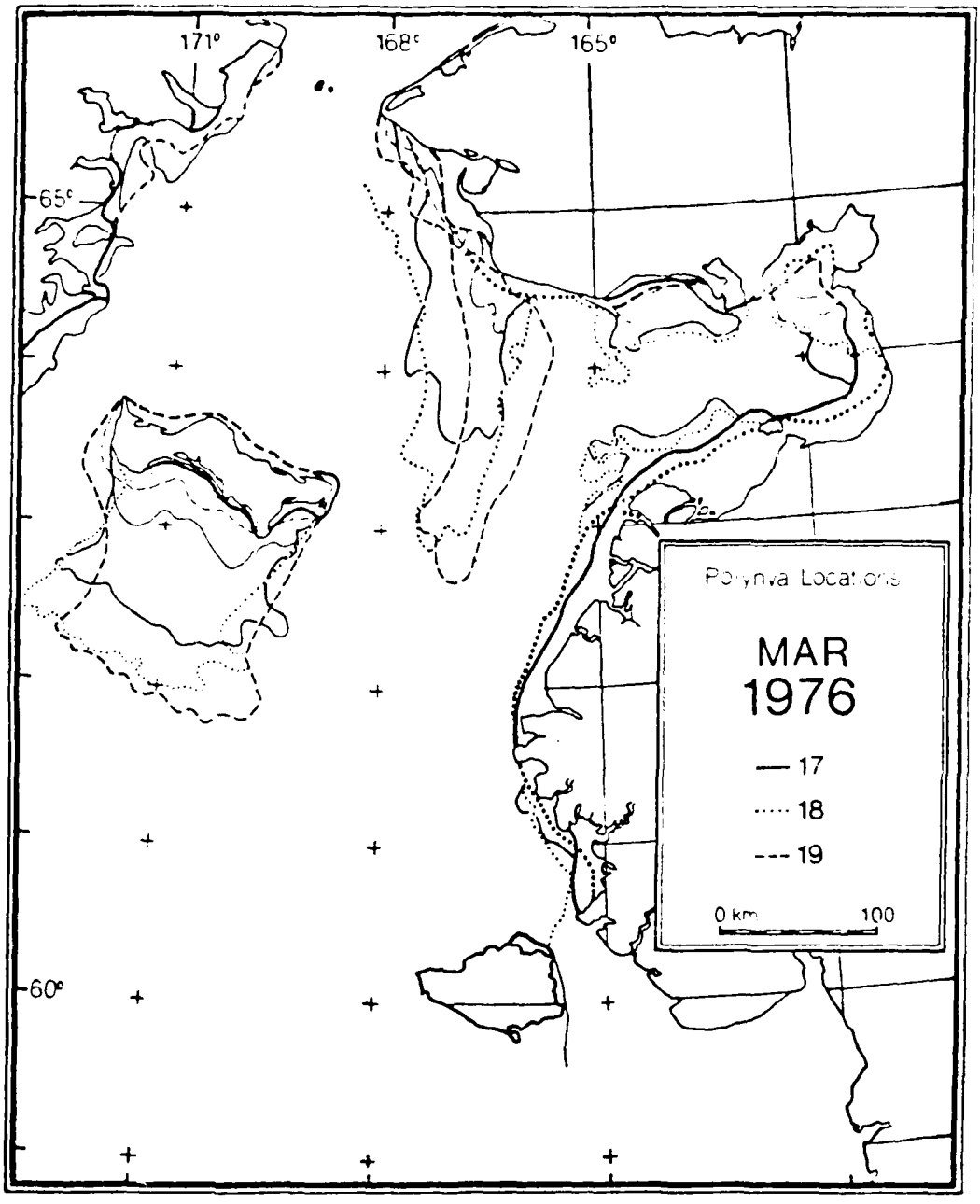

Fig. 14. Examples of two recurring polynyas, one south of Cape Prince of Wales, the other along the southern coast of St. Lawrence I. (from McNutt, 1981).

The other item of interest is the historical occurrences of salinities above 34 ‰. There are only two instances, in BURTON ISLAND 1951 in February near the present Station 55 and in GLACIER 1971 east of St. Lawrence I. in March. At no other times were salinities above 33.5 ‰ found. Because of the relative rarity of winter observations in the area of interest, this suggests only that salinities greater than 34 ‰ probably do not form every year.

Stations 58-61 have salinities between 32.9 and 33.1 ‰, distinctly less saline than the waters north or south of St. Lawrence I. This water is in the salinity range (< 33 ‰, > 32.75 ‰) that CAT (p. 72) describe as Anadyr Water. The extension through Anadyr Strait of water in the Anadyr Water salinity range suggests a possible northward movement of water through the strait, in agreement with CAT conclusions. If this movement does occur, it could only be reconciled with the general southward flow of ice by concluding that southern water moves northward along the bottom and northern water is carried southward in an upper layer. The flow might well be sporadic and convection could be expected to mix the water columns top-to-bottom, so there is no reason to expect the stratification due to the assumed flow to be evident. In actuality, only Station 60 is appreciably stratified, to the extent of 0.035 ‰, beginning at 34 m depth. However, in view of the few stations involved and the non-conservative nature of salinity under freezing conditions, the evidence for northward flow is inconclusive.

The waters south of St. Lawrence I. are typified by Stations 62-64 in Fig. 15. Station 63 is not notably stratified but Station 64 has a salinity 0.9 ‰ greater at the bottom. We believe the high bottom salinity at this station was generated in the shallow-water parts of the polynya usually extending southward from St. Lawrence I. and probably near the southeast point of the island (Fig. 14). The brine-enriched water would then flow westward and

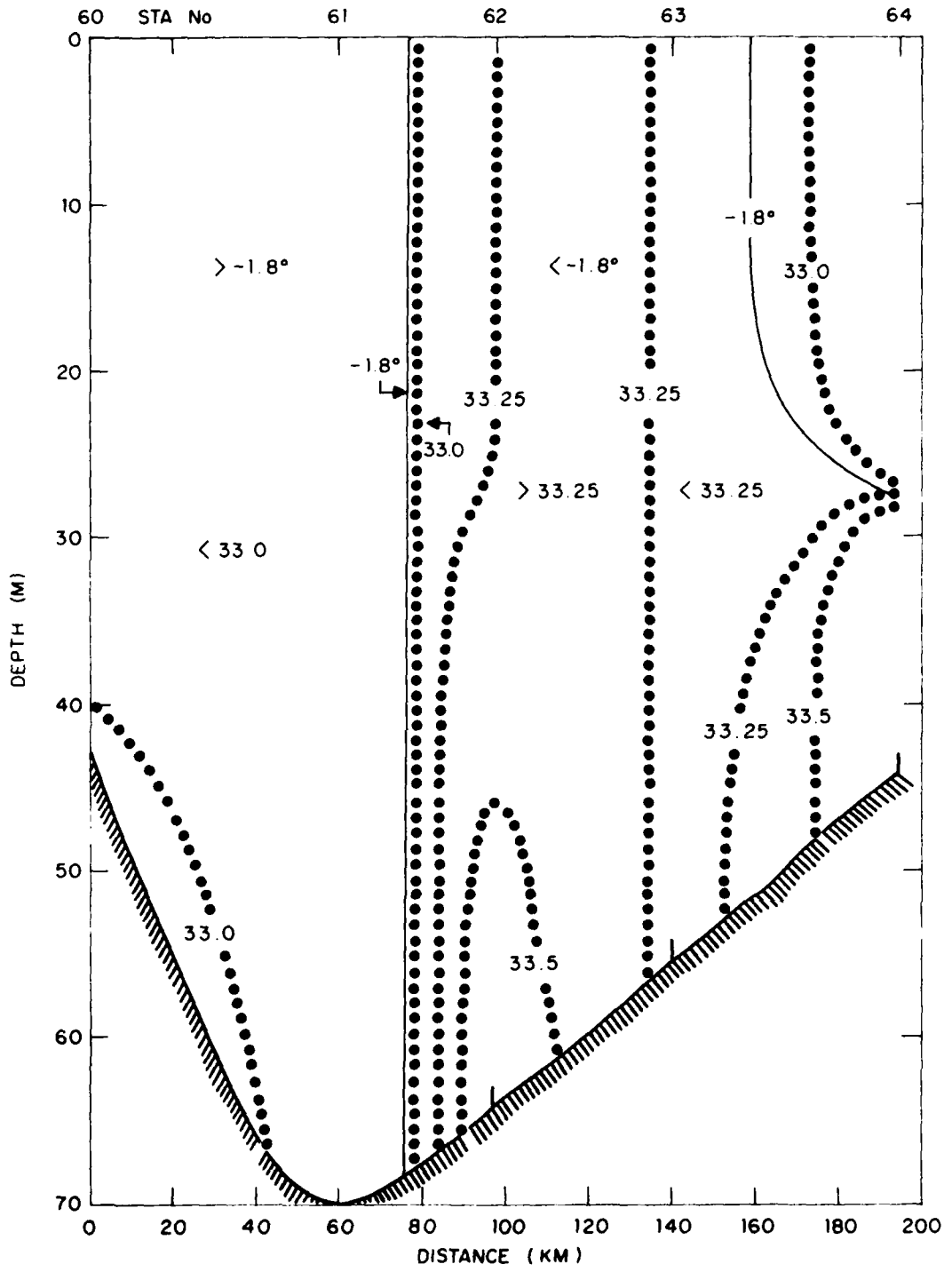

Fig. 15. Temperature and salinity cross-section from the line of stations (60-64) southwest of St. Lawrence I. The high bottom salinity at Station 64 probably flowed downslope from a shallower coastal brine-generating area.

downslope along the bottom to the approximate location of Station 64 to produc the two-layered condition observed.

9. RELATION OF TEMPERATURE TO THE FREEZING POINT

Much of the initial information of this section relating to the observed temperature-salinity correlation is taken in modified form from the earlier report of Newton and Anderson (1980). The correlation between temperature and salinity values for the surface and bottom waters is shown in Figs. 16 and 17. The near-surface temperature-salinity plot includes points from all stations within the ice (Stations 10-78 inclusive). From this list the bottom layer temperature-salinity plot also excludes stations near the ice edge obviously warmed by admixture of southern Bering Sea water. These additional exclusions are Stations 10 and 70-78 which were warmer than -1.5° C. Each plot includes the freezing point curve from Doherty and Kester (1974).

Near-surface temperatures within the ice ranged from -1.549° C (Station 26) to a minimum at Station 39H of -1.905° C. At the majority of the stations, near-surface temperatures were within 0.02° C of the freezing point line (Fig. 16). Stations with temperatures in excess of 0.02° C above the freezing point are identified on Fig. 16 and their geographic distribution is indicated in Fig. 18. Surface waters with temperatures notably above the freezing point appear to be concentrated in two areas: along the Alaskan coast of Norton Sound and near the ice edge.

Six stations along the Alaskan coast south of the Yukon delta had near-surface temperatures > 0.02° C above freezing. All of these stations were associated with the low-salinity (< 32.5 ‰) water along the coast (Fig. 8). The near-shore, lowest salinity surface waters tended to be somewhat more elevated above their respective freezing points than were near-surface water

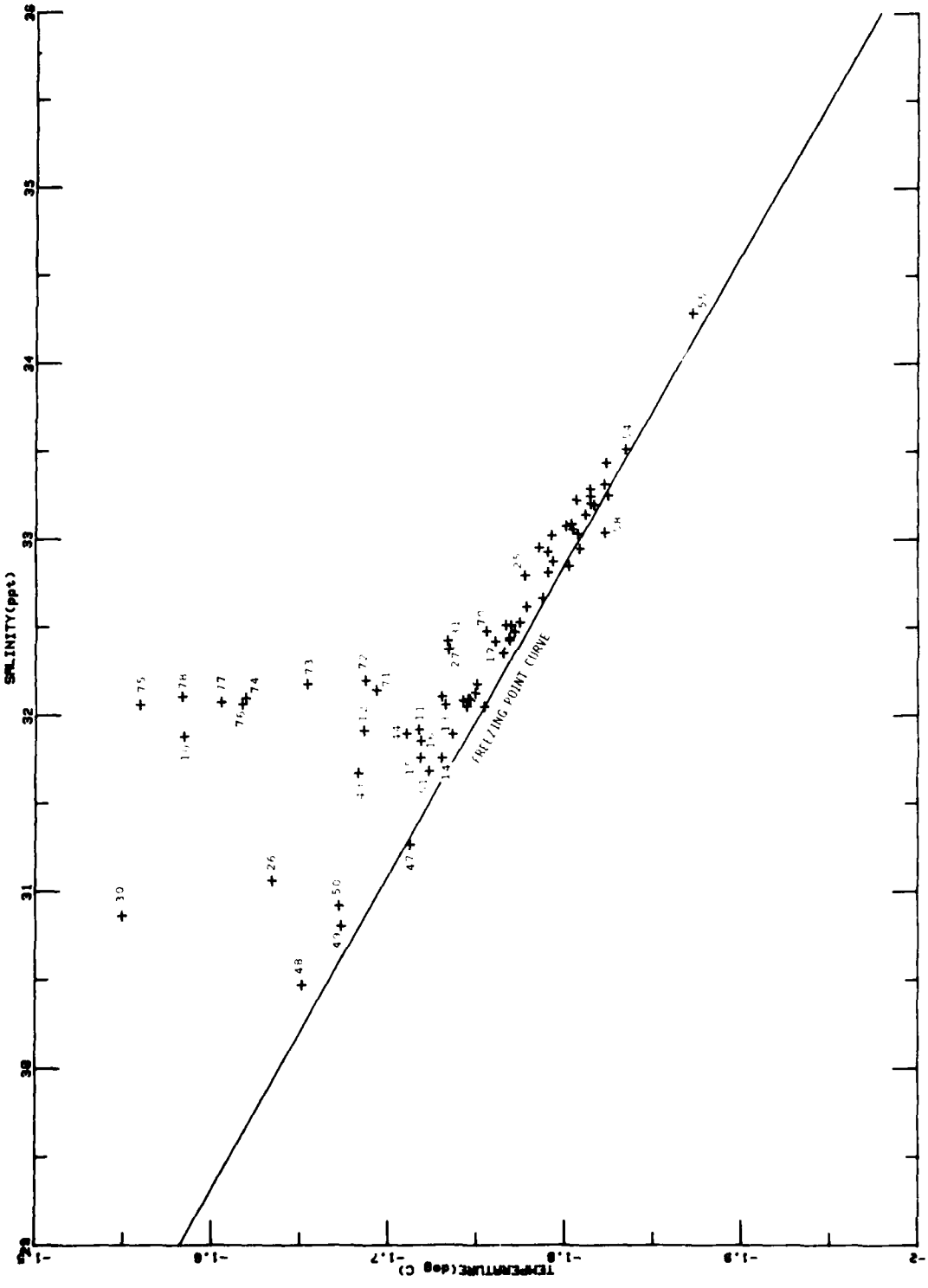

Fig. 16. Near-surface temperature-salinity pairs from all stations within the ice (Stations 10-78) plotted in relation to the Doherty and Kester (1974) freezing point curve.

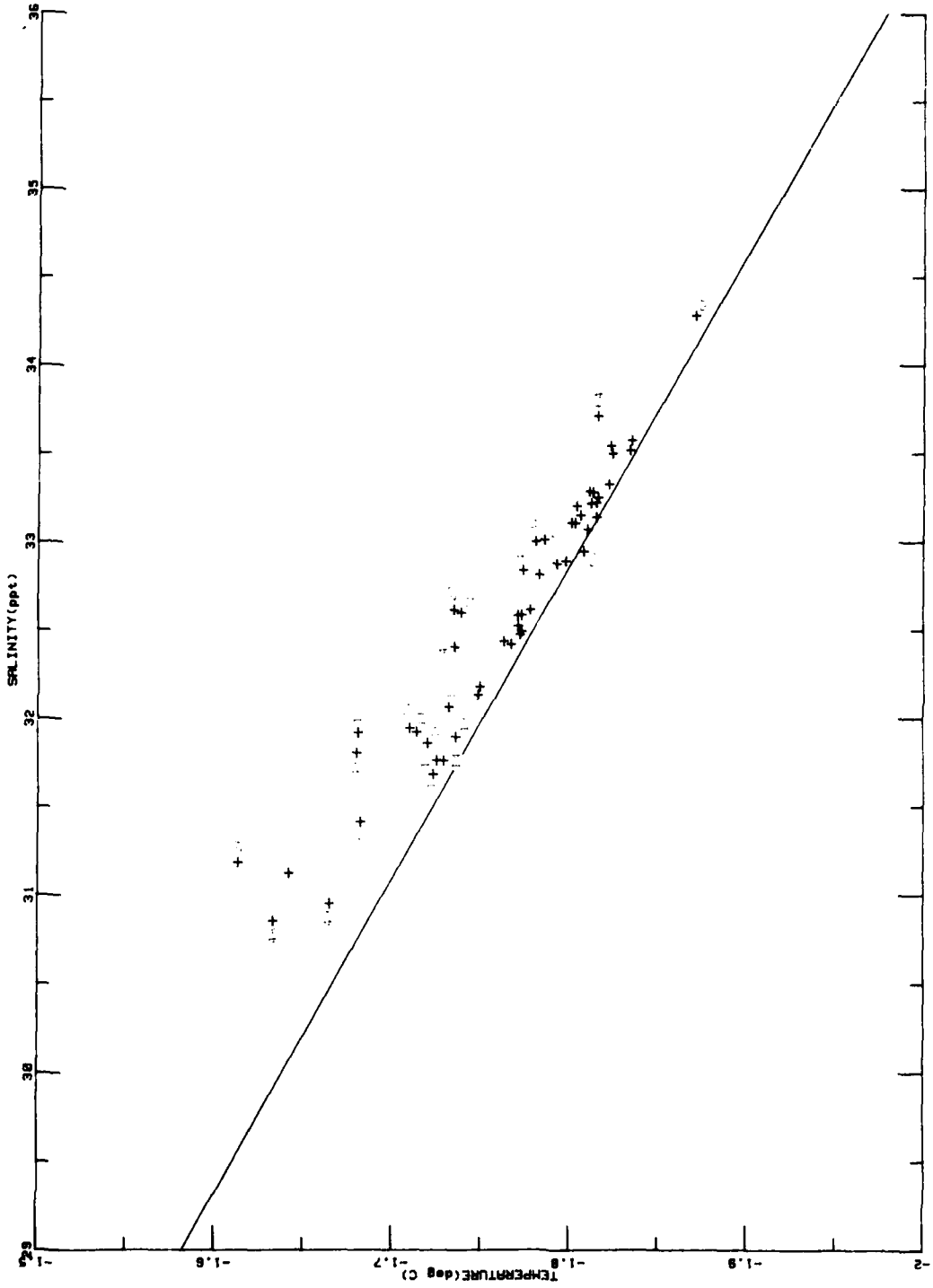

Fig. 17. Near-bottom temperature-salinity pairs for stations within the ice having temperatures colder than -1.5° C (Stations 11-69) plotted in relation to the Doherty and Kester (1974) freezing point curve.

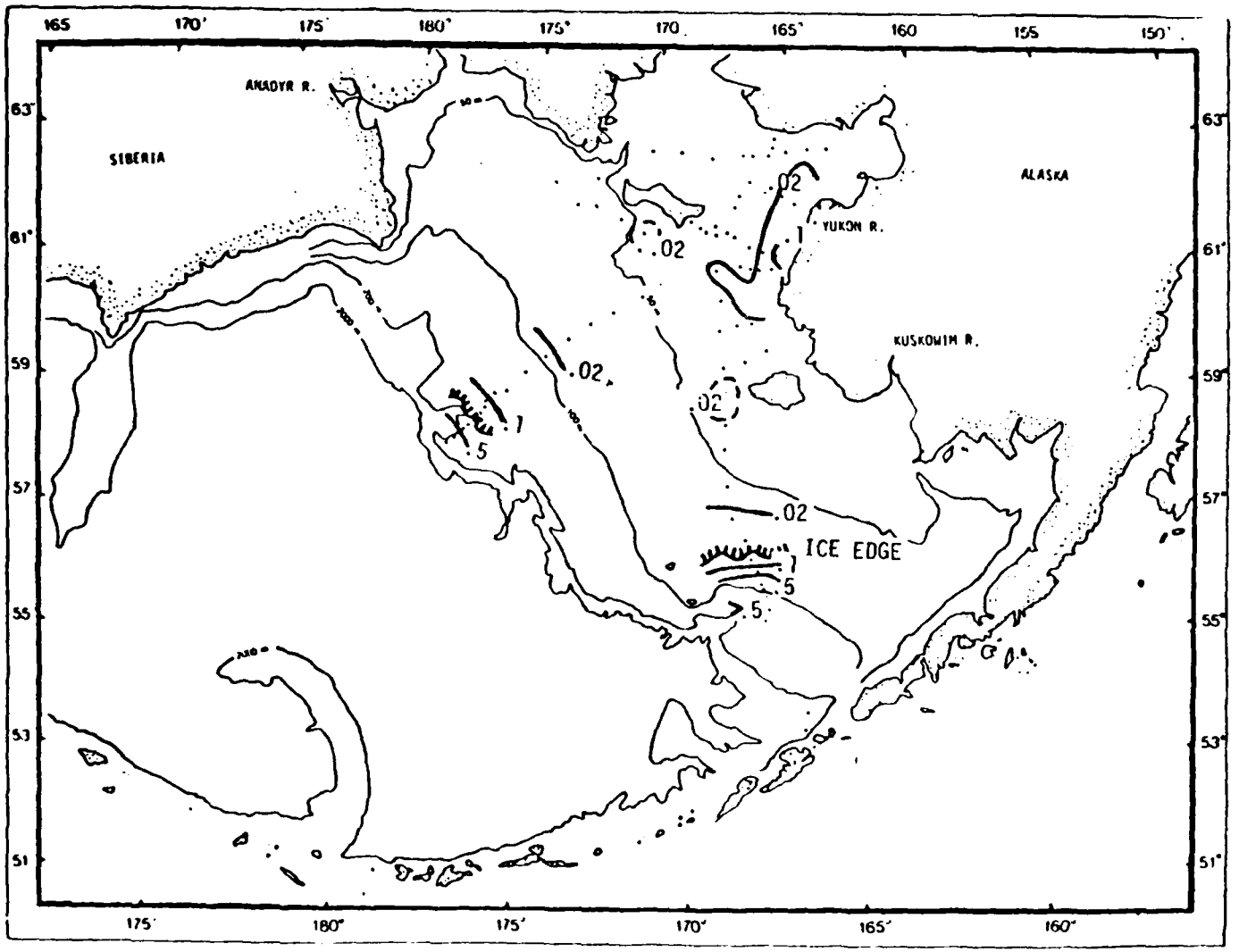

Fig. 18. Geographic distribution of near-surface temperatures which were ≤ 0.02° C above the freezing point (observed temperature minus freezing point). The freezing point was calculated from Doherty and Kester (1974) (from Newton and Anderson, 1980).

at adjacent stations located farther from shore with higher salinities. This can be seen in Fig. 16 by observing the temperature-salinity trends from Stations 30 to 31, 43 to 44 and 26 to 27 which in each case illustrate the temperature-salinity changes proceeding outward from the coast.

The second region with near-surface temperatures above the freezing point was located near the ice edge. For the eastern crossing of the ice edge (essentially at Station 10) near-surface temperatures were elevated above freezing for a distance of about 80 km into the ice pack (Stations 11 and 12). For the western crossing near-surface temperatures were elevated above freezing for nearly 200 km into the ice pack (Stations 70 through 78). The trend in temperature-salinity characteristics proceeding from the ice edge (Stations 10 and 78) into the pack ice (toward Stations 12 and 70) was one of decreasing temperature (although not always monotonic) with perhaps a slight increase in salinity.

Because of the warm, high salinity water which extended under the ice pack during the western crossing, near-bottom temperatures covered a significantly greater range than did the near-surface waters, -1.905° C to > 3.0° C. Stations with near-bottom temperatures > 0.02° C above the freezing point have been identified on Fig. 17 and their geographic distribution is indicated in Fig. 19. Near the ice edge the spatial extent of bottom waters with temperatures above freezing is similar to that of the surface waters although the magnitude of departure is greater in the lower layers because of the warm water extending under the ice to the 100 m contour. The region near the Yukon delta with above freezing near-bottom temperatures is extended to the north and covers those stations in Norton Sound. Here bottom temperatures were approximately 0.02° C warmer than surface values but 0.1 to 0.3 ‰ more saline. As was the case for the surface waters, there appears to be a general

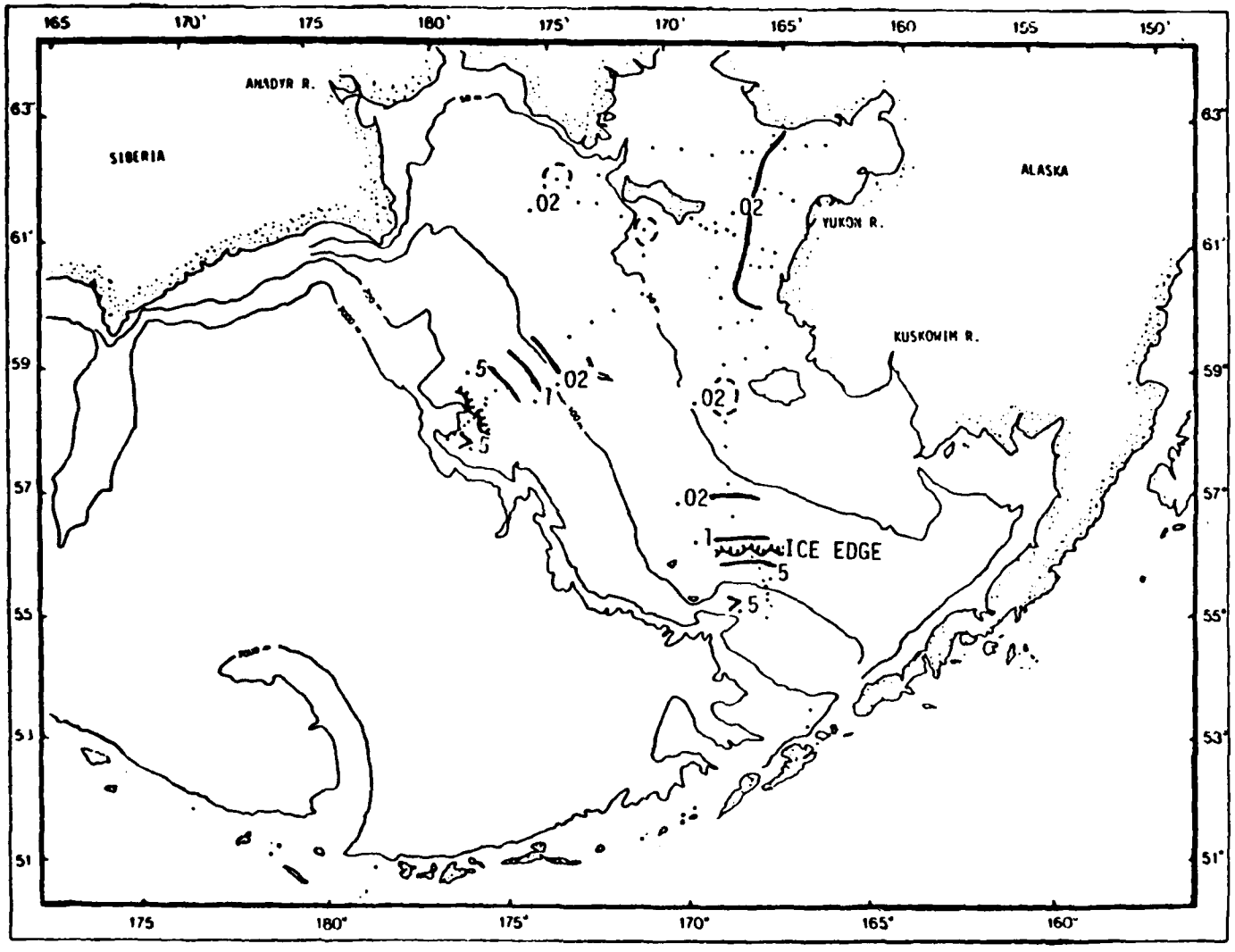

Fig. 19. Geographic distribution of near-bottom temperatures which were $\geq$ 0.02°C above the freezing point (observed temperature minus freezing point). The freezing point was calculated from Doherty and Kester (1974) (from Newton and Anderson, 1980).

tendency for the greatest temperature departures from freezing to be associated with the lower salinities.

The correlation of temperatures above freezing with the presence of admixed Yukon water is surprising because Yukon water, having flowed for thousands of miles in intimate contact with ice could be expected to be exceedingly close to 0° C or perhaps slightly colder, if it contained appreciable salts. The non-constancy of specific heat with salinity and temperature and the slight non-linearity of the Doherty and Kester (1974) equation are not great enough to cause apparent warming of more than about 0.002° C when mixing freezing fresh and saline waters. This result assumes the accuracy of the Cox and Smith (19[illegible] specific heats and extrapolates them below 0° C. There appear to be no measurements of specific heat below 35 ‰ in the minus temperature range. There is no alternative to the conclusion that the warmth must be due to the frequent baring of the water surface near the mouth of the river, a condition which also was observed during this cruise. There is then a large decrease in the albedo for incoming diffuse light as compared to ice-covered water, particularly if the ice has some snow cover. There is an opposite change in the back-radiated energy due to the relative warmth of a bare water surface, but the result is very sensitive to ice temperature. Without precise temperatures and a good estimate of incoming and net longwave radiation it is impossible to compute the energy exchange with sufficient precision. However, it would not be surprising to find warming preponderating over cooling in March when the ice-forming processes are nearly at a balance with melting.

Newton and Anderson's (1980) analysis shows surface temperatures averaging 0.010° C above the Doherty and Kester (1974) prediction at low salinities (< 32 ‰) and 0.008° C above at higher salinities. Bottom temperatures average, respectively, 0.002° and 0.001° C warmer than the above. To explore

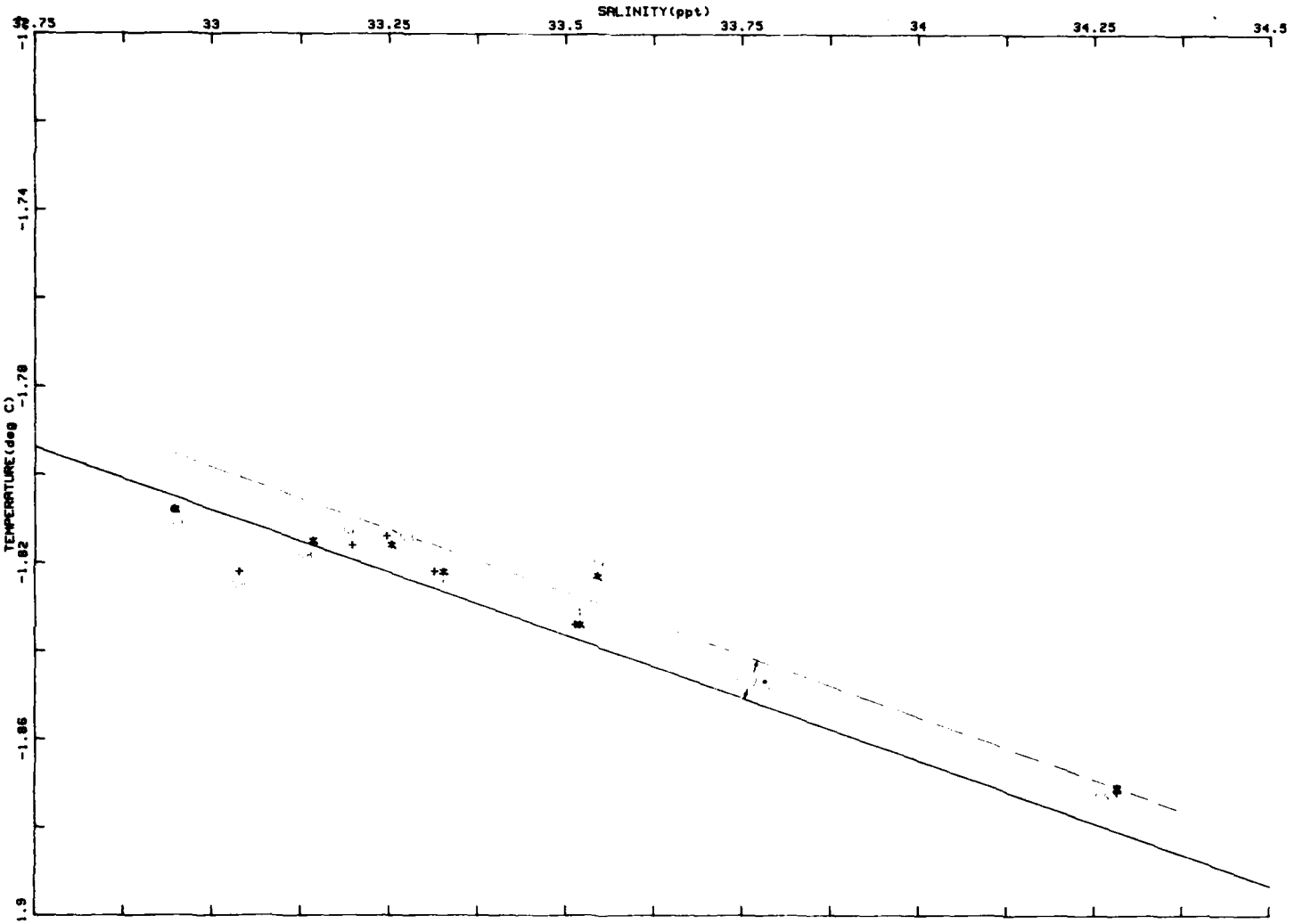

Fig. 20. A plot of near-surface (+) and near-bottom (*) temperature-salinity pairs from stations north of St. Lawrence I. (Stations 53-58) well-removed from the warming influence of either Bering Sea or Yukon River water. The freezing point curve is from Doherty and Kester (1974). The implication is that the CTD is reading about 0.01° C too high.

this trend further, temperature-salinity pairs from the portion of the cruise most isolated from either southern Bering Sea or Yukon River influence were plotted in Fig. 20. These also average above 0.01° C higher than the Doherty and Kester prediction. The logical conclusion from these results is that the CTD calibration is about 0.01° C too high, in opposition to the reversing thermometer comparisons which showed the CTD 0.009° C too low.

If the temperatures in all the data, Figs. 16 and 17, are decreased by 0.01° C, 24 points fall below the freezing-point line in the surface data and 17 fall below the line in the bottom data. There are no indications of supercooling greater than 0.02° C. In view of the unlikelihood of supercooling, as expressed by Lewis and Lake (1971), we prefer not to suggest that supercooling was even as great as 0.01° C until we know a great deal more about the stability and accuracy of the NBIS CTD.

10. REFERENCES

Becker, P., Light aircraft deployable CTD system, Proc. Third S/T/D Conference and Workshop, Plessey Environmental Systems, San Diego, 1975.

Bloom, G.L., Water transport and temperature measurements in the eastern Bering Strait 1953-1958, J. Geophys. Res., 69, 3335-3354, 1964.

Coachman, L.K., and K. Aagaard, Reevaluation of water transports in the vicinity of Bering Strait, in: The Eastern Bering Sea Shelf: Oceanography and Resources, D.W. Hood and J.A. Calder, Eds., U.S. Gov. Print. Office, Wash., D.C., 1980.

Coachman, L.K., K. Aagaard, and R.B. Tripp, Bering Strait: The regional physical oceanography, Univ. of Washington Press, Seattle, 1975.

Cox, R.A., and N.D. Smith, The specific heat of sea water, Proc. Roy. Soc., A, 252, 51-62, 1959.

Doherty, B.T. and D.R. Kester, Freezing point of seawater, J. Mar. Res., 32, 285-300, 1974.

Hughes, F.W., L.K. Coachman, and K. Aagaard, Circulation, transport, and water exchange in the western Bering Sea, in: Oceanography of the Bering Sea, Hood, D.W. and E.J. Kelley (eds.), Institute of Marine Science, University of Alaska, 1974.

Lewis, E.L., and R.A. Lake, Sea ice and supercooled water, J. Geophys. Res., 76(24), 5836-5841, 1971.

Lohrmann, W.R., Winter and spring oceanographic conditions in and under the ice of the Bering Sea, Tech. Rept. NPS 68-79-001, Naval Postgraduate School, Monterey, 1979.

Maykut, G.A., Energy exchange over young sea ice in the central Arctic, AIDJEX Bulletin No. 31, 45-74, 1976.

McNutt, Lyn, Ice conditions in the eastern Bering Sea from NOAA and LANDSAT imagery: winter conditions 1974, 1976, 1977, 1979, NOAA Tech. Memo. ERL PMEL-24, 1981.

Muench, R.D. and K. Ahlnäs, Ice movement and distribution in the Bering Sea from March to June 1974, J. Geophys. Res., 81(24), 4467-4481, 1976.

Newton, J.L., and B.G. Anderson, MIZPAC 80A; USCGC POLAR STAR (WAGB-10) Arctic west operations, March 1980: Bering Sea, SAI202-80-460-LJ, Science Applications, Inc., La Jolla, 1980.

Paquette, R.G., and R.H. Bourke, The oceanographic cruise of the USCGC GLACIER to the marginal sea-ice zone of the Chukchi Sea--MIZPAC 78, Tech. Rept. NPS 68-79-003, Naval Postgraduate School, Monterey, 1979.

Pease, C.H., Eastern Bering Sea ice processes, Mon. Wea. Rev., 108, 2015-2023, 1980.

Potocsky, G.J., Alaskan area 15- and 30-day ice forecasting guide, Nav. Oceanog. Office Spec. Pub. No. 263, U.S. Govt. Print. Off., 1975.

Stommel, H. and G. Veronis, Barotropic response to cooling, J. Geophys. Res., 85, (C11), 6661-6666, 1980.

Sverdrup, H.U., M.W. Johnson, and R.H. Fleming, The Oceans, Prentice-Hall, Englewood Cliffs, 1942.

U.S. Geological Survey, Water discharge records for Alaska, Water Resources Div., Anchorage, 1980 (ser.).

APPENDIX A

INSTRUMENTATION AND METHODS

Two CTD's were used during the cruise. Generally used from shipboard was a Neil Brown Instrument Systems (NBIS) Mark III CTD with a Beckman oxygen cell. The conductivity cell was the standard 3 cm in legnth, the system was provided with a rapid-response thermometer stabilized by a platinum resistance thermometer and the pressure sensor had a range of 320 dbar. The digital data stream was read into a Hewlett-Packard 9835-B computer, which is fast enough to store about 15 complete binary data records (C,T,D, and O_2) per second and has enough memory to hold about 3500 such records. The rate of data acceptance was slowed to about 12 per second which was amply fast for the present purpose, although it was only about 40% as fast as the NBIS system produces data. To conserve cassette storage space the computer was programmed also to operate with 1750 or 875 memory records in shallow water. Typically, 875 records sufficed to reach bottom at depths of about 60 m, deeper than most of the shelf, and 3500 records sufficed to reach 300 m. Usually, the upward traverse of the instrument was recorded as well as the downward traverse, a practice which is highly useful in revealing instrument artifacts.

The system was programmed to plot the data on a 28 × 38 cm digital flatbed plotter, Hewlett-Packard Model 9872A. Plot scaling could easily be changed to accommodate different depths and to expand scales when desired. The data were stored in their original binary form on the cassette, which is part of the computer. They were eventually transferred to 9-track tape, corrected, edited and replotted by techniques already developed during previous work (see, for example, Paquette and Bourke, 1979).

The CTD was standardized by means of a Nansen bottle and reversing thermometers on the wire 6 m above the sensors. Twenty-one comparisons were made leading to an average temperature error of -0.0088° C with standard deviation 0.014° and an average salinity error of 0.0029 ‰ with standard deviation 0.013 ‰. Since the standard deviations were greater than the errors, no corrections were applied.

Operating a CTD in ice under freezing conditions presents several problems. The first is to find or make a hole in the ice. Sometimes leads could be used. More commonly, the ship would swing in an arc and then back or drift away from the ice ahead into the widened channel made by the swinging ship. This method was successful where the ice was thin and not under pressure, which was about two-thirds of the time. In heavier ice, the ship might have to maneuver considerably to widen the channel. Then, the floating ice was thick enough to present considerable hazard to the CTD. In thick, close-packed ice, neither technique worked and it was necessary to wait for a lead to appear along the route or stop and drop the portable CTD (to be described later) into the broken channel astern or through a drilled hole.

Backing of the ship undoubtedly increased the likelihood that a somewhat stirred water column would be encountered in the upper 10 m during the CTD lowering, particularly since it was seldom possible to wait more than 5 to 10 minutes for the disturbed water to drift away. Little difficulty was evident because of this problem, possibly because there was little structure under the ice sheet to be disturbed. More difficulty was caused by heat and effluents from the ship, as will be discussed below.

There was usually slush, brash ice and blocks of various sizes and concentrations alongside the ship. Quick action often was required to get the instrument down and back without excessive hazard. It was fortunate that the

water was shallow. Deep, time-consuming lowerings would have been impossible much of the time without the use of a protective ice shield. The so-called "Northwind donut" was available but clumsy and time-consuming in application. After one initial test of its operation, further usage was abandoned.

The ice was a hazard to the delicate sensors. Also, the electrical connector at the top of the pressure case was close enough to the shackle to be broken off by a kink at that point. The connector was also vulnerable to the ice. The sensor pod was close to the bottom of the instrument and, since it was desired to lower to bottom, extra length had to be added to the instrument guard frame. The way in which these problems were overcome is shown in Fig. 21. The guard frame was covered with stout wire mesh and the sensor pod was covered additionally with plastic mesh. A clamp-on steel guard protected the connector. The protective mesh undoubtedly slowed response a little and must have had some tendency to smooth microstructure. However, we believe it was essential. In spite of all this protection, the conductivity cell was sometimes plugged by fine slush, a condition yielding low or zero salinity readings in the NBIS instrument.

A problem due to cold air began to develop after the air temperature dropped below -1.8° C after Station 9. The underwater unit, if left on deck in the cold, would freeze water in the conductivity cell and in the port of the pressure transducer when lowered into the water. The seawater, being at the freezing point, would not melt out the ice thereafter. The remedy was to bring the instrument back to deck level, warm it with warm salt water from a hose and immediately lower it again into the water. We soon took to keeping the instrument in the quartermaster's shelter near the "hydro" platform with a small electric heater and then limiting its time in the cold air to a minimum. Later in the cruise, near Station 40, the air temperature

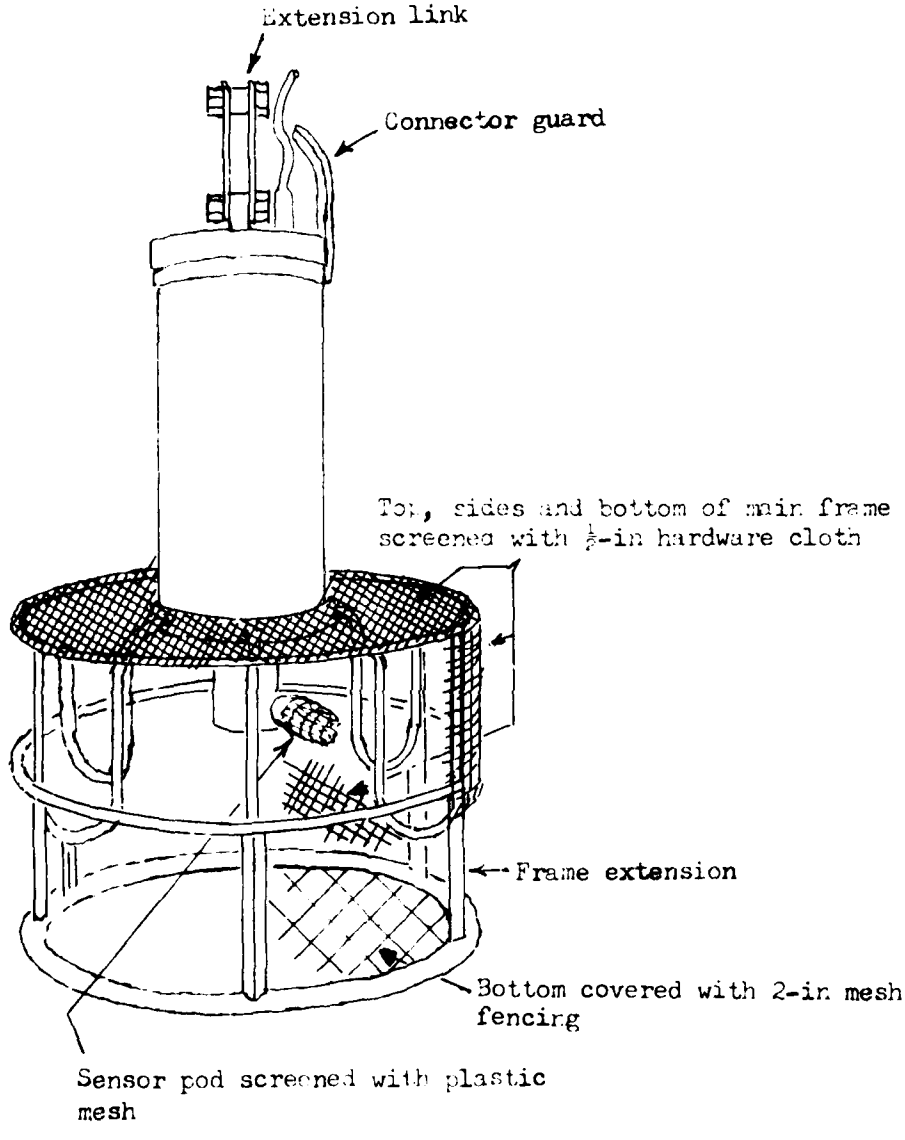

Fig. 21. Sketch of NBIS CTD showing modifications to protect it from ice damage.

dropped below -5° C and then below -15° C. Under these conditions it was hard to keep the instrument warm and the heater was moved closer and closer to the sensors. In the vicinity of Station 66-1 the sensors were being warmed to 30° C and in this location an anomaly in the salinity was observed, apparently due to the heating. This anomaly will be described later. Beginning with Station 67, we were careful to soak the instrument and move it up and down in the water until any initial temperature anomaly had disappeared.

The CTD supplied by the University of Washington Applied Physics Laboratory (APL) (Becker, 1975), being an admirably portable instrument, was used primarily from helicopters, which took a number of the stations to either side of the central ship's track. This instrument also had a tendency to freeze ice in the conductivity cell and the principal remedy was the same as with the other CTD: keep it warm.

A number of comparisons with the NBIS CTD were made and a deviation of temperature from the true temperature was found, essentially linear with the length of cable immersed in the water. The cause was eventually traced to a poor ground connection. Sufficient calibration data were obtained to correct the earlier results satisfactorily. Intercomparison with the NBIS CTD was possible at 8 stations, both near surface and near bottom. The APL CTD was determined to have a mean temperature difference 0.005° C less than the NBIS CTD reading and a mean salinity difference 0.014 ‰ greater (Newton and Anderson, 1980).

The APL CTD also records on a magnetic tape cassette. The data were plotted aboard and later transferred to nine-track tape by APL. After this, they were handled by the same library of computer programs as had been used for earlier data.

Editing of the data from both CTD's was less difficult than usual because there were few temperature transients capable of generating a salinity spike.

There were the usual number of noise spikes on the APL CTD and a few on the NBIS CTD. The latter were formed by more than one data point, were always in salinity and negative-going, which leads us to believe that they were due to slush dislodged from the mesh cage, producing a partial temporary blockage of the conductivity cell. Both systems required the removal of useless sections of record at the top and bottom of a record where the CTD was stopped; both required treatment by the RACHET routine to remove inversions in depth caused by the ship's roll when in open water.

As previously mentioned, the NBIS instrument had an interesting salinity anomaly of small magnitude, apparently due to stored heat in the instrument. In extreme cases it caused the apparent salinity to be several hundredths of a p.p.t. too low, as compared with the up trace, which was more nearly isohaline under ice. The temperature, at the same time, would be either slightly too low or essentially the same as on the up trace. The most severe manifestation of the phenomenon occurred at Station 66-2 where the sensors were warmest, about 30° C. The salinity and temperature profiles from this station are shown, highly expanded, in Fig 22. The salinity is evidently 0.07 ‰ too low at the beginning of the lowering and the anomaly decreases with either time or distance of travel through the water. In terms of an exponential decay, the time constant is about 30 sec. The down-cast temperature at the same time is too high, but by only one-fifth as much as is necessary to cause the salinity anomaly, if we exclude the uncertain zone shallower than 15 m which is contaminated by ship's effluent. In other cases the salinity anomaly decreases linearly rather than exponentially with depth and the temperature may have little or no anomaly. We have no good explanation which satisfies all the symptoms. Where the effect is notable, we have chosen the up trace rather than the down trace during editing.

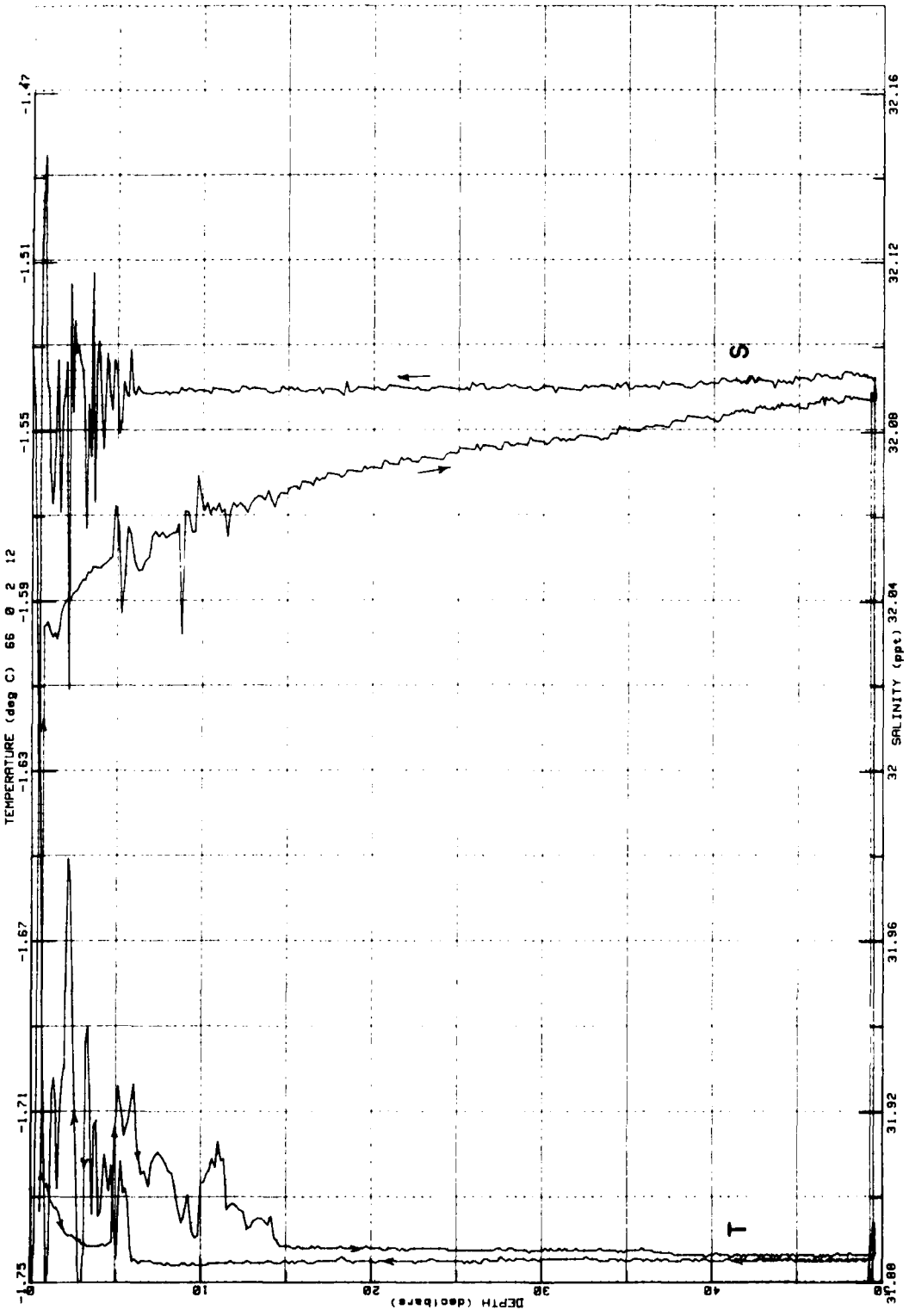

Fig. 22. Temperature and salinity profiles from Station 66-2 showing the salinity error of the downtrace apparently due to excessive pre-warming of the instrument and failure to bring it to equilibrium prior to lowering.

Perturbations will be noted in many of the profiles in the upper 5 to 15 m of the water column. These were due to effluents from the ship. The perturbations were usually less marked on the up trace, possibly because of the diminution of turbulence remaining from the motion of the ship and screws and the tendency of warm effluents to rise in the absence of stirring. In the majority of cases we elected to use the up trace rather than the down trace because the former was notably less disturbed.

The NBIS CTD was provided with a Beckman oxygen cell, but it was not possible to standardize it against Nansen bottle samples. If the conventional conversion equation and constants are used, the results are unreasonable. Some progress has been made in the ad hoc adjustment of constants, basically trying to make the down and up traces match and yield a maximum of 100% saturation at the surface. We have too little confidence in the results to report them at this time.

Artifacts and errors such as those described in the paragraphs above could be found because brine-convected water columns are excellent test baths with nearly constant properties. Measurement under these conditions, combined with the comparison of up and down traces has revealed effects which would never be clearly characterized or even found in other, more variable waters.

APPENDIX B

EXPLANATION OF HEADING CODES

The heading of the printed output uses the coding and format from NODC Publication M-2, August 1964, with a few exceptions. Heading entries which are not self-explanatory are as follows: MSQ is the Marsden Square, and DPTH is the water depth in meters. Wave source direction is in tens of degrees, but the direction 99 indicates no observation. The significant wave height is coded by Table 10 (Code $\div$ 2 $\simeq$ height in meters) and the wave period is coded by Table 11 (Code $\div$ 2 $\simeq$ period in sec); in each case X indicates no observation. Wind speed, V, is coded as Beaufort force, Table 17. The barometer is in millibars, less 1000 if more than 3 digits; wet and dry bulb temperature in degrees C. The present weather is from Table 21 with cloud type and amount from Tables 25 and 26, respectively. The combination 4 X9 indicates that clouds cannot be observed usually because of fog conditions. The visibility is from Table 27 which is roughly in powers of two with Code 4 = 1-2 km. The ice concentration, ICE, is in tenths; amounts less than 1 tenth are preceded by a minus sign and indicate concentrations in powers of ten, e.g., 10^{-4} = -4.

The entry, NAV, is a code to identify the accuracy of each station position based upon the navigation system used. Code 1 indicates a position determined by visual sightings, radar or by navigation satellite; Code 2 a position determined by Omega or Loran; and Code 3 a position determined by dead reckoning.

The heading data are listed sequentially with increasing station number. Those stations taken from a helicopter are followed with an H, e.g., Station 26H. Shipboard stations taken with the APL-UW CTD are followed by a W, e.g., Station 33W. Several lowerings over a period of four days were made at Station 66; these are numerically sequentially coded, e.g., Station 66-1.

MIZPAC 80 CTD STATIONS

NAT	SHIP	LAT	LONG	MSQ	MO	DY	YR	HR	STA	DPTH	NAV	ICE	WVD	HT	WND	V	BAR	DRY	WET	WTHR	CL	AMT	VIS
31	PS	54-20.0	166-17.0	197	02	29	80	00.3	001	774	1	0	13	2	13	6	999	3.0	2.9	1	7	8	7
31	PS	54-36.0	166-12.0	197	02	29	80	02.6	002	401	2	0	12	3	12	5	002	4.3	3.2	5	7	8	7
31	PS	56-15.0	167-16.0	197	02	29	80	12.5	003	118	2	0	13	5	13	8	003	2.5	1.9	1	6	7	7
31	PS	56-23.5	167-08.0	197	02	29	80	15.0	004	112	2	0	18	5	16	5	004	2.9	2.1	2	6	8	7
31	PS	56-30.0	167-12.0	197	02	29	80	16.5	005	105	2	0	18	3	12	5	006	2.1	1.8	2	7	8	7
31	PS	56-37.0	167-14.0	197	02	29	80	17.3	006	93	2	0	18	3	15	6	006	2.1	1.7	2	6	8	7
31	PS	56-47.5	167-20.0	197	02	29	80	18.8	007	88	2	0	14	3	14	4	007	2.1	1.9	2	7	8	7
31	PS	56-50.0	167-23.0	197	03	01	80	00.9	008	82	2	0	13	2	13	4	007	1.0	0.1	2	3	7	7
31	PS	57-00.8	167-30.4	197	03	01	80	02.5	009	76	2	-4	16	3	12	5	006	0.	0.	2	3	8	7
31	PS	57-14.5	167-39.7	197	03	01	80	06.4	010	74	2	9			09	5		0.9	-1.2	1	6	8	7
31	PS	57-35.7	167-55.0	197	03	01	80	11.7	011	70	2	9			07	5	000	-1.9	-2.1	3	7	8	7
31	PS	57-57.0	168-10.0	197	03	01	80	20.6	012	69	2	10			07	8	995	-2.2	-3.8	3	7	8	7
31	PS	58-30.0	168-16.0	197	03	03	80	04.0	013	57	2	10			03	6	993	-1.2	-1.1	3	7	8	5
31	PS	59-05.0	168-08.0	197	03	03	80	18.5	014	41	2	10			04	4	986	0.8	0.8	3	6	8	3
31	PS	59-36.0	168-10.0	197	03	03	80	23.8	015	39	2	8			10	7	991	1.1	0.6	2	7	8	7
31	PS	59-52.1	168-16.5	197	03	04	80	04.1	016	37	2	1						0.	0.				
31	PS	60-03.3	168-12.8	233	03	04	80	05.4	017	33	2	5			11	5	992	0.0	0.6	7	7	8	7
31	PS	60-34.0	168-09.0	233	03	04	80	09.0	018	31	2	9						0.	0.				
31	PS	60-41.5	167-28.0	233	03	04	80	16.0	019	23	2	3			11	5	994	0.0	0.5	7	7	8	1
31	PS	60-49.0	166-48.0	233	03	04	80	19.4	020	22	2	9			13	5	992	0.5	-1.5	7	7	7	6

MIZPAC 80 C.D STATIONS

NAT	SHIP	LAT	LONG	MSQ	MO	DY	YR	HR	STA		DPTH	NAV	ICE	WVD	HT	WND	V	BAR	DRY	WET	WTHR	CL	AMT	VIS
31	PS	61-18.0	167-07.0	233	03	04	80	23.2	021		23	2	9			12	6	993	2.1	1.8	7	7	8	7
31	PS	61-16.0	167-36.0	233	03	05	80	01.3	022		25	2	8						1.9	0.				
31	PS	61-10.0	168-08.0	233	03	05	80	03.5	023		30	2	10			25	3	993	0.3	0.1	1	7	8	7
31	PS	61-43.0	168-04.0	233	03	05	80	08.9	024		29	2	10			12	4	995	-1.2	-1.5	1	7	8	6
31	PS	62-09.7	168-09.0	233	03	05	80	15.6	025		22	2	9			10	4	002	0.2	0.0	2	7	8	7
31	PS	62-09.0	166-16.0	233	03	05	80	19.7	026	H	10	2	0						0.	0.				
31	PS	62-12.0	166-39.0	233	03	05	80	20.0	027	H	17	2	0						0.	0.				
31	PS	62-14.5	166-59.5	233	03	05	80	20.2	028	H	34	2	0						0.	0.				
31	PS	62-19.2	167-22.0	233	03	05	80	20.4	029	H	29	2	9						0.	0.				
31	PS	62-26.0	166-02.0	233	03	06	80	01.8	030	H	15	2	0						0.	0.				
31	PS	62-30.0	166-36.0	233	03	06	80	02.0	031	H	14	1							0.	0.				
31	PS	62-40.0	167-00.0	233	03	06	80	13.1	032		30	2	10			10	4	009	-1.5	-1.5	2	7	8	6
31	PS	62-44.0	167-30.0	233	03	06	80	23.7	033	W	31	2	10			09	4	006	-1.0	-1.8	1	0	2	7
31	PS	62-52.0	167-47.0	233	03	07	80	18.9	034		26	2	10			11	3	998	0.9	-1.2	7	5	8	4
31	PS	62-52.0	168-05.0	233	03	08	80	05.6	035		33	2	10			08	2	998	-1.0	-1.3	7	7	8	6
31	PS	62-53.0	168-03.0	233	03	08	80	17.2	036		30	2	10						0.	0.	7	7	8	5
31	PS	62-55.7	168-24.0	233	03	09	80	01.8	037	H	41	2							0.	0.				
31	PS	63-03.5	169-05.0	233	03	09	80	02.4	038	H	26	2							0.	0.				
31	PS	62-59.0	168-44.0	233	03	09	80	02.6	039	H	38	2							0.	0.				
31	PS	62-55.0	168-14.0	233	03	09	80	09.5	040		38	2	9			36	3	006	-14.8	-13.9	3	7	8	5

MIZPAC 80 CTD STATIONS

NAT	SHIP	LAT	LONG	MSQ	MO	DY	YR	HR	STA		DPTH	NAV	ICE	WVD	HT	WND	V	BAR	DRY	WET	WTHR	CL	AMT	VIS
31	PS	63-16.0	167-28.0	233	03	10	80	07.2	041		35	2	9			33	4	007	-16.0	-16.5	1	7	4	7
31	PS	63-27.0	167-11.0	233	03	10	80	21.6	042		26	2	10			32	4	011	-19.0	-19.0	1	3	1	7
31	PS	63-17.0	165-23.9	233	03	11	80	01.4	043	H	19	2							0.	0.				
31	PS	63-24.7	165-40.3	233	03	11	80	01.6	044	H	23	2							0.	0.				
31	PS	63-32.9	166-15.5	233	03	11	80	01.9	045	H	26	2							0.	0.				
31	PS	63-43.8	166-56.2	233	03	11	80	02.3	046	H	32	2							0.	0.				
31	PS	64-05.0	166-00.0	233	03	11	80	18.2	047		21	2	9			03	4	014	-14.9	-15.1	1	7	4	9
31	PS	64-08.2	163-47.5	233	03	11	80	20.8	048	H	22	2							0.	0.				
31	PS	64-06.8	164-36.7	233	03	11	80	21.1	049	H	19	2							0.	0.				
31	PS	64-07.2	165-18.8	233	03	11	80	21.4	050	H	18	2							0.	0.				
31	PS	64-14.5	165-55.0	233	03	11	80	22.3	051		20	1	9			32	5	017	-15.0	-16.0	1	4	2	9
31	PS	64-24.0	165-50.0	233	03	12	80	07.7	052		25	2	8						0.	0.	1	4	2	7
31	PS	64-04.0	166-31.0	233	03	14	80	11.2	053		29	2	10			09	3	024	-19.2	-20.4	0		0	7
31	PS	64-06.5	166-59.0	233	03	15	80	03.7	054		32	2	9			09	1	018	-17.2	-17.8	0		0	7
31	PS	64-05.0	168-07.0	233	03	15	80	18.8	055		38	2	10			30	2	016	-23.0	-25.0	0		0	7
31	PS	64-16.0	169-17.0	233	03	19	80	07.0	056		37	2	10			03	5	999	-6.0	-6.2	7	4	8	6
31	PS	64-17.0	170-30.0	234	03	20	80	04.5	057		33	2	10			02	5	999	-6.9	-7.1	7	7	8	5
31	PS	64-03.0	172-06.0	234	03	20	80	17.3	058		50	2	1			33	5	989	-6.5	-6.0	3	7	8	5
31	PS	63-49.0	172-46.0	234	03	20	80	20.2	059		37	2	1			03	9	988	-5.2	-5.0	3	7	8	6
31	PS	63-45.0	174-15.0	234	03	20	80	23.7	060		42	2	10			04	6	987	-3.2	-3.0	2	4	7	7

MIZPAC 80 CTD STATIONS

NAT	SHIP	LAT	LONG	MSQ	MO	DY	YR	HR	STA		DPTH	NAV	ICE	WVD	HT	WND	V	BAR	DRY	WET	WTHR	CL	AMT	VIS
31	PS	63-22.0	173-24.0	234	03	21	80	02.5	061		70	2	10			06	0	983	-9.6	-10.0	3	4	8	6
31	PS	63-19.0	172-40.0	234	03	21	80	07.2	062		64	2	9			03	8	977	-2.2	-2.2	3	5	8	5
31	PS	63-08.0	171-54.0	234	03	21	80	10.1	063		55	2	10			06	5	976	0.0	0.2	7	7	8	4
31	PS	62-52.0	171-00.0	234	03	21	80	13.5	064		43	2	8			07	5	976	0.6	0.0	7	7	8	4
31	PS	62-25.0	171-00.0	234	03	21	80	17.7	065		42	2	8			14	4	978	0.0	0.6	7	7	8	4
31	PS	61-52.0	171-01.0	234	03	24	80	15.7	066	1	52	2	8			06	5	996	-3.3	-3.9	7	5	8	3
31	PS	61-52.0	171-08.0	234	03	25	80	07.8	066	2	52	3	7			07	5	990	-1.4	-2.0	7	6	8	7
31	PS	61-52.0	171-12.0	234	03	25	80	08.2	066	3	52	3	9						0.	0.				
31	PS	61-52.0	171-24.0	234	03	26	80	03.0	066	4W	54	3	9						0.	0.				
31	PS	61-52.0	171-41.0	234	03	27	80	03.0	066	5W	54	3	9						0.	0.				
31	PS	61-36.0	172-08.0	234	03	28	80	19.3	067	W	61	2	10						0.	0.				
31	PS	61-19.0	172-52.0	234	03	29	80	23.3	068		68	2	10			04	6	996	-7.2	-7.8	1	6	6	7
31	PS	61-01.0	173-40.0	234	03	30	80	20.0	069		68	2	10						0.	0.				
31	PS	60-42.0	174-25.0	234	03	31	80	11.2	070		90	2	8			34	5	996	-8.8	-9.0	7	7	8	4
31	PS	60-24.0	175-08.0	234	03	31	80	21.2	071		109	2	7			01	5	998	-7.2	-7.0	7	7	8	4
31	PS	60-03.5	175-52.5	234	04	01	80	05.2	072		126	2	6			04	6		-3.3	-3.9	2	7	8	7
31	PS	60-01.0	176-04.0	234	04	01	80	06.3	073		129	2	7			04	6	994	-2.8	-3.3	2	7	8	7
31	PS	59-54.0	176-30.0	198	04	01	80	15.9	074		140	2	7			03	6	991	-4.4	-4.0	7	7	8	4
31	PS	59-49.0	176-30.0	198	04	01	80	20.5	075		139	2	10			01	5	995	-2.8	-3.3	2	7	8	7
31	PS	59-45.0	176-35.0	198	04	02	80	00.5	076		138	2	6			36	5	995	-5.4	-5.6	2	7	8	7

MIZPAC 80 CTD STATIONS

NAT	SHIP	LAT	LONG	MSQ	MO	DY	YR	HR	STA	DPTH	NAV	ICE	WVD	HT	WND	V	BAR	DRY	WET	WTHR	CL	AMT	VIS
31	PS	59-42.0	176-45.0	198	04	02	80	02.0	077	140	2	6						0.	0.				
31	PS	59-39.0	176-53.0	198	04	02	80	04.2	078	152	2	6			03	5	997	-3.3	-1.1	2	7	8	7
31	PS	59-33.0	177-02.0	198	04	02	80	09.3	079	162	2	0			36	4	999	-7.2	-7.0	2	7	8	7
31	PS	59-29.0	177-07.0	198	04	02	80	10.5	080	151	2	-2			36	4	000	0.	0.	7	7	8	7
31	PS	59-26.0	177-14.0	198	04	02	80	11.6	081	159	2	0			36	4	000	-7.4	-7.8	7	7	8	7
31	PS	59-20.0	177-24.0	198	04	02	80	13.5	082	171	2	0			33	5	001	-8.2	-9.3	2	7	8	7
31	PS	59-16.0	177-45.0	198	04	02	80	15.6	083	280	2	0			34	4	005	-8.3	-9.0	1	6	7	7

APPENDIX C

PROPERTY PROFILES FOR MIZPAC 80 STATIONS

This section contains plots of temperature, salinity, sound speed, and sigma-t for the 83 stations of MIZPAC 80. Shipboard stations were taken with the Neil Brown CTD while the helicopter stations employed the APL-UW CTD. The helicopter stations are sequentially incorporated in the station numbering scheme and are denoted with an H after the station number, e.g., station 26H. However, five stations were taken using the APL-UW instrument from the ship. These are marked with a W: Station 33W, 66-2W, 66-4W, 66-5W, and 67W. The salinities of stations 37H, 38H and 39H are computed from the temperature assuming freezing conditions due to freezing of the salinity port. Three series of stations are slightly out of numerical sequence: Stations 30-36, 43-51, and 66-69.

Because of the small range of properties, we have used expanded T, S and D scales. This has necessitated variable scaling to be used, sometimes with an awkward scale interval, e.g., for Station 1, one temperature unit equals 0.4°C. The shallow water stations are plotted four per page while the deep water stations are shown two per page. To assist in distinguishing between curves the temperature profile has been darkened three times while the salinity trace only twice. The curves are also labeled, T for temperature, S for salinity, SV for sound velocity, and ST for sigma-t.

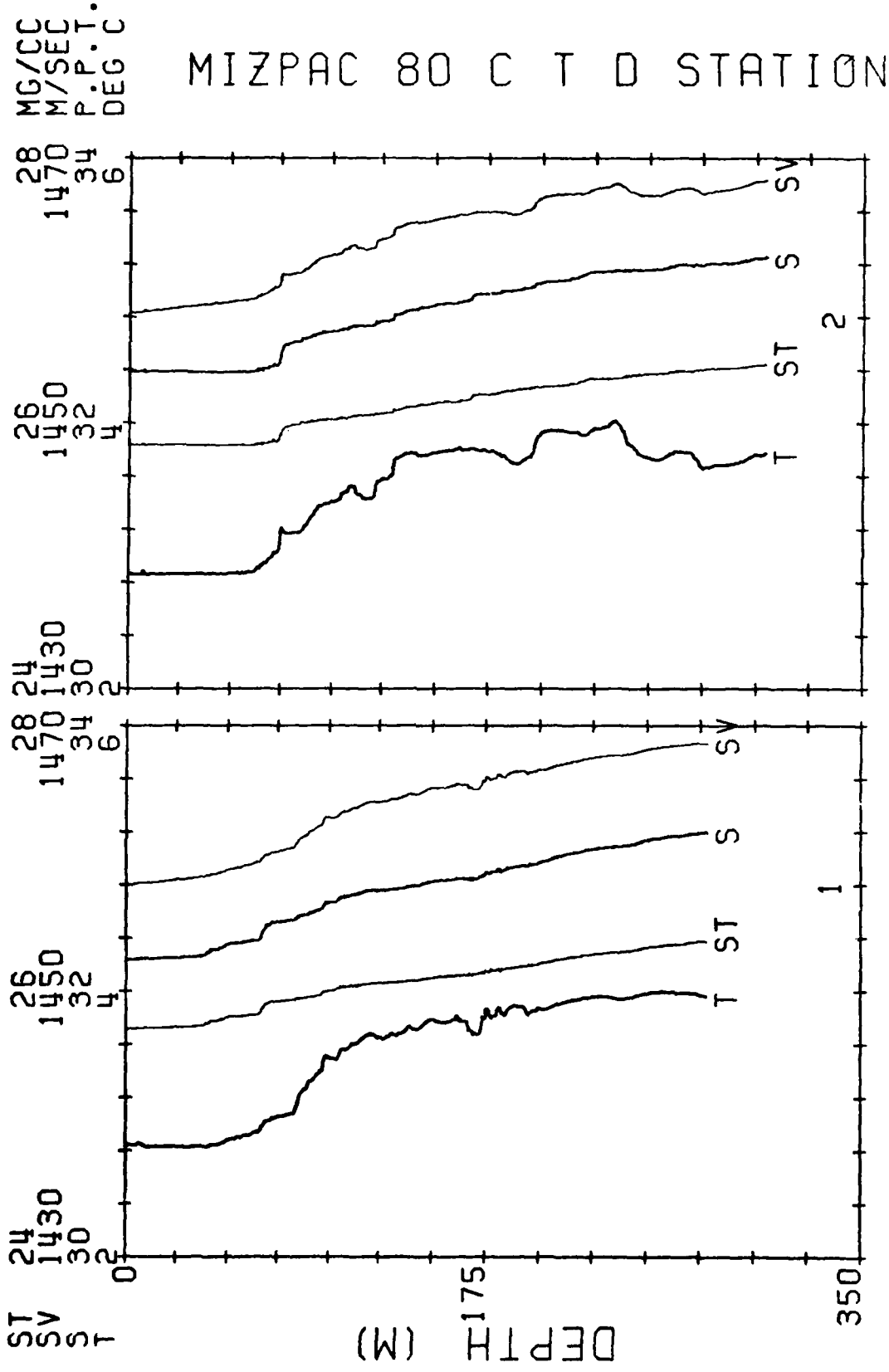
MIZPAC 80 C T D STATIONS
MG/CC
M/SEC
P.P.T.
DEG C
28
1470
34
6
26
1450
32
4
24
1430
30
2
SV
S
ST
T
2
1
0
175
350
DEPTH (M)

MIZPAC 80 C T D STATIONS

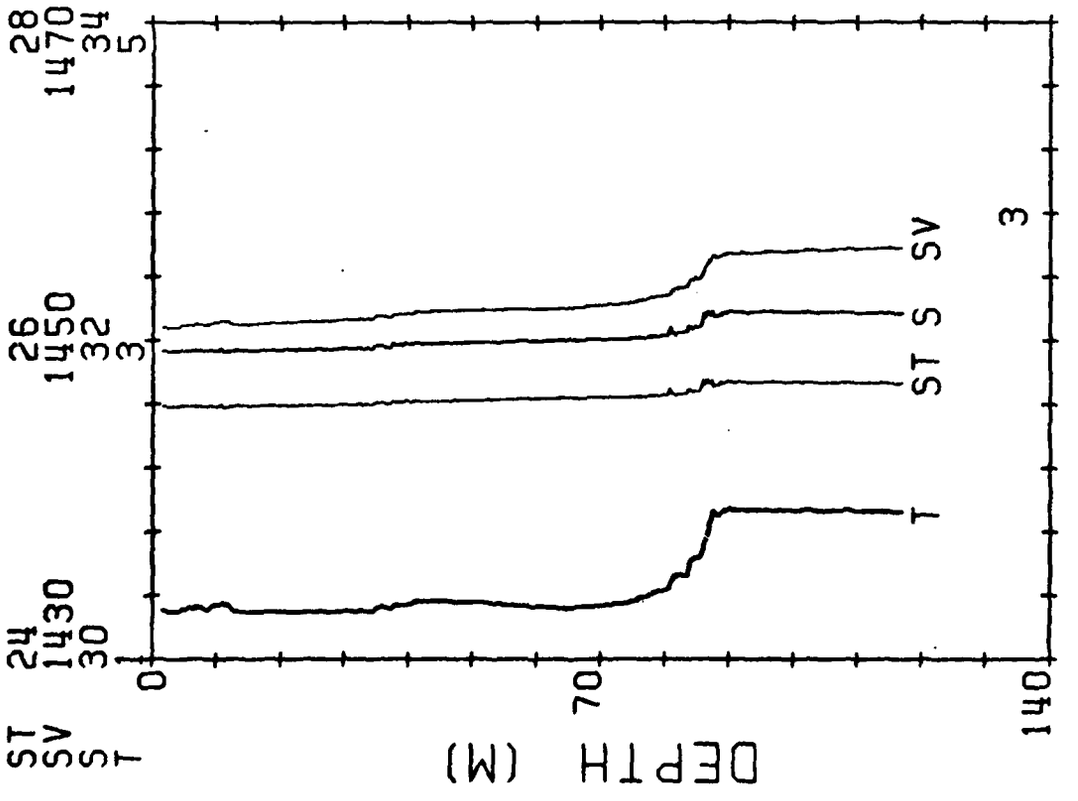

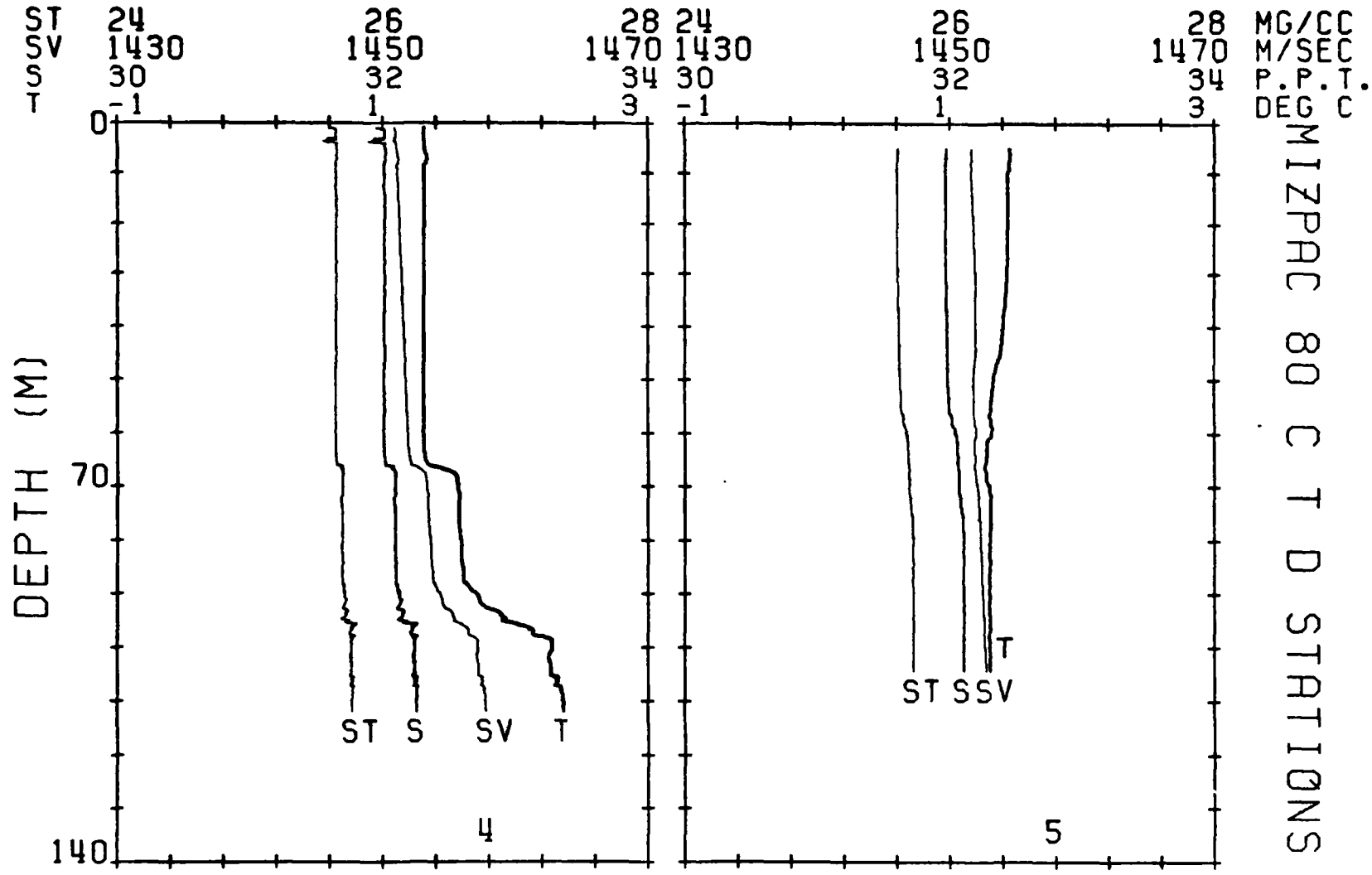
ST 24 26 28 24 26 28 MG/CC
SV 1430 1450 1470 1430 1450 1470 M/SEC
S 30 32 34 30 32 34 P.P.T.
T -1 1 3 -1 1 3 DEG C
0
70
140
DEPTH (M)
ST S SV T
4
ST S SV T
5
MIZPAC 80 C T D STATIONS

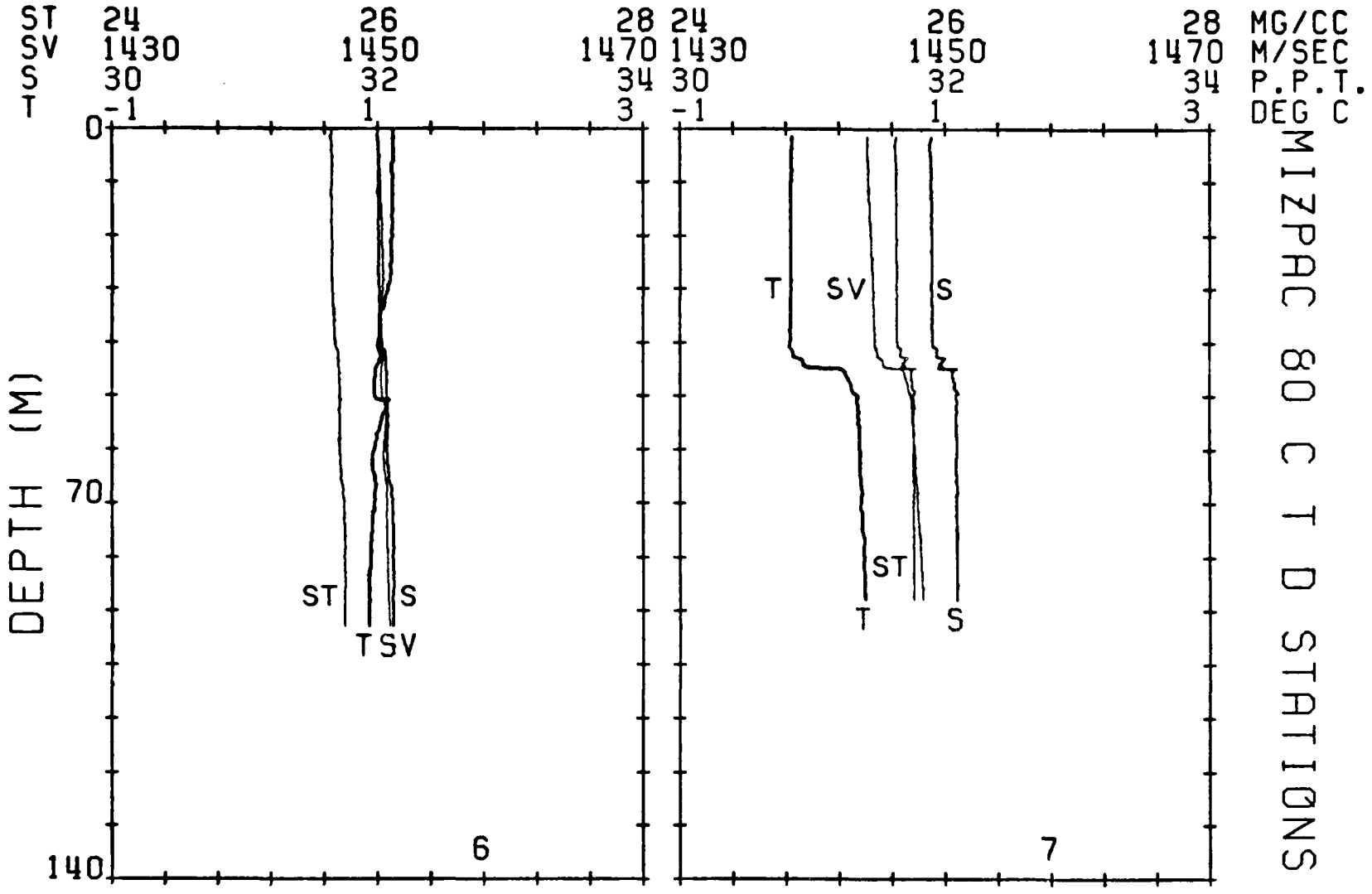
ST 24 26 28 24 26 28 MG/CC
SV 1430 1450 1470 1430 1450 1470 M/SEC
S 30 32 34 30 32 34 P.P.T.
T -1 1 3 -1 1 3 DEG C
0
70
140
DEPTH (M)
ST
S
T SV
6
T
SV
S
ST
T
S
7
MIZPAC 80 C T D STATIONS

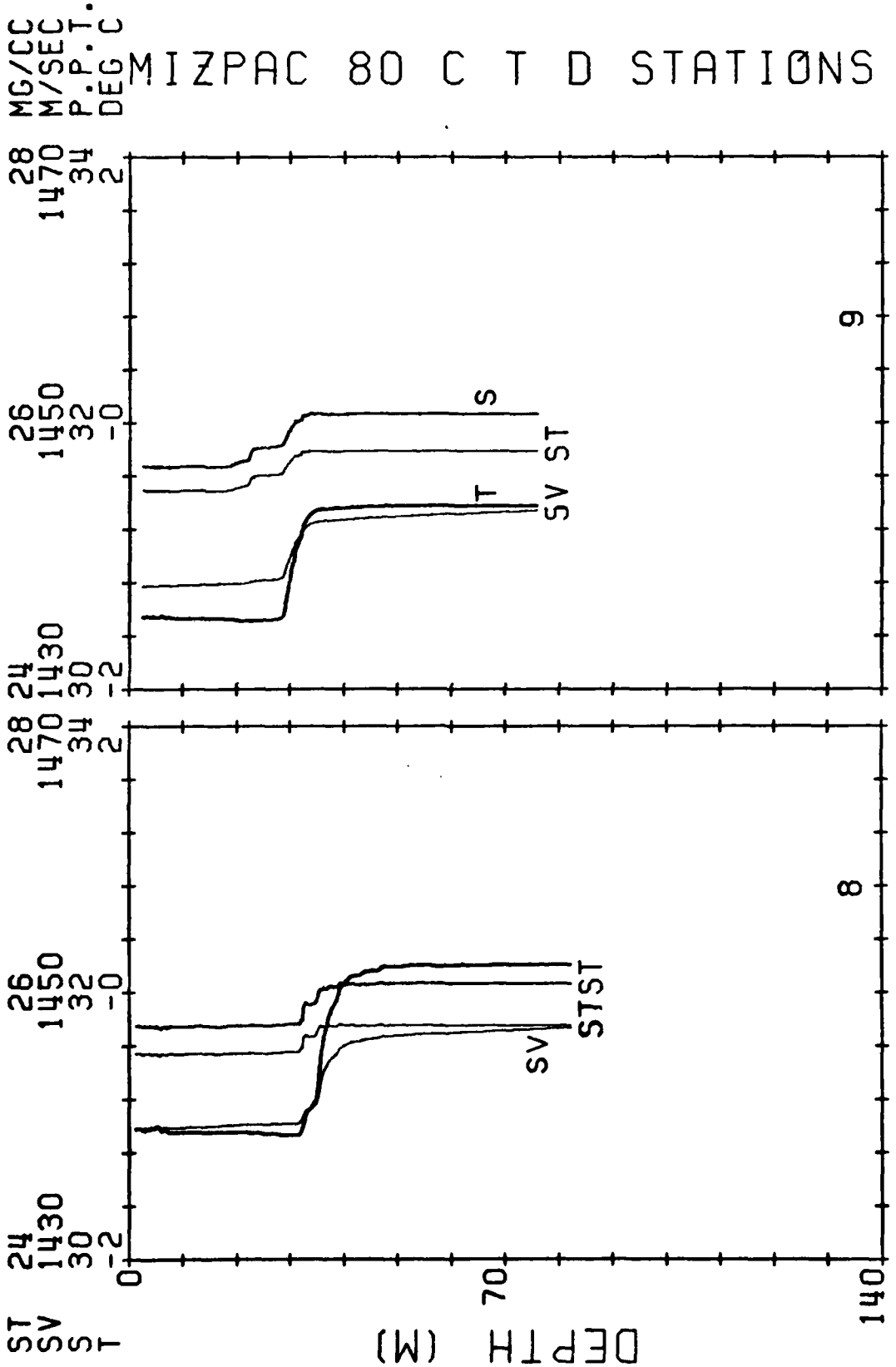
MIZPAC 80 C T D STATIONS
MG/CC
M/SEC
P.P.T.
DEG C
28
1470
34
2
26
1450
32
-0
24
1430
30
-2
S
ST
T
SV
9
8
STST
SV
0
70
140
DEPTH (M)
ST
SV
S
T

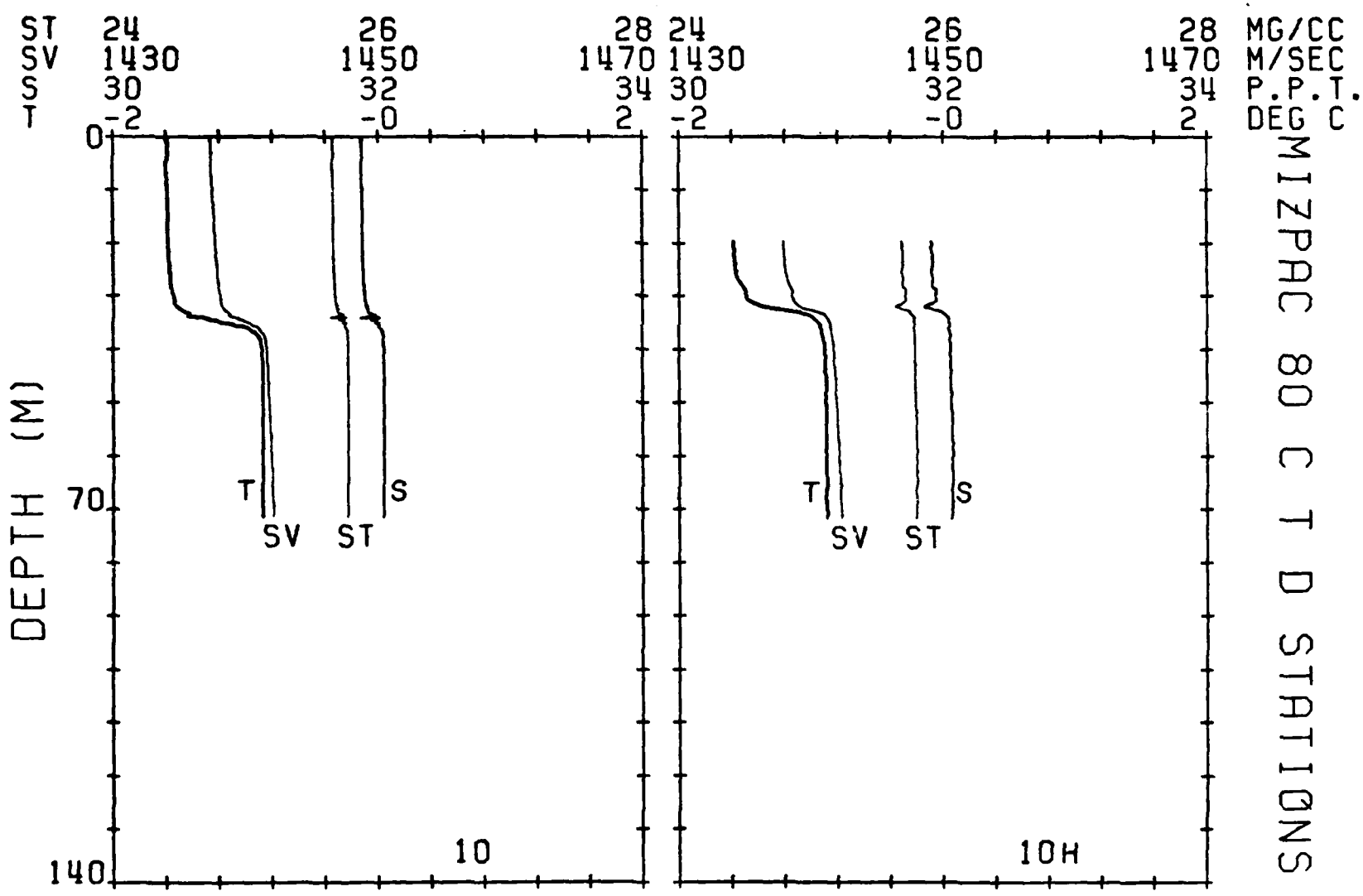
ST 24 26 28 24 26 28 MG/CC
SV 1430 1450 1470 1430 1450 1470 M/SEC
S 30 32 34 30 32 34 P.P.T.
T -2 -0 2 -2 -0 2 DEG C
MIZPAC 80 C T D STATIONS
DEPTH (M)
0
70
140
T
SV
ST
S
10
10H

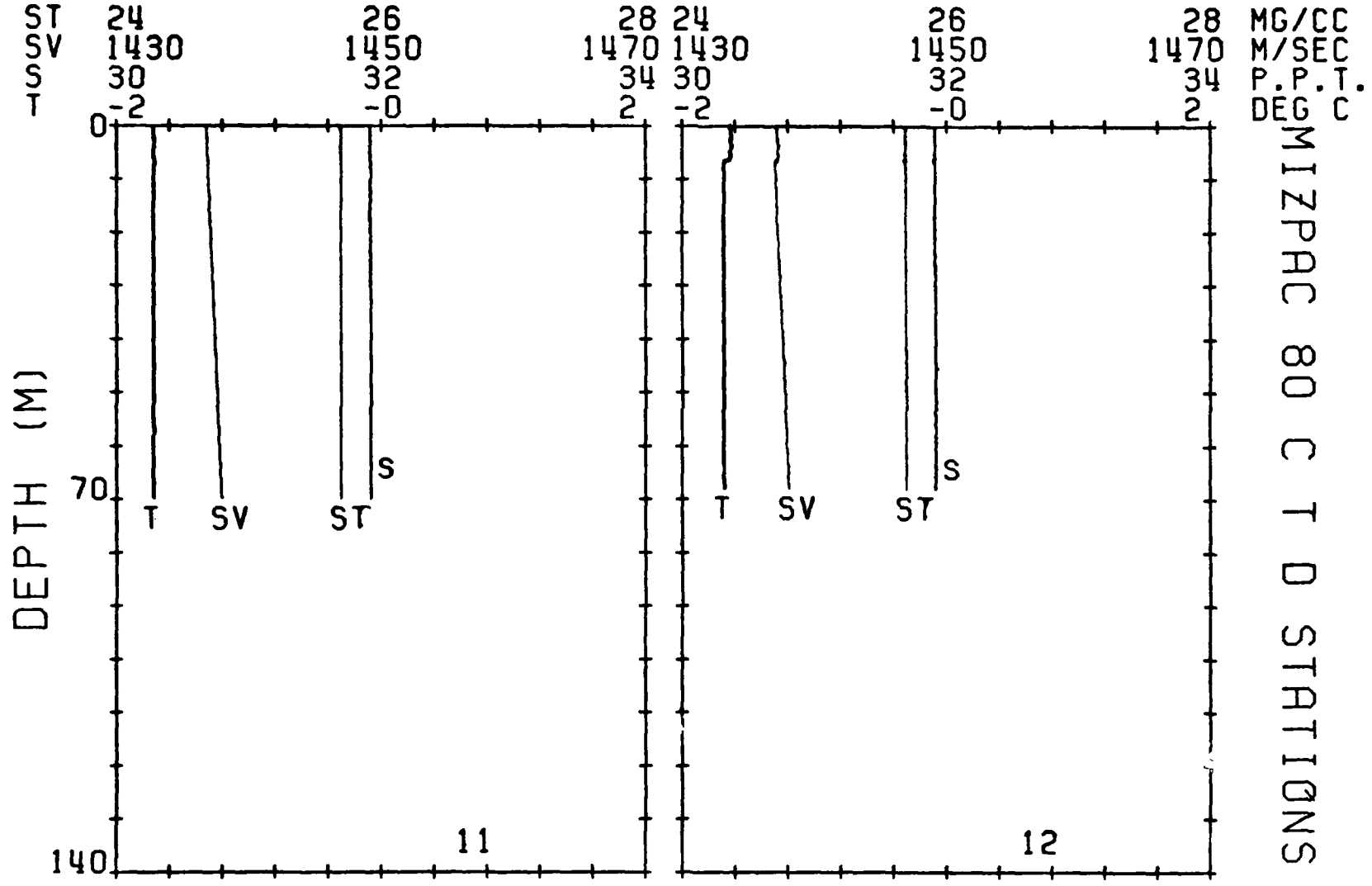
ST 24 26 28 24 26 28 MG/CC
SV 1430 1450 1470 1430 1450 1470 M/SEC
S 30 32 34 30 32 34 P.P.T.
T -2 -0 2 -2 -0 2 DEG C
0
70
140
DEPTH (M)
T
SV
ST
S
11
12
MIZPAC 80 C T D STATIONS

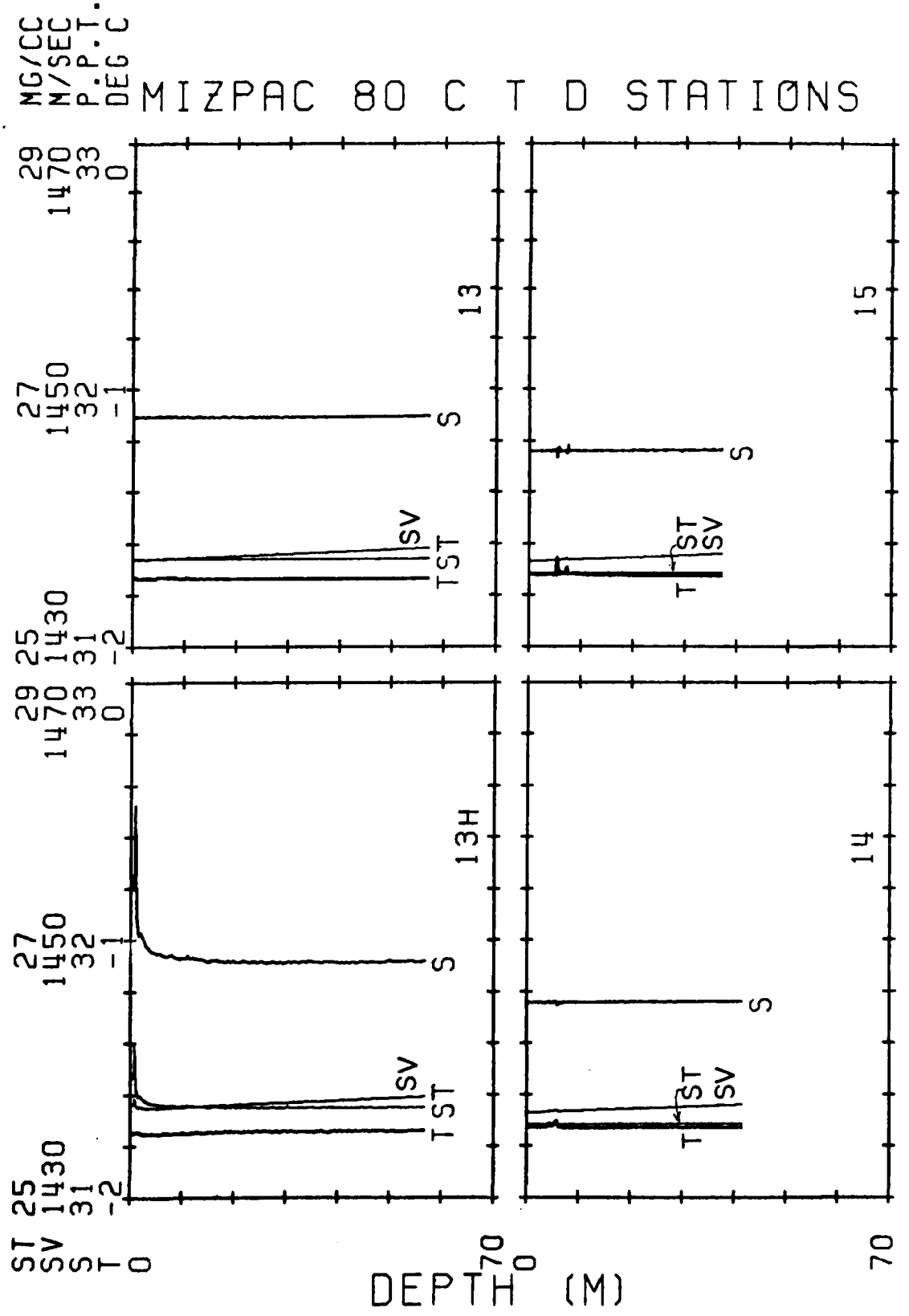
MG/CC
M/SEC
P.P.T.
DEG C
MIZPAC 80 C T D STATIONS
29
1470
33
0
27
1450
32
-1
25
1430
31
-2
S
SV
ST
T
13
15
13H
14
ST
SV
T
S
0
70
DEPTH (M)

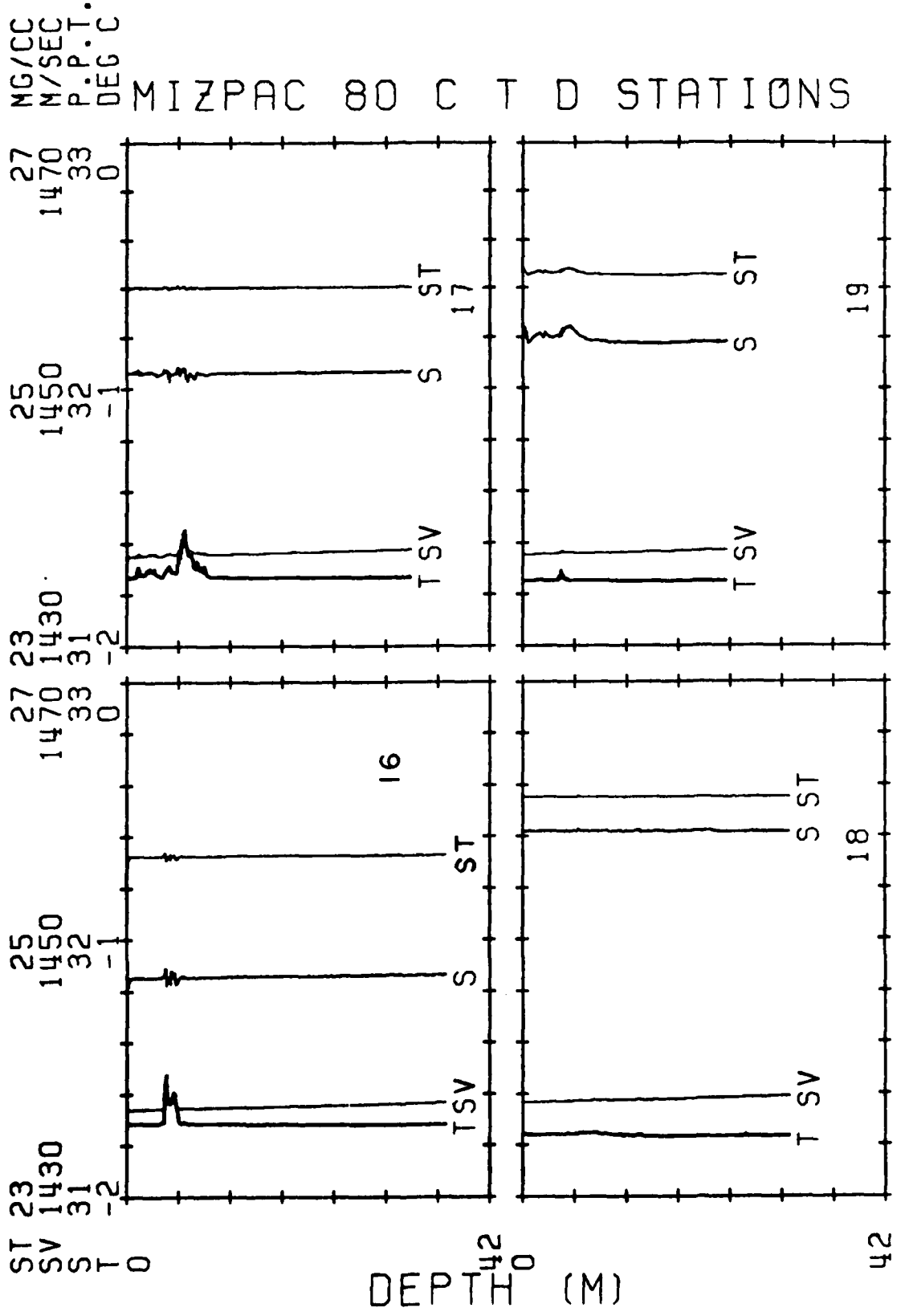
MIZPAC 80 C T D STATIONS
MG/CC
M/SEC
P.P.T.
DEG C
27
1470
33
0
25
1450
32
-1
23
1430
31
-2
ST
SV
S
T
17
19
16
18
DEPTH (M)
42

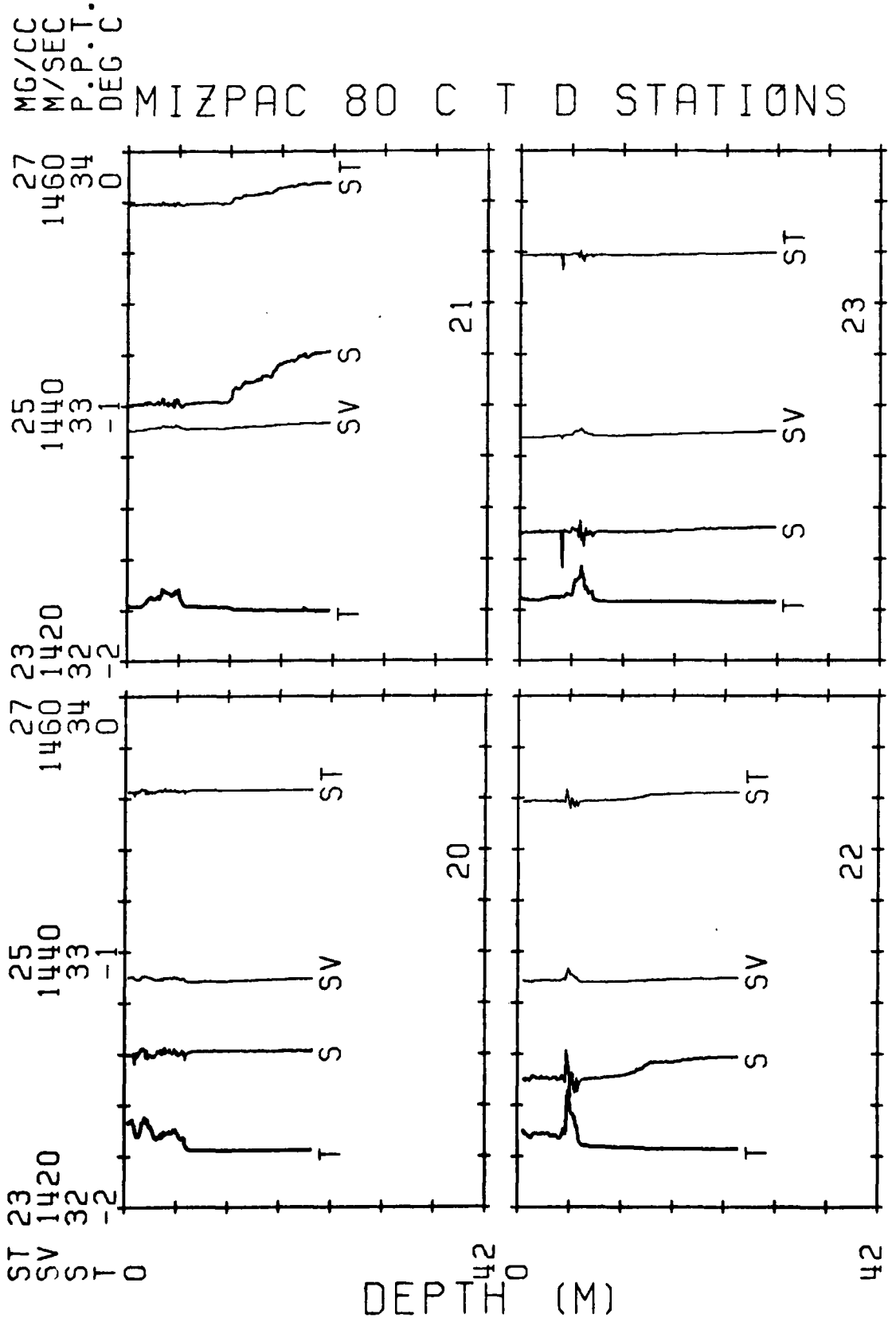
MIZPAC 80 C T D STATIONS
MG/CC
M/SEC
P.P.T.
DEG C
27
1460
34
0
ST
25
1440
33
-1
SV
S
T
23
1420
32
-2
21
23
20
22
DEPTH (M)
42
0

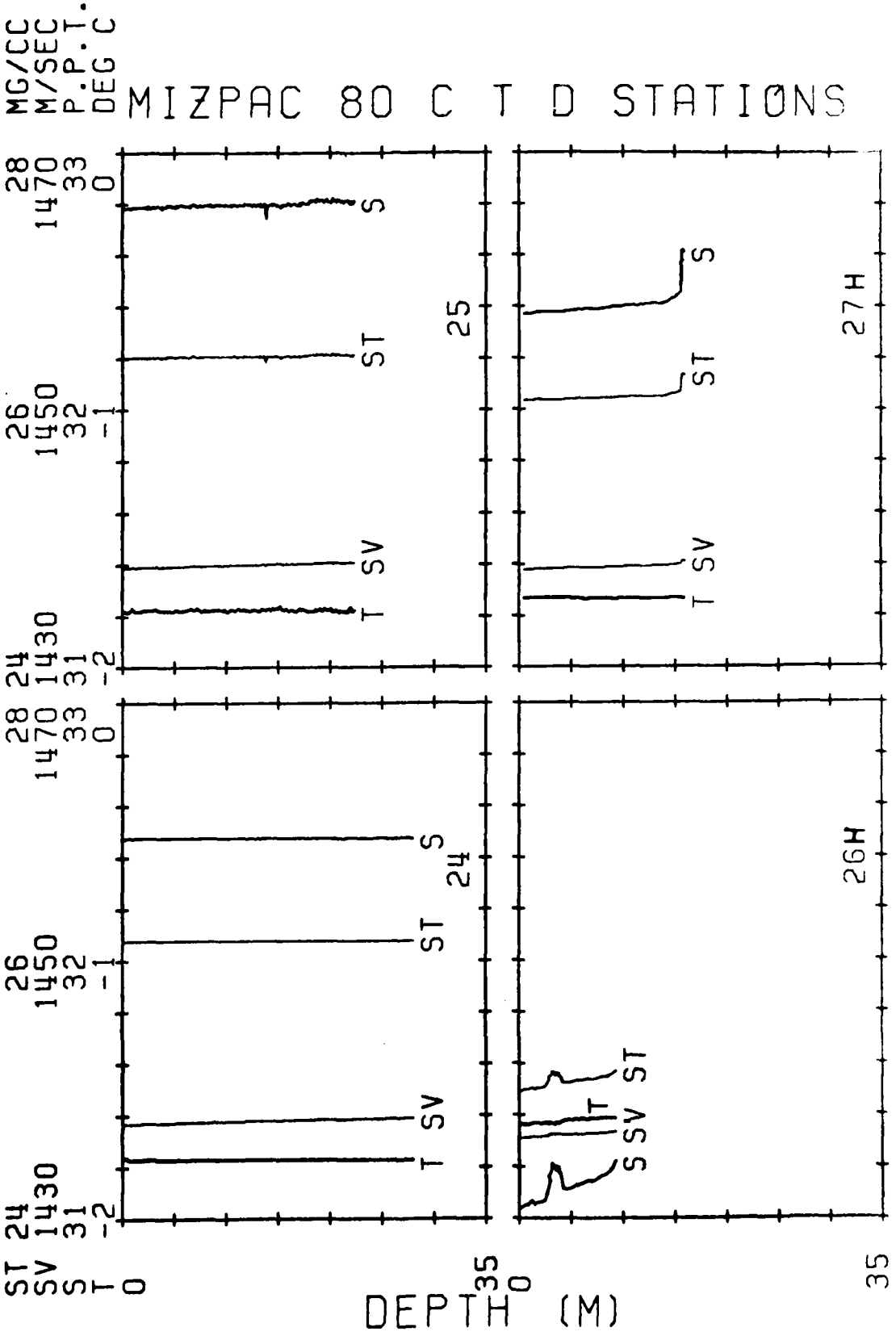
MIZPAC 80 C T D STATIONS
MG/CC
M/SEC
P.P.T.
DEG C
28
1470
33
0
S
ST
25
26
1450
32
-1
T SV
24
1430
31
-2
27H
26H
DEPTH (M)
0
35

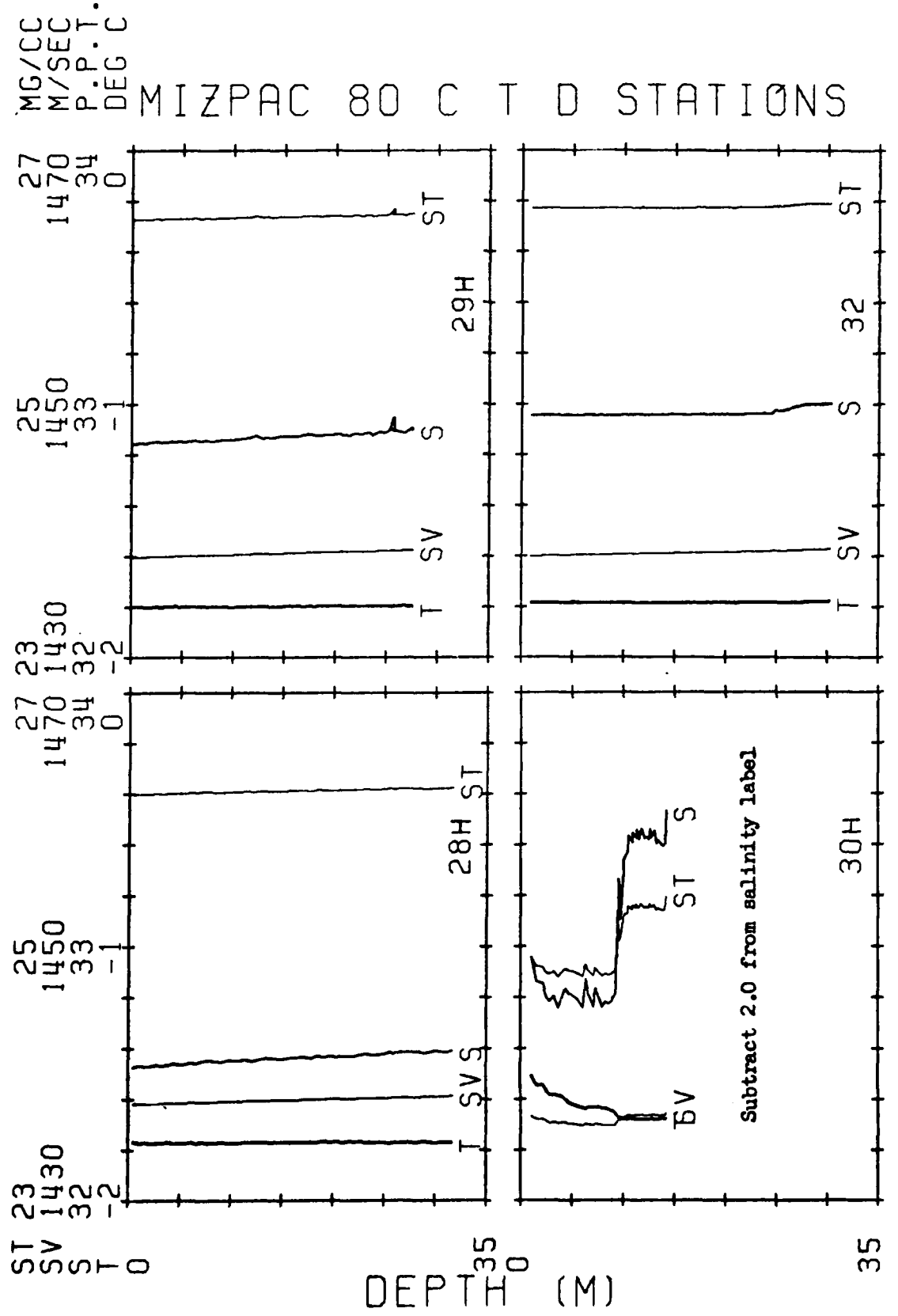
MG/CC
M/SEC
P.P.T.
DEG C
MIZPAC 80 C T D STATIONS
27
1470
34
0
25
1450
33
-1
23
1430
32
-2
ST
S
SV
T
29H
32
28H
30H
Subtract 2.0 from salinity label
ST 23
SV 1430
S 32
T -2
0
35
DEPTH (M)

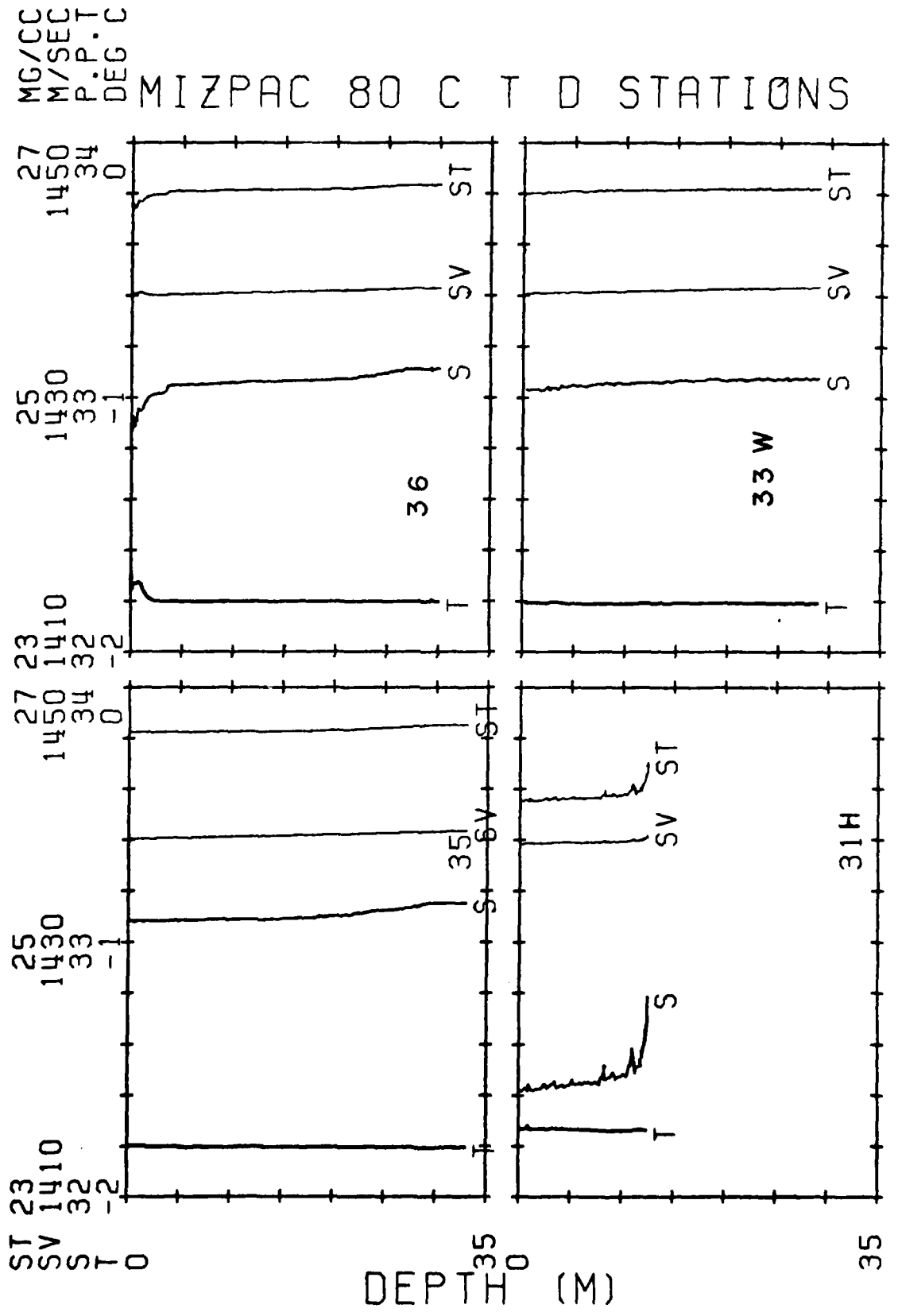
MIZPAC 80 C T D STATIONS
MG/CC
M/SEC
P.P.T.
DEG C
27
1450
34
0
25
1430
33
-1
23
1410
32
-2
ST
SV
S
T
36
33 W
35
31H
DEPTH (M)
0
35

MIZPAC 80 C T D STATIONS

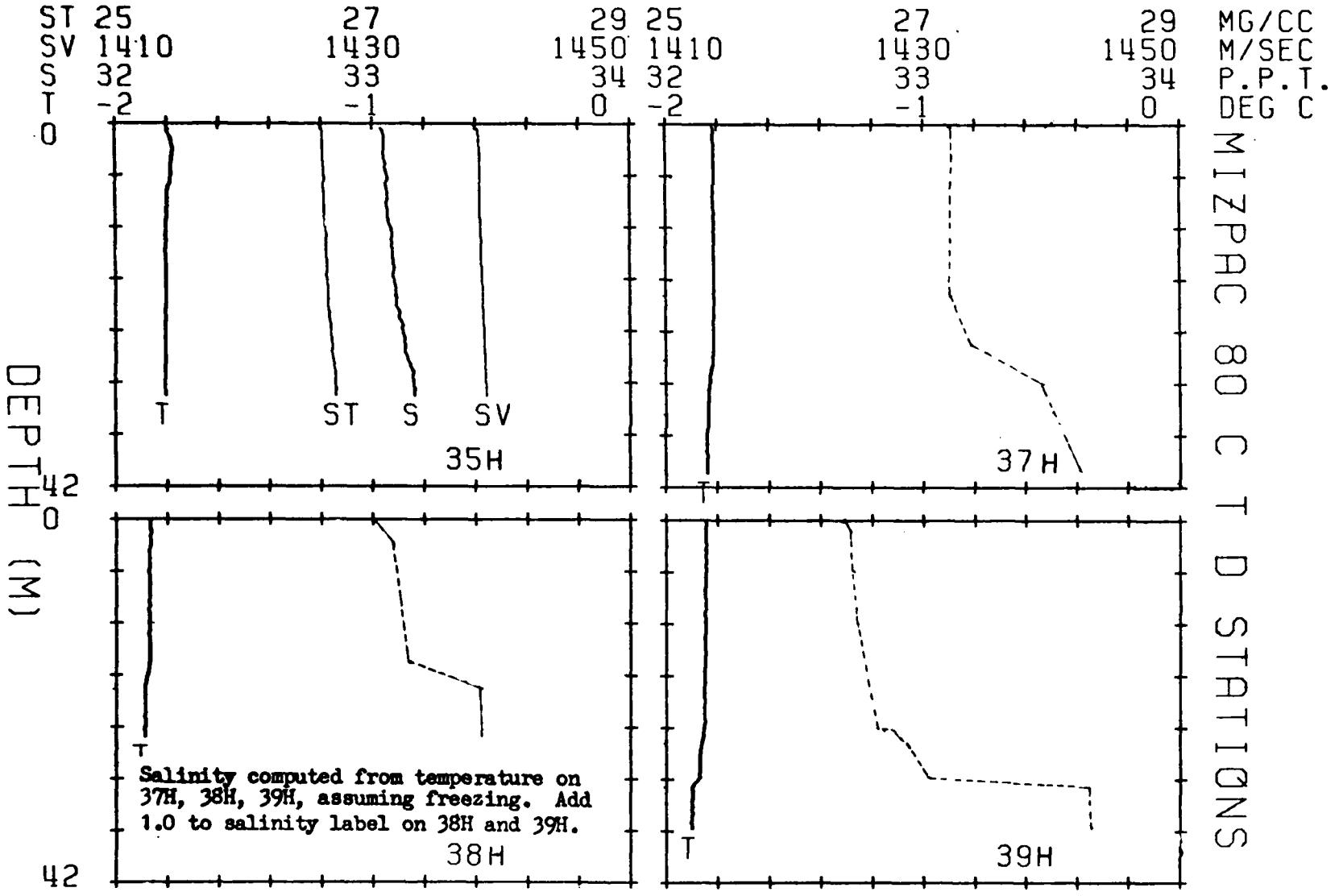
ST 25 27 29 25 27 29 MG/CC
SV 1410 1430 1450 1410 1430 1450 M/SEC
S 32 33 34 32 33 34 P.P.T.
T -2 -1 0 -2 -1 0 DEG C
0
T
ST
S
SV
35H
37H
42
0
DEPTH (M)
T
Salinity computed from temperature on 37H, 38H, 39H, assuming freezing. Add 1.0 to salinity label on 38H and 39H.
38H
T
39H
42
MIZPAC 80 C T D STATIONS

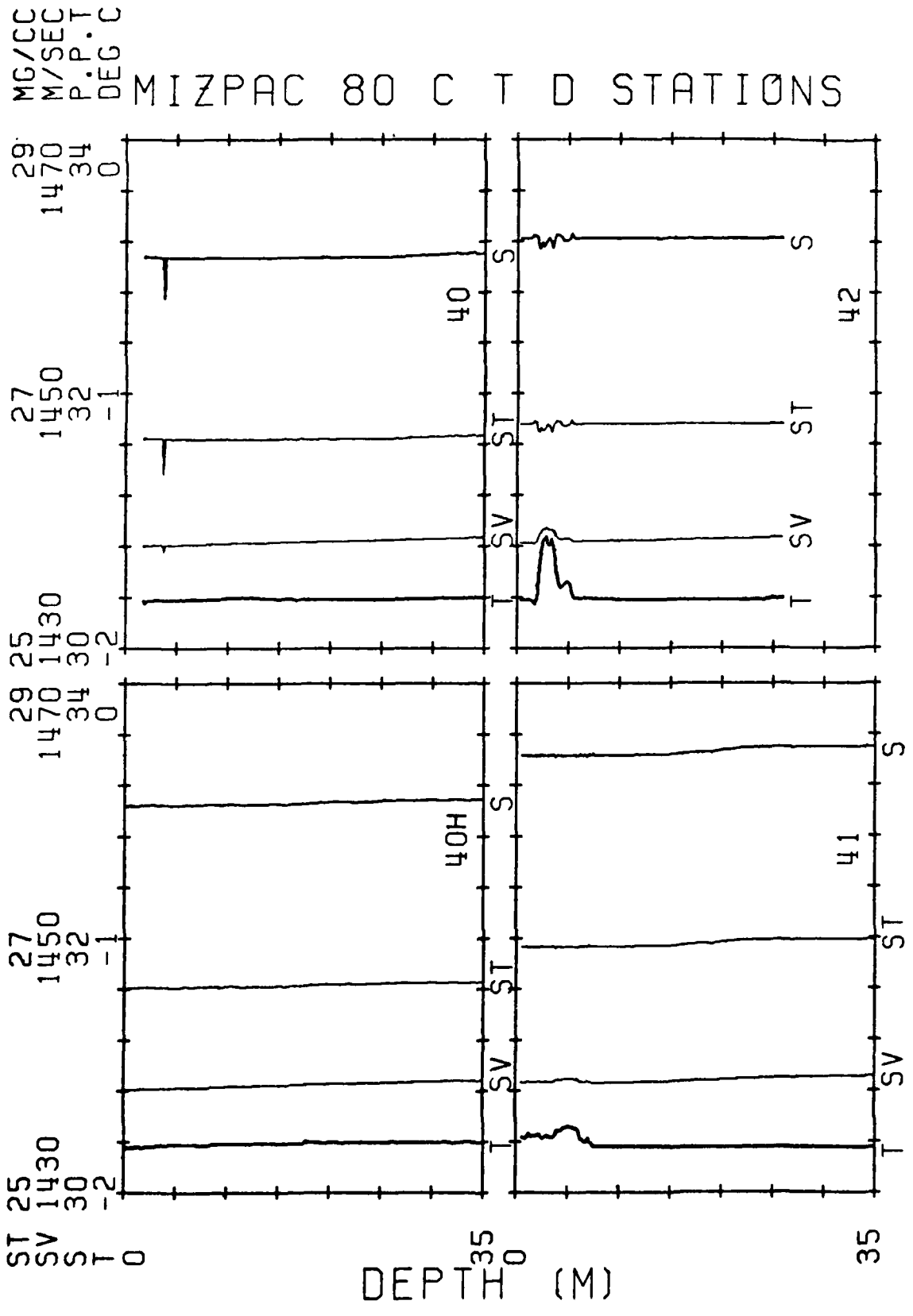
MG/CC
M/SEC
P.P.T.
DEG C
MIZPAC 80 C T D STATIONS
29
1470
34
0
27
1450
32
-1
25
1430
30
-2
40
42
40H
41
S
ST
SV
T
35
DEPTH (M)

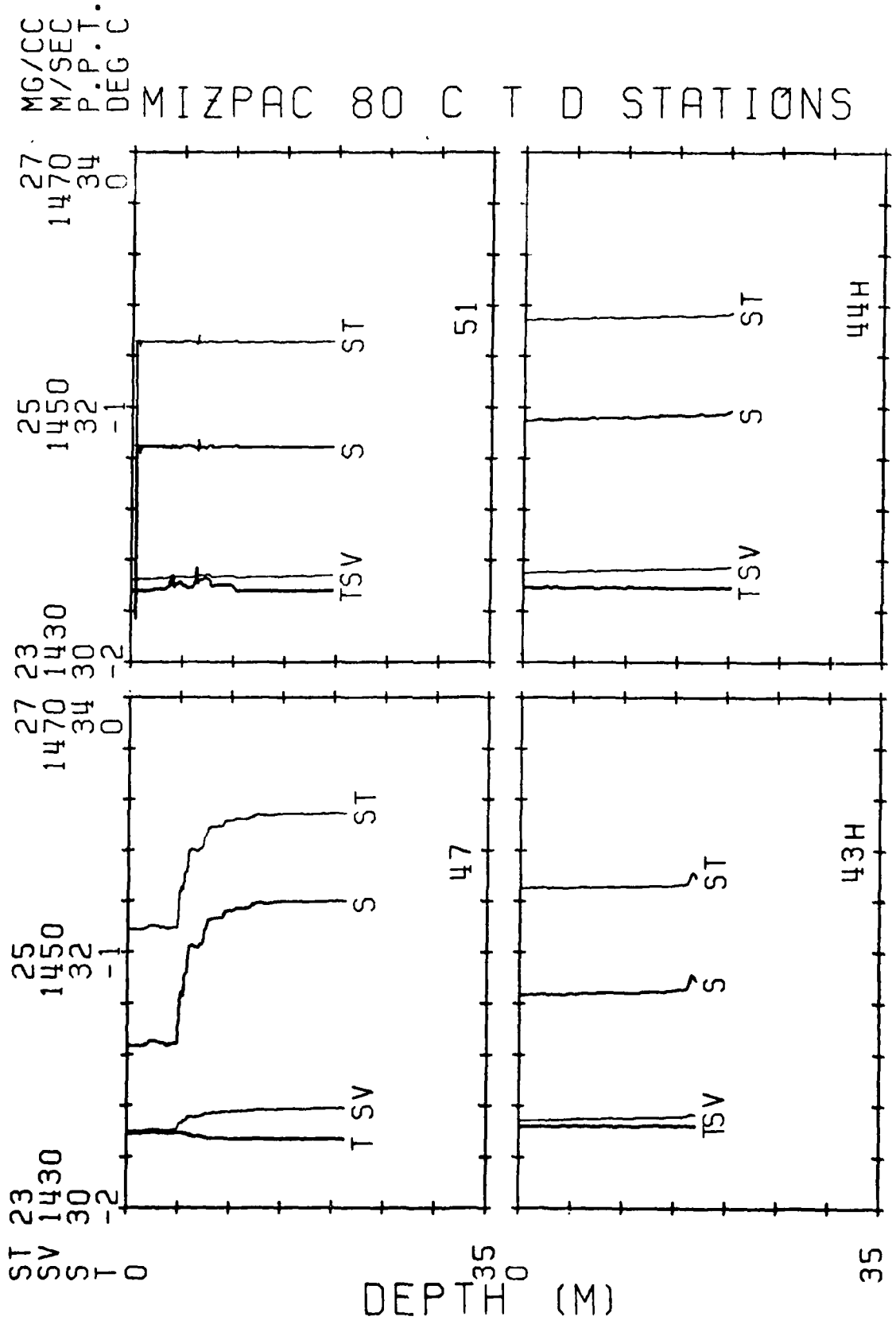
MIZPAC 80 C T D STATIONS
MG/CC
M/SEC
P.P.T.
DEG C
27
1470
34
0
25
1450
32
-1
23
1430
30
-2
ST
S
TSV
51
44H
47
43H
0
35
DEPTH (M)

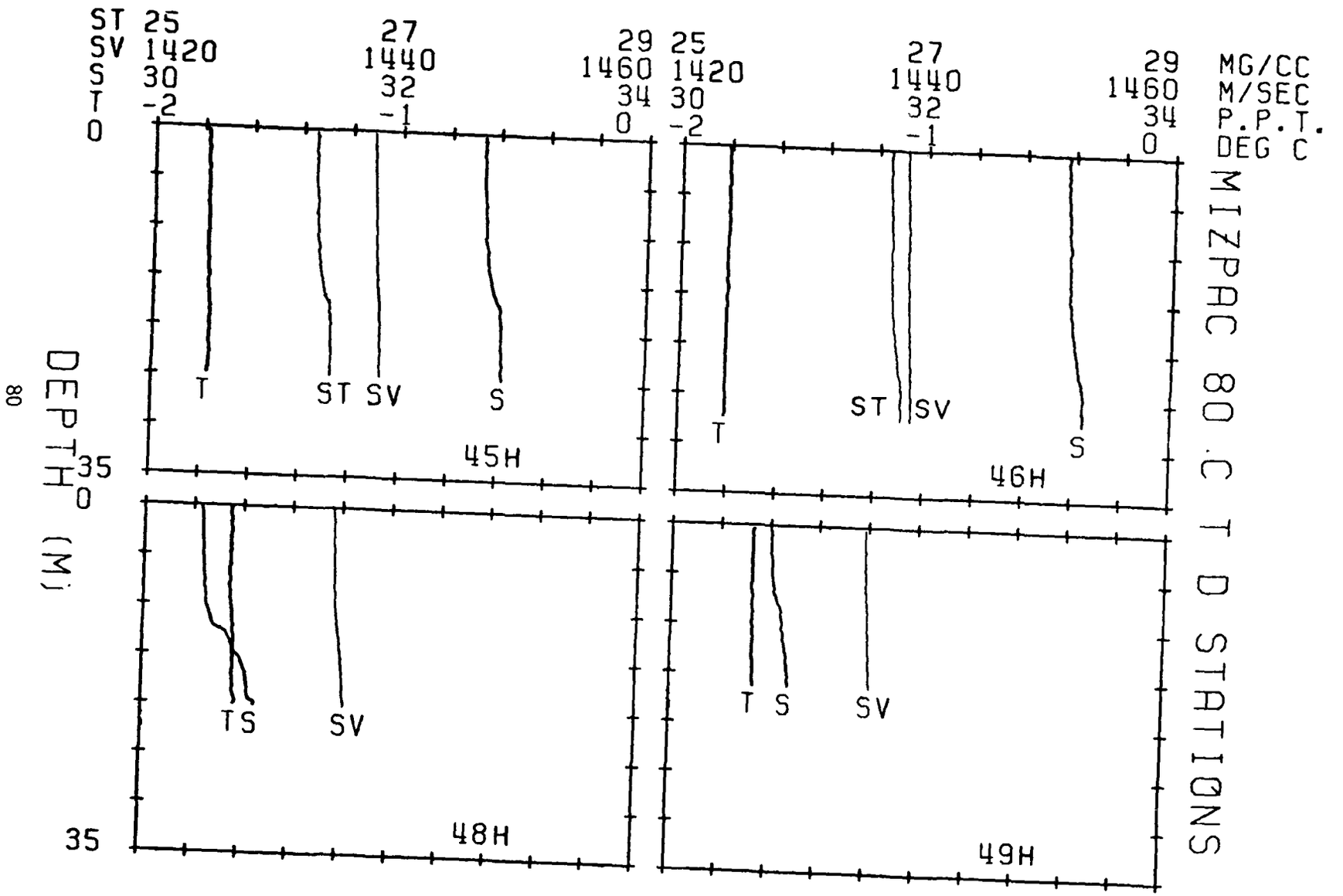
MIZPAC 80 C T D STATIONS
MG/CC
M/SEC
P.P.T.
DEG C
DEPTH (M)
ST 25 27 29
SV 1420 1440 1460
S 30 32 34
T -2 -1 0
0
35
T
ST SV
S
45H
46H
48H
49H
TS
SV

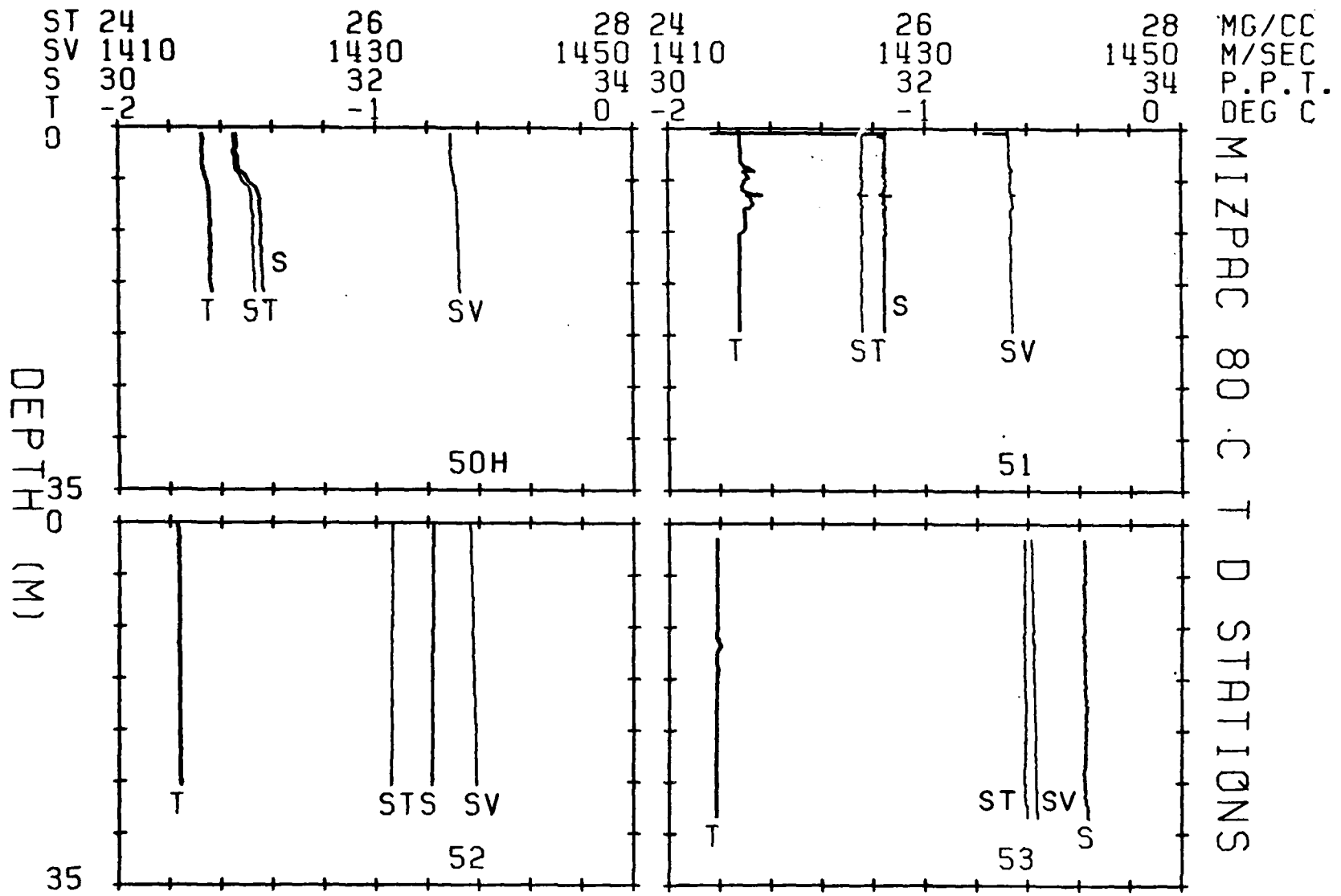
ST 24 26 28 24 26 28 MG/CC
SV 1410 1430 1450 1410 1430 1450 M/SEC
S 30 32 34 30 32 34 P.P.T.
T -2 -1 0 -2 -1 0 DEG C
MIZPAC 80 C T D STATIONS
DEPTH (M)
0
35
T ST S SV
50H
T ST S SV
51
T STS SV
52
T ST SV S
53

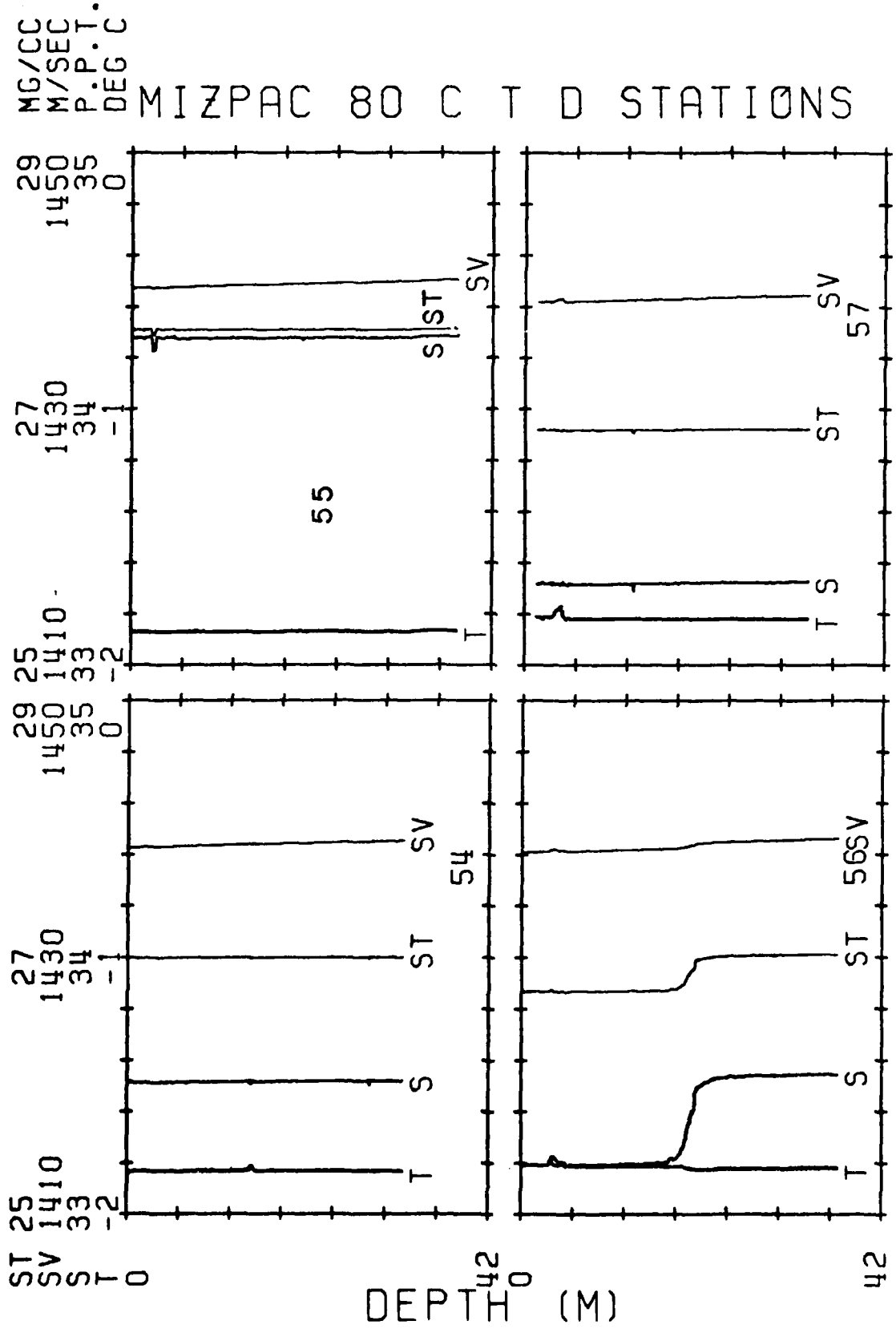
MIZPAC 80 C T D STATIONS
MG/CC
M/SEC
P.P.T.
DEG C
29
1450
35
0
27
1430
34
-1
25
1410
33
-2
ST
SV
S
T
55
54
57
56
SV
ST
S
T
0
42
DEPTH (M)

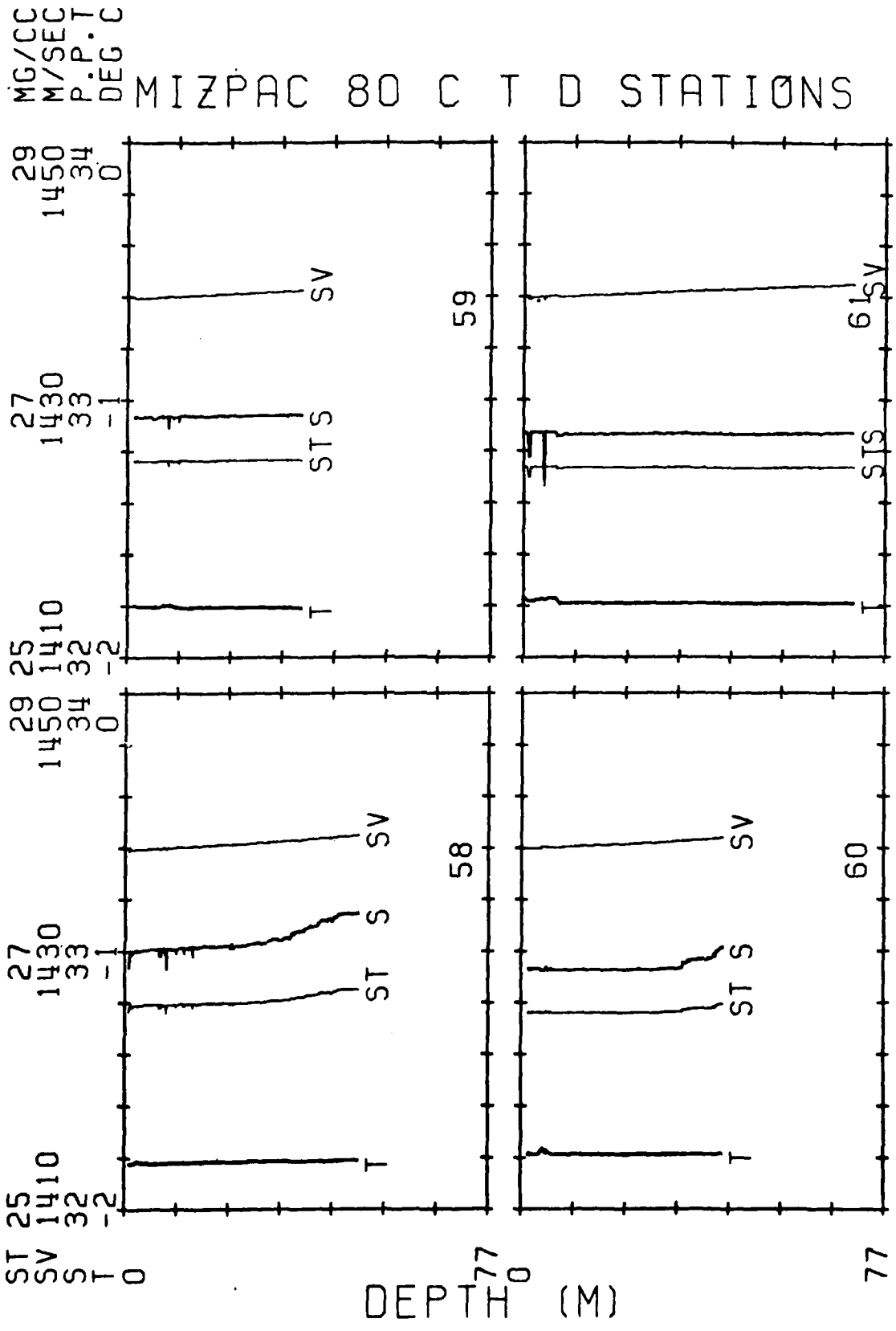
MIZPAC 80 C T D STATIONS
MG/CC
M/SEC
P.P.T.
DEG C
29
1450
34
0
27
1430
33
-1
25
1410
32
-2
SV
S
T
59
61
58
60
ST
SV
S
T
0
77
DEPTH (M)

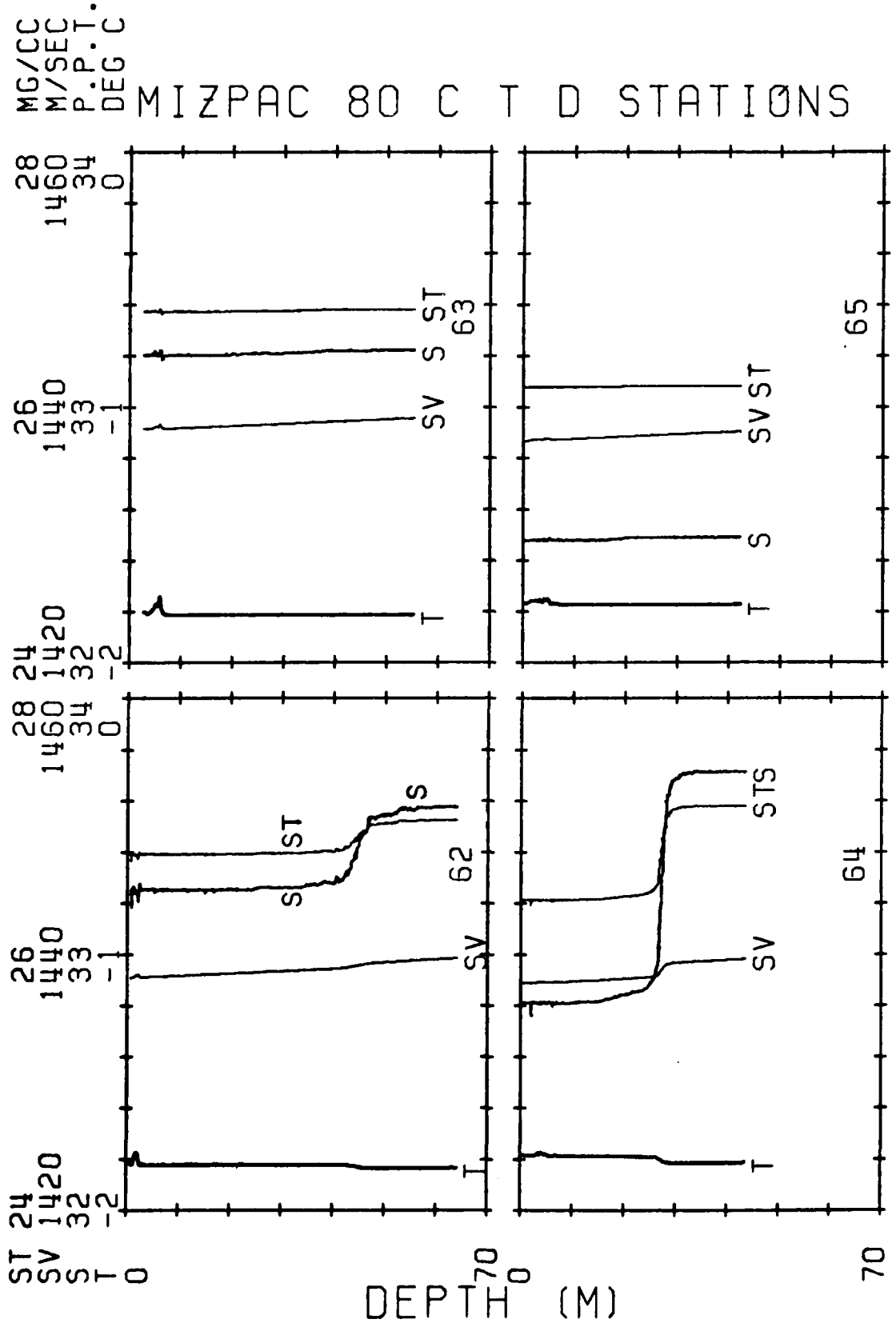
MIZPAC 80 C T D STATIONS
MG/CC
M/SEC
P.P.T.
DEG C
28
1460
34
0
26
1440
33
-1
24
1420
32
-2
ST
SV
S
T
63
65
62
64
SV ST
S
T
STS
DEPTH (M)
0
70

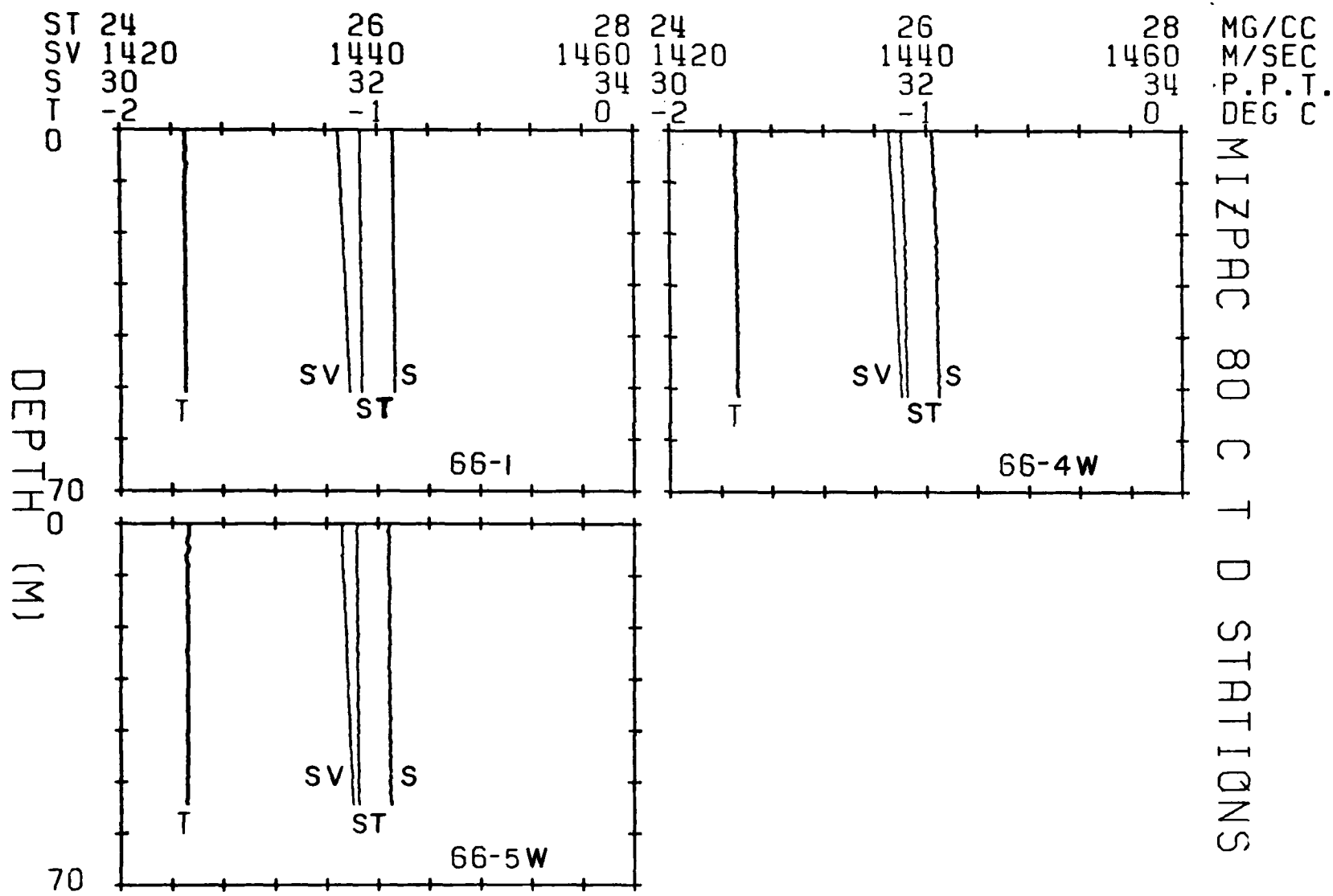
ST 24 26 28 24 26 28 MG/CC
SV 1420 1440 1460 1420 1440 1460 M/SEC
S 30 32 34 30 32 34 P.P.T.
T -2 -1 0 -2 -1 0 DEG C
0
DEPTH (M)
70
T
SV
S
ST
66-1
66-4W
66-5W
MIZPAC 80 C T D STATIONS

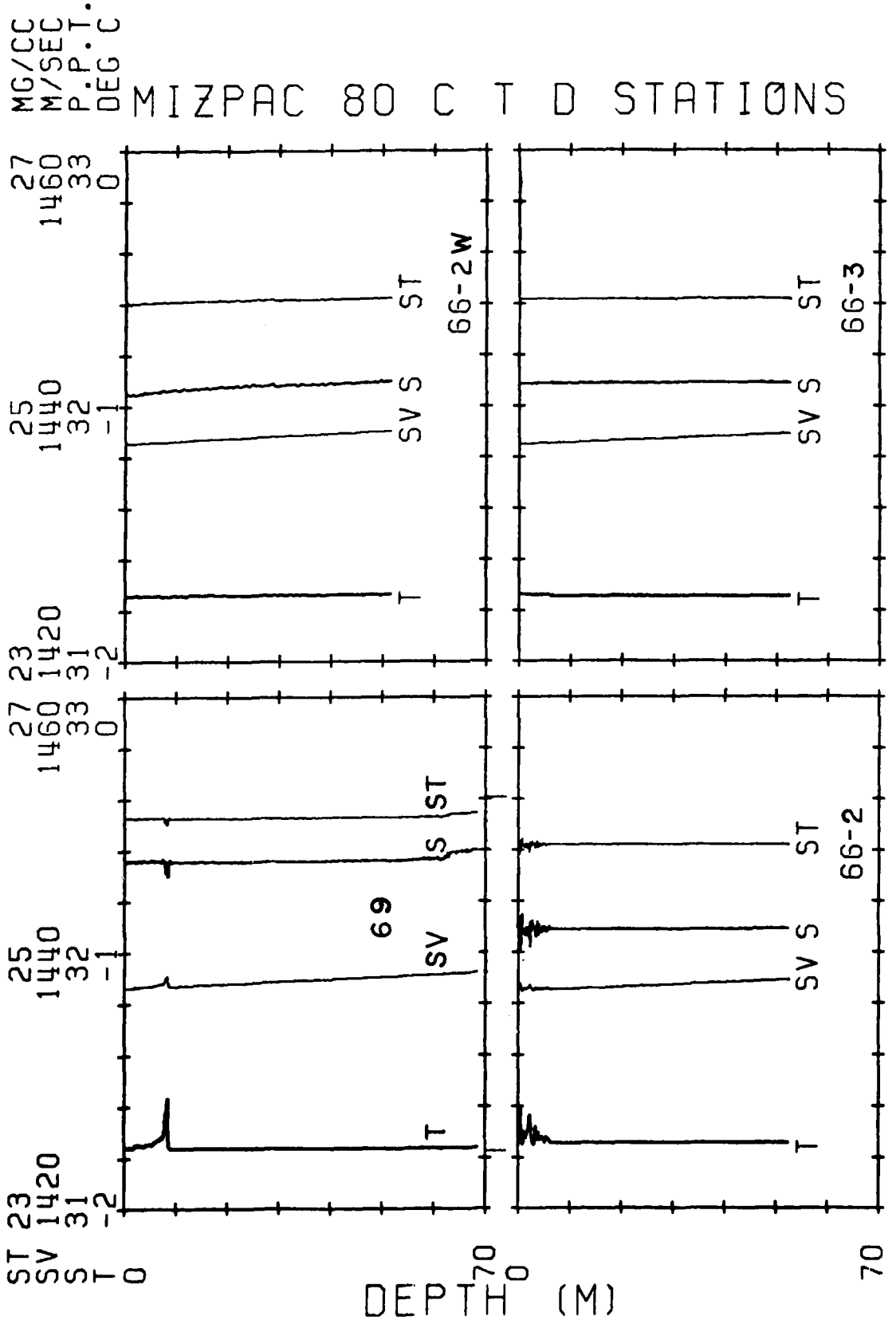
MIZPAC 80 C T D STATIONS
MG/CC
M/SEC
P.P.T.
DEG C
27
1460
33
0
25
1440
32
-1
23
1420
31
-2
ST
SV
S
T
66-2W
66-3
66-2
69
0
70
DEPTH (M)

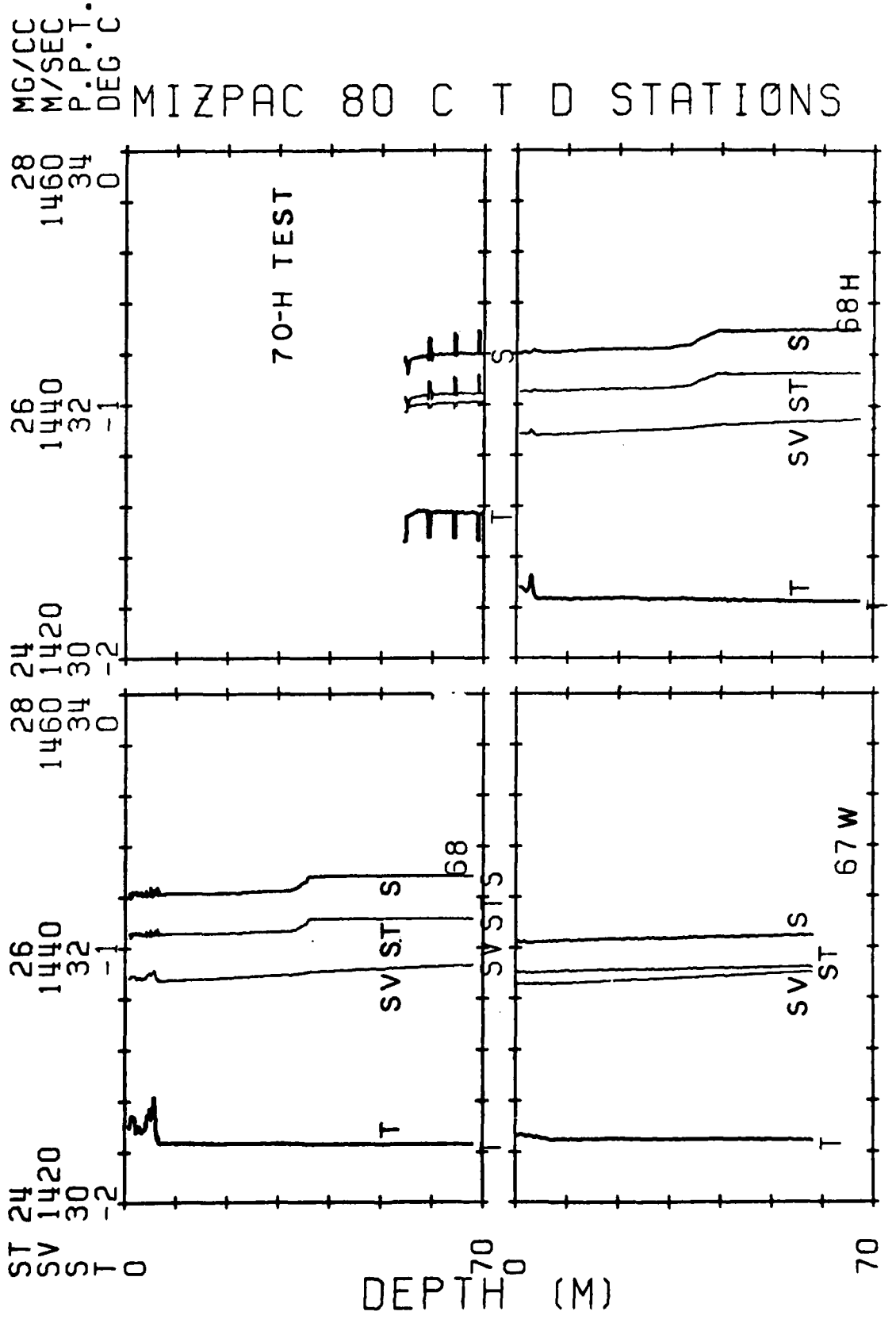
MIZPAC 80 C T D STATIONS
MG/CC
M/SEC
P.P.T.
DEG C
70-H TEST
68H
68
67 W
S
ST
SV
T
28
1460
34
0
26
1440
32
-1
24
1420
30
-2
DEPTH (M)
70

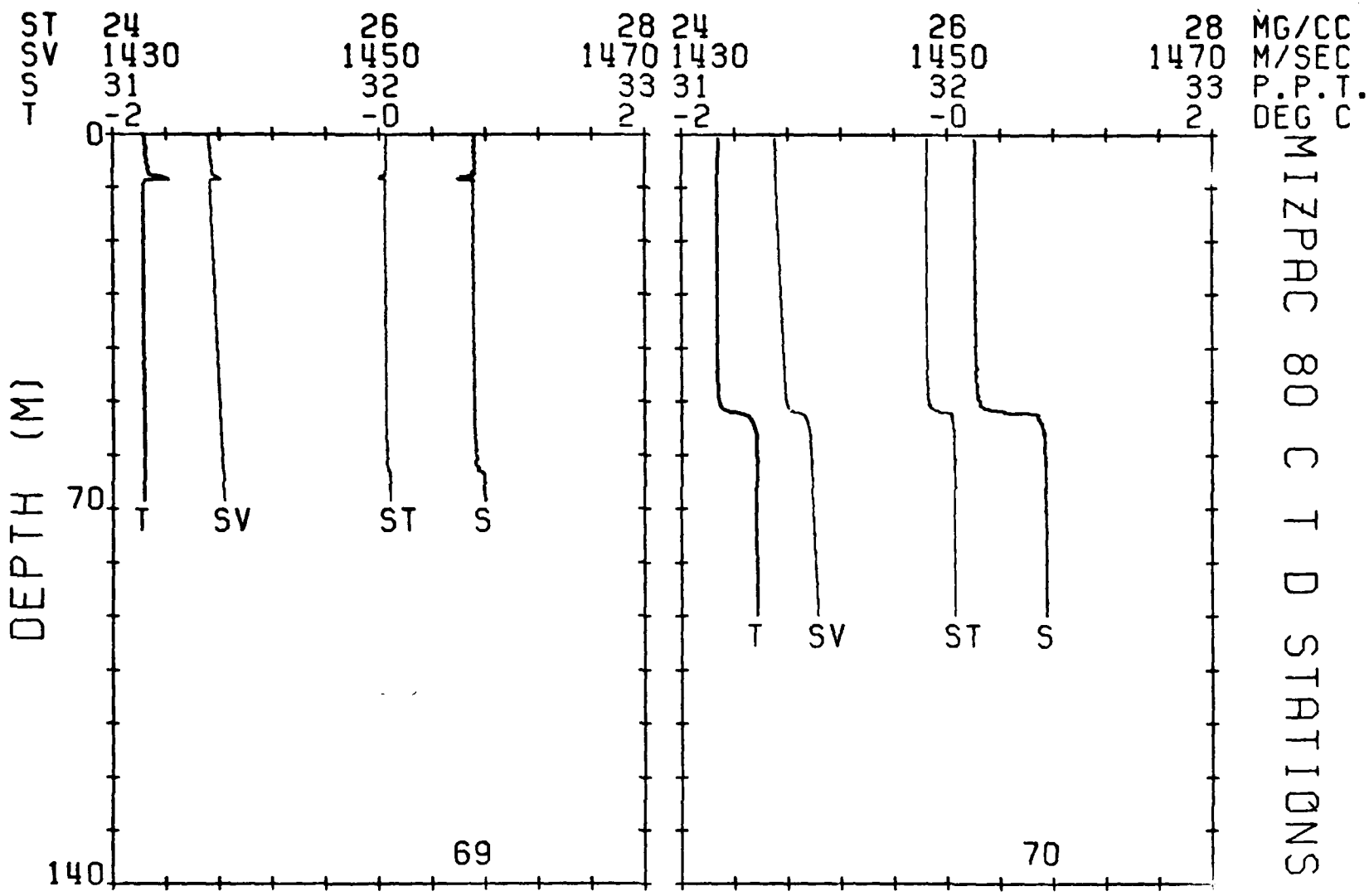
ST 24 26 28 24 26 28 MG/CC
SV 1430 1450 1470 1430 1450 1470 M/SEC
S 31 32 33 31 32 33 P.P.T.
T -2 -0 2 -2 -0 2 DEG C
MIZPAC 80 C T D STATIONS
DEPTH (M)
0
70
140
T
SV
ST
S
69
70

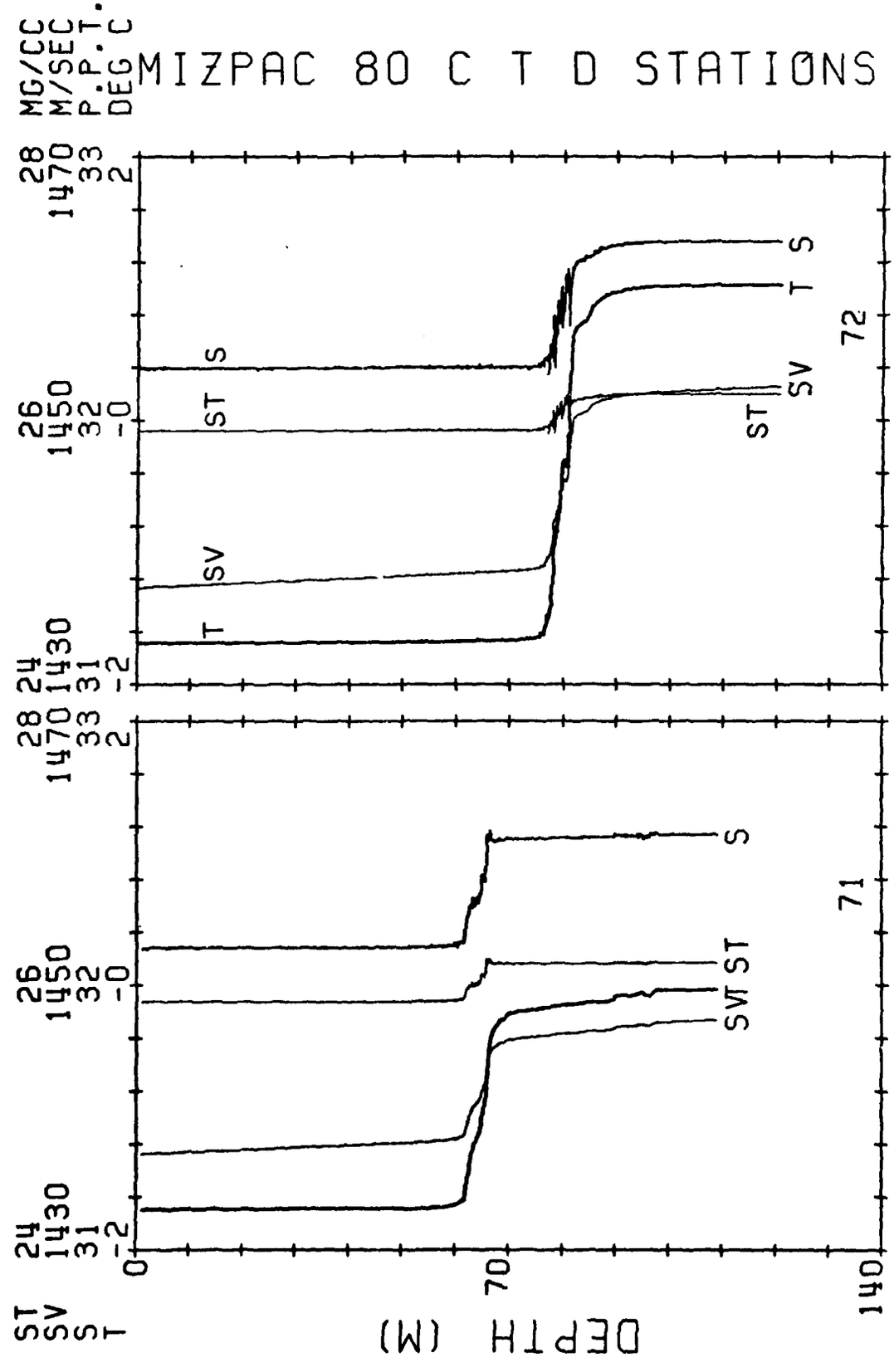
MIZPAC 80 C T D STATIONS
MG/CC
M/SEC
P.P.T.
DEG C
28
1470
33
2
26
1450
32
-0
24
1430
31
-2
ST
SV
S
T
72
71
0
70
140
DEPTH (M)

AD-A122 443 WINTER CONDITIONS IN THE BERING SEA(U) NAVAL POSTGRADUATE SCHOOL MONTEREY CA R H BOURKE ET AL. MAY 81 NPS-68-81-004 2/2

UNCLASSIFIED F/G 8/10 NL

END
DATE FILMED
DTIC

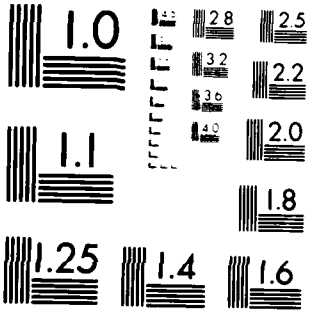

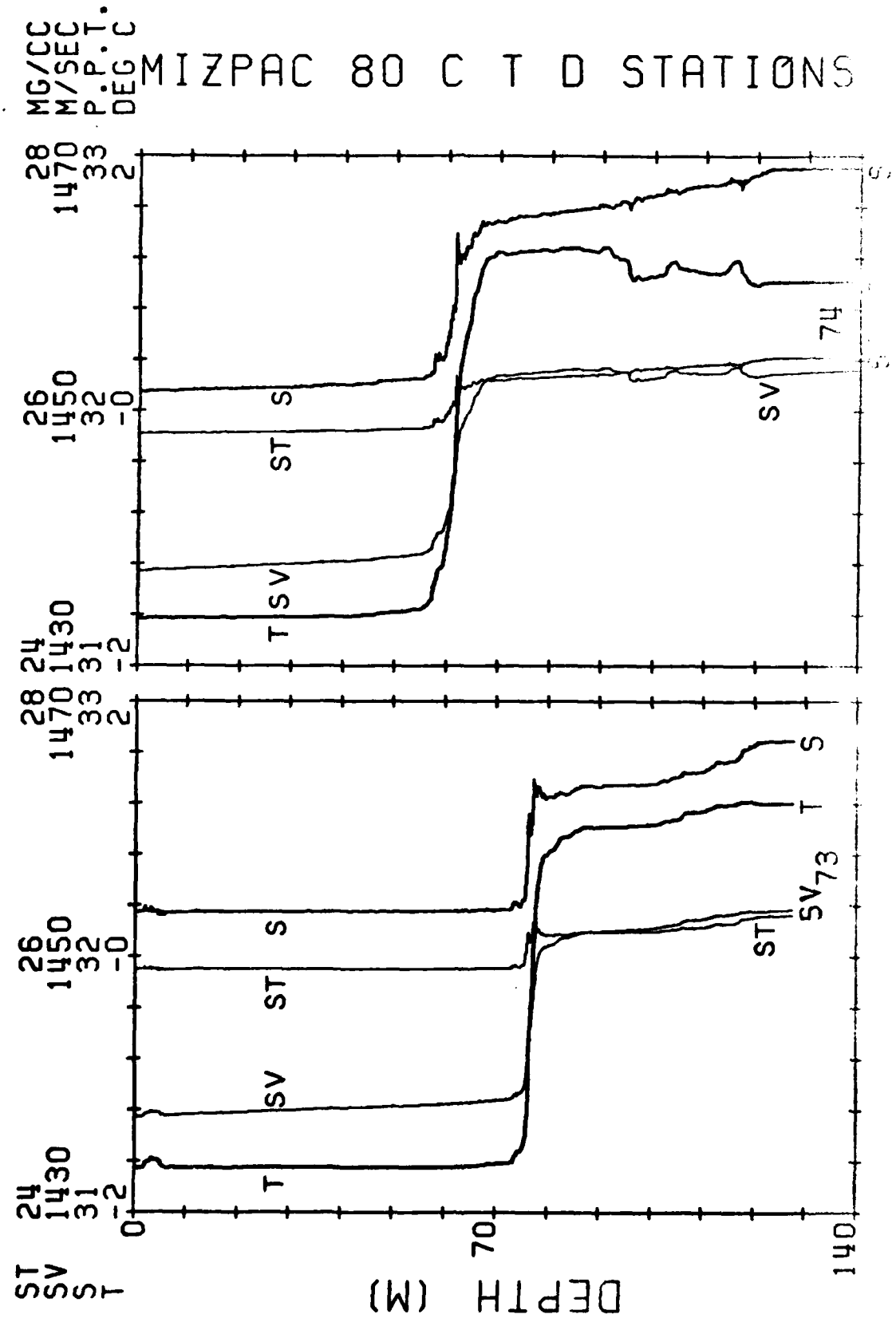
MIZPAC 80 C T D STATIONS
MG/CC
M/SEC
P.P.T.
DEG C
28
1470
33
2
26
1450
32
-0
24
1430
31
-2
ST
SV
T
S
74
73
0
70
140
DEPTH (M)

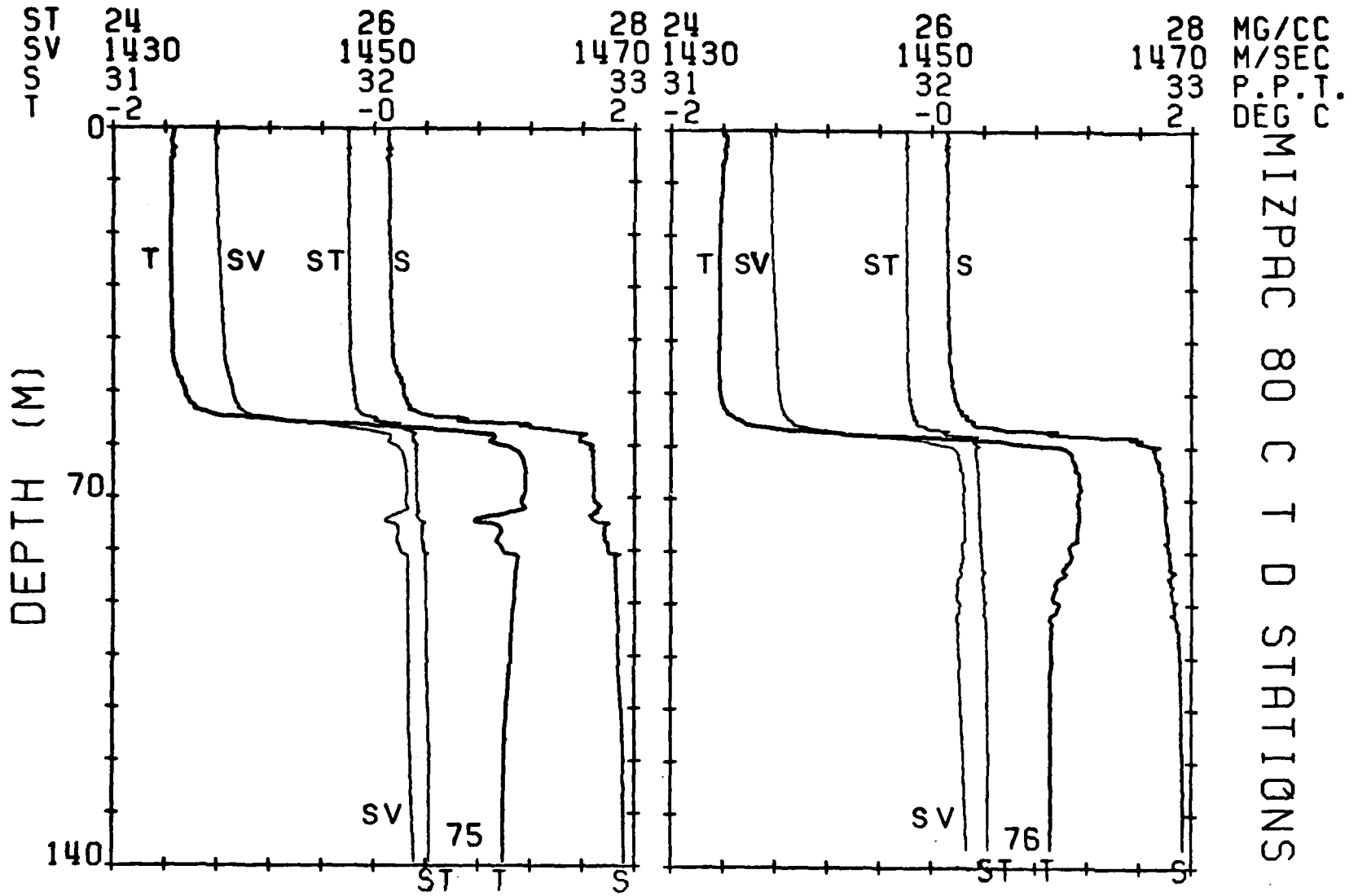
ST 24 26 28 24 26 28 MG/CC
SV 1430 1450 1470 1430 1450 1470 M/SEC
S 31 32 33 31 32 33 P.P.T.
T -2 -0 2 -2 -0 2 DEG C
0
70
140
DEPTH (M)
T
SV
ST
S
SV
75
ST T S
T SV ST S
SV
76
ST T S
MIZPAC 80 C T D STATIONS

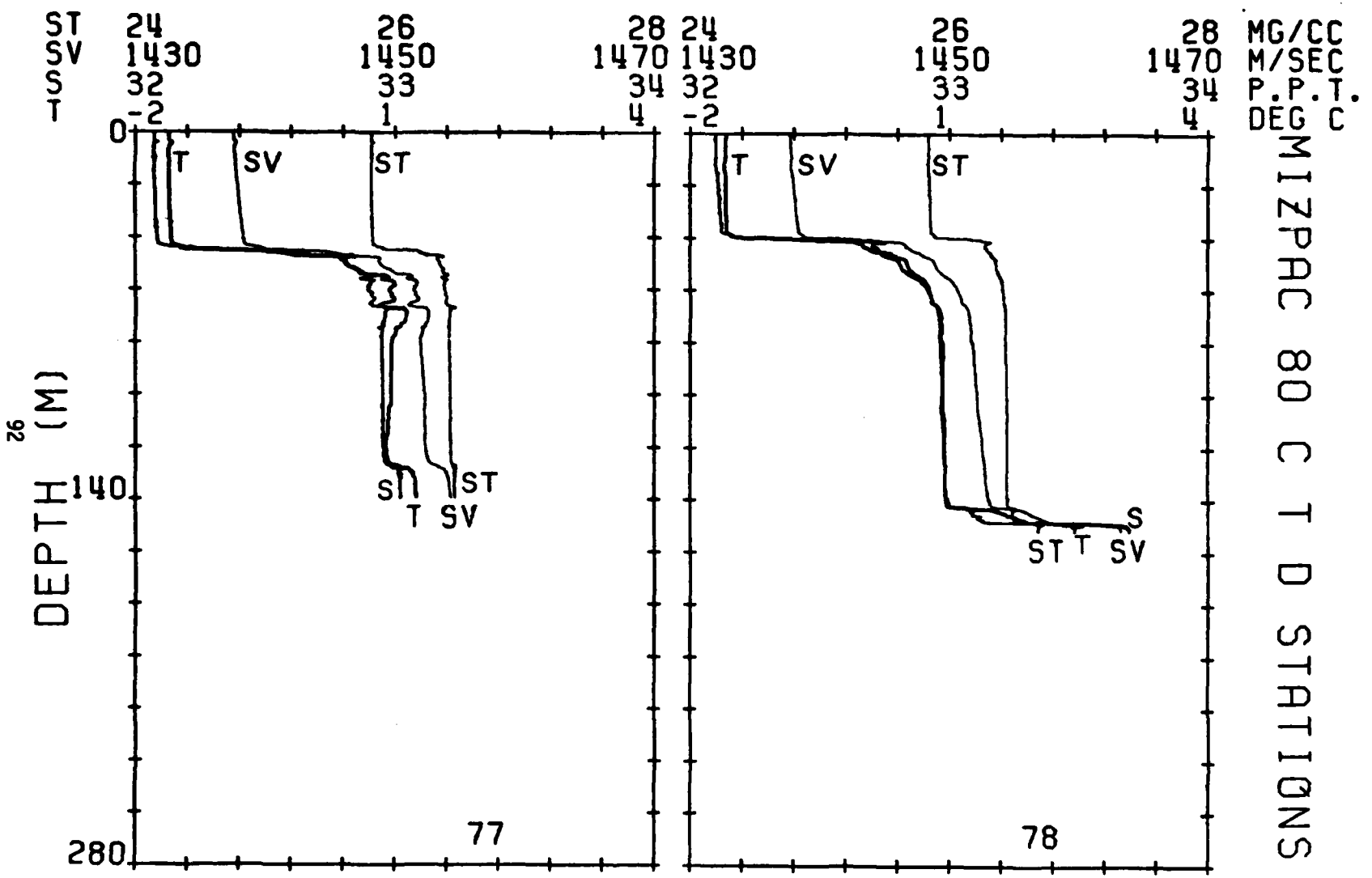
ST 24 26 28 24 26 28 MG/CC
SV 1430 1450 1470 1430 1450 1470 M/SEC
S 32 33 34 32 33 34 P.P.T.
T -2 1 4 -2 1 4 DEG C
MIZPAC 80 C T D STATIONS
DEPTH (M)
0
140
280
T
SV
ST
S
77
78

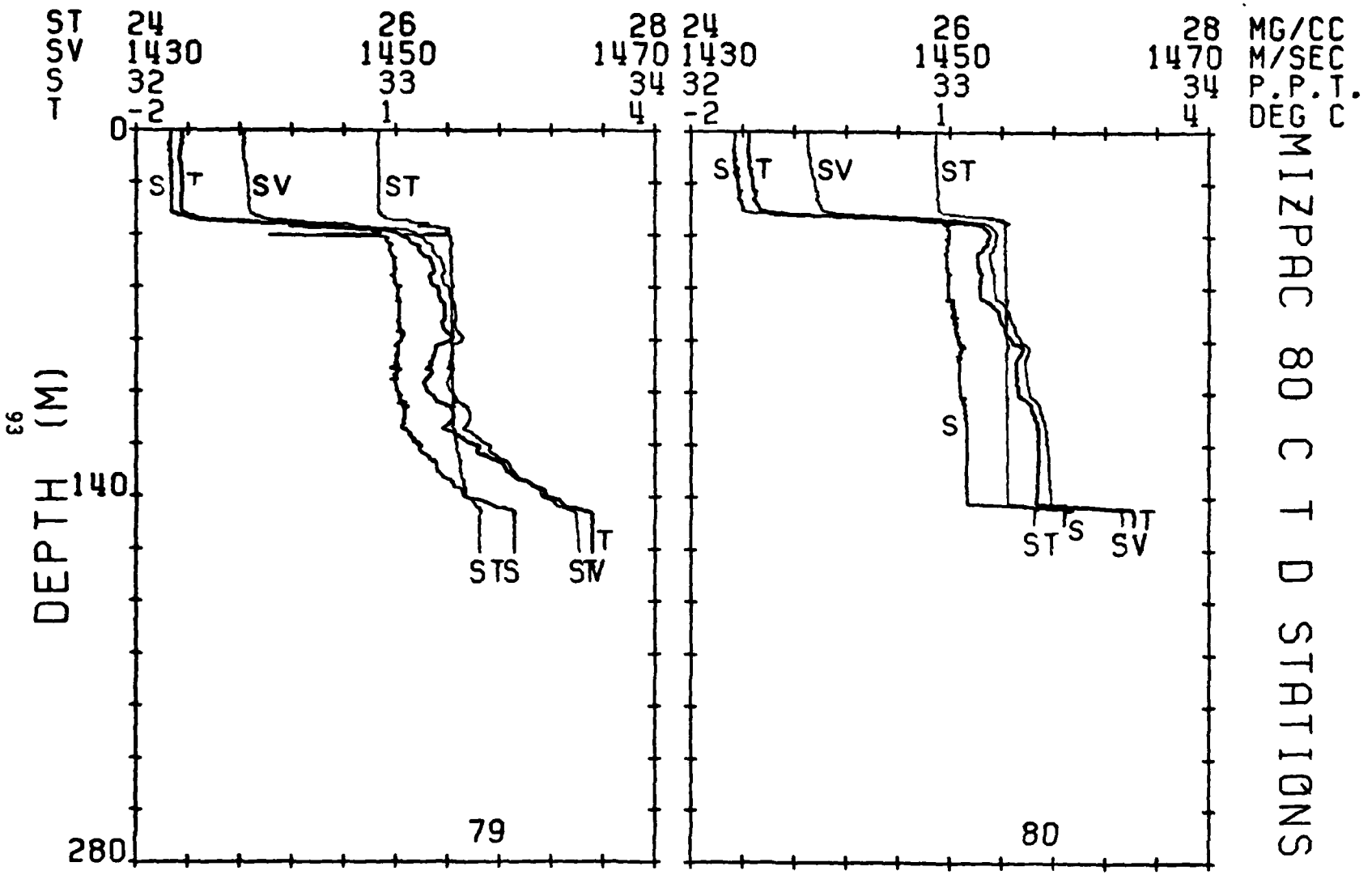
ST 24 26 28 24 26 28 MG/CC
SV 1430 1450 1470 1430 1450 1470 M/SEC
S 32 33 34 32 33 34 P.P.T.
T -2 1 4 -2 1 4 DEG C
MIZPAC 80 C T D STATIONS
DEPTH (M)
0
140
280
S
T
SV
ST
STS
STV
79
80

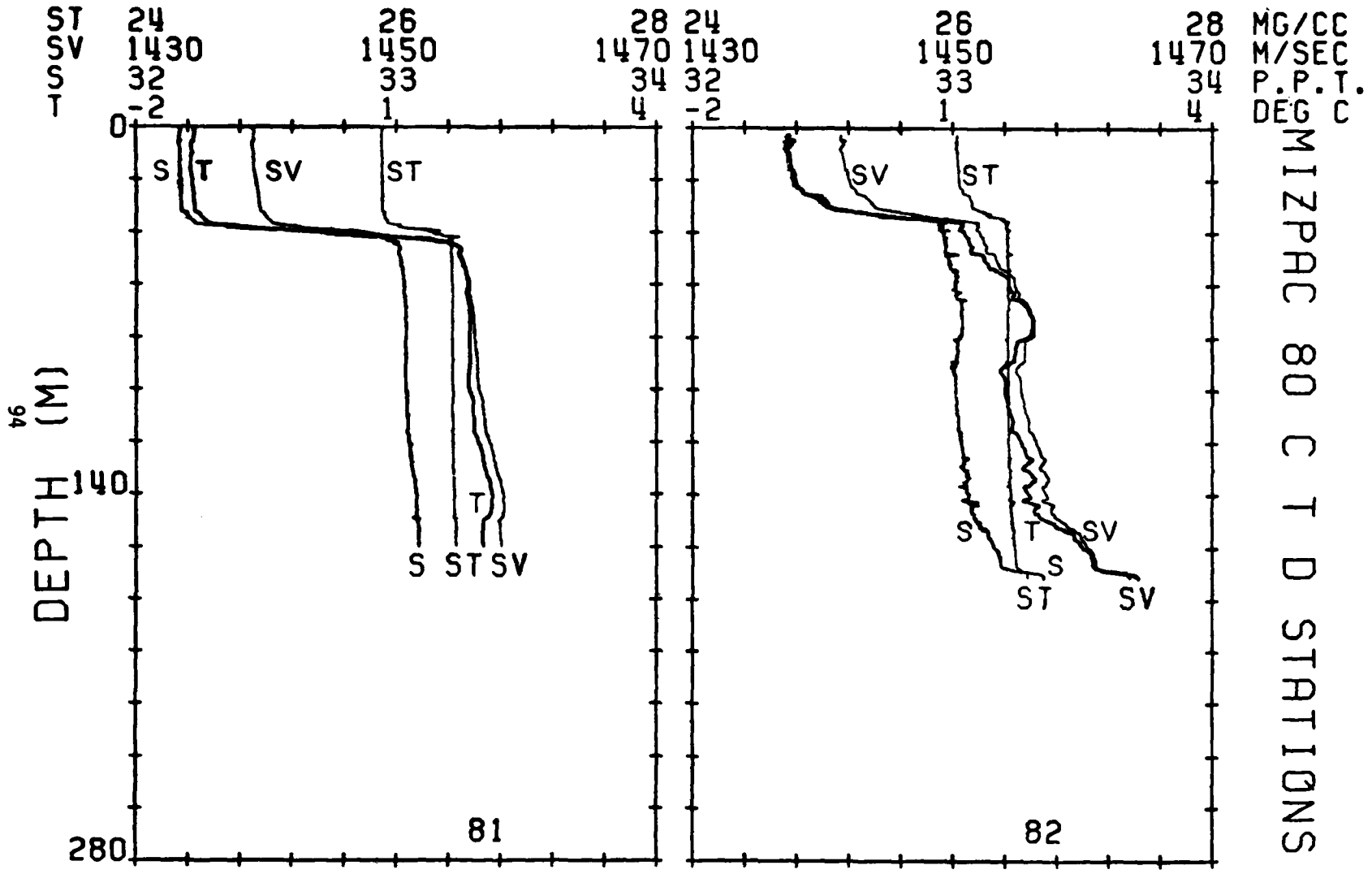
ST 24 26 28 24 26 28 MG/CC
SV 1430 1450 1470 1430 1450 1470 M/SEC
S 32 33 34 32 33 34 P.P.T.
T -2 1 4 -2 1 4 DEG C
MIZPAC 80 C T D STATIONS
DEPTH (M)
0
140
280
S T SV ST
S ST T SV
SV ST
S T SV S ST SV
81
82

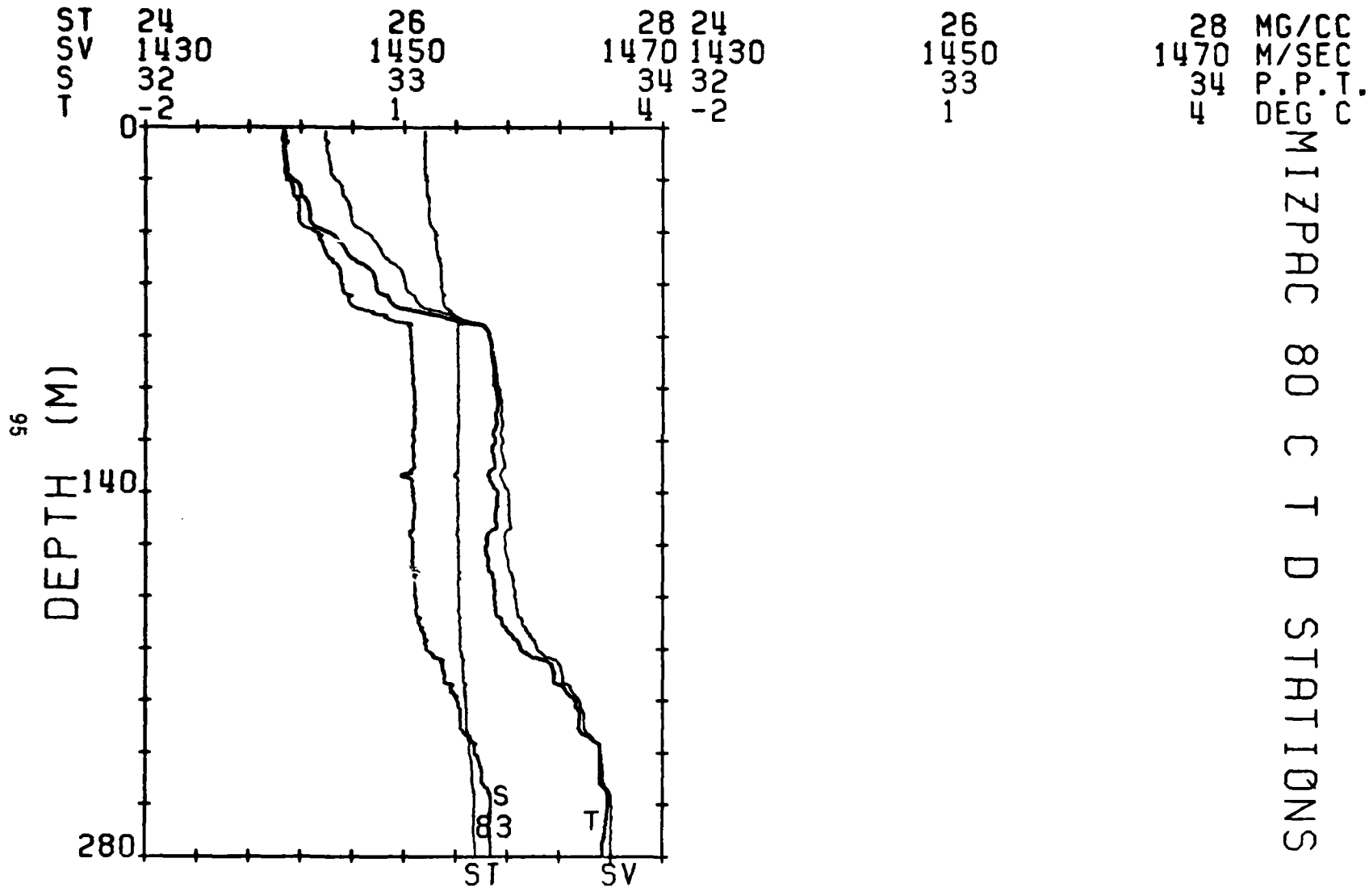

MIZPAC 80 C T D STATIONS

INITIAL DISTRIBUTION LIST

	No. Copies
Director Applied Physics Laboratory University of Washington 1013 Northeast 40th Street Seattle, Washington 98195	
Mr. Robert E. Francois	1
Mr. E. A. Pence	1
Mr. G. R. Garrison	1
Library	1
Director Arctic Submarine Laboratory Code 54, Building 371 Naval Ocean Systems Center San Diego, California 92152	25
Superintendent Naval Postgraduate School Monterey, California 93940	
Library, Code 0142	2
Dr. R. G. Paquette Code 68Pa	5
Dr. R. H. Bourke Code 68Bf	5
Code 68	2
Polar Research Laboratory, Inc. 123 Santa Barbara Street Santa Barbara, California 93101	2
Chief of Naval Operations Department of the Navy Washington, D. C. 20350	
NOP-02	1
NOP-22	1
NOP-946D2	1
NOP-095	1
NOP-098	1
Commander Submarine Squadron THREE Fleet Station Post Office San Diego, California 92132	1
Commander Submarine Group FIVE Fleet Station Post Office San Diego, California 92132	1

Dr. John L. Newton — 2
Science Applications, Inc.
1200 Prospect St.
P.O. Box 2351
La Jolla, Ca 92038

Director — 1
Marine Physical Laboratory
Scripps Institution of Oceanography
San Diego, California 92132

Comanding Officer — 1
Naval Intelligence Support Center
4301 Suitland Road
Washington, D. C. 20390

Commander — 1
Naval Electronic Systems Command
Department of the Navy
Washington, D. C. 20360
NESC 03 — 1
PME 124 — 1

Director — 1
Woods Hole Oceanographic Institution
Woods Hole, Massachusetts 02543

Commanding Officer — 1
Naval Coastal Systems Laboratory
Panama City, Florida 32401

Commanding Officer — 1
Naval Submarine School
Box 700, Naval Submarine Base, New London
Groton, Connecticut 06340

Assistant Secretary of the Navy — 2
(Research and Development)
Department of the Navy
Washington, D. C. 20350

Director of Defense Research and Engineering — 1
Office of Assistant Director (Ocean Control)
The Pentagon
Washington, D. C. 20301

Commander, Naval Sea Systems Command — 4
Department of the Navy
Washington, D. C. 20362

Chief of Naval Research — 1
Department of the Navy
800 North Quincy Street
Arlington, Virginia 22217
Code 102-OS — 1
Code 220 — 1
Code 425 (Arctic) — 1

Project Manager 1
Anti-Submarine Warfare Systems Project
Office (PM4)
Department of the Navy
Washington, D. C. 20360

Commanding Officer 1
Naval Underwater Systems Center
Newport, Rhode Island 02840

Commander 2
Naval Air Systems Command
Headquarters
Department of the Navy
Washington, D. C. 20361

Commander 2
Naval Oceanographic Office
Washington, D. C. 20373
Attention: Library Code 3330

Director 1
Advanced Research Project Agency
1400 Wilson Boulevard
Arlington, Virginia 22209

Commander SECOND Fleet 1
Fleet Post Office
New York, New York 09501

Commander THIRD Fleet 1
Fleet Post Office
San Francisco, California 96601

Commander
Naval Surface Weapons Center
White Oak
Silver Spring, Maryland 20910
Mr. M. M. Kleinerman 1
Library 1

Officer-in-Charge 1
New London Laboratory
Naval Underwater Systems Center
New London, Connecticut 06320

Commander 1
Submarine Development Group TWO
Box 70
Naval Submarine Base
New London
Groton, Connecticut 06340

Commander 1
Naval Weapons Center
China Lake, California 93555
Attention: Library

Commander 1
Naval Electronics Laboratory Center
271 Catalina Boulevard
San Diego, California 92152
Attention: Library

Director 3
Naval Research Laboratory
Washington, D. C. 20375
Attention: Technical Information Division

Director 1
Ordnance Research Laboratory
Pennsylvania State University
State College, Pennsylvania 16801

Commander Submarine Force 1
U. S. Atlantic Fleet
Norfolk, Virginia 23511

Commander Submarine Force
U. S. Pacific Fleet
N-21 1
FPO San Francisco, California 96860 1

Commander 1
Naval Air Development Center
Warminster, Pennsylvania 18974

Commander 1
Naval Ship Research and Development Center
Bethesda, Maryland 20084

Chief of Naval Material
Department of the Navy
Washington, D. C. 20360
NMAT 03 2
NMAT 034 1
NMAT 0345 1

Commandant 2
U. S. Coast Guard Headquarters
400 Seventh Street, S.W.
Washington, D. C. 20590

Commander 1
Pacific Area, U. S. Coast Guard
630 Sansome Street
San Francisco, California 94126

Commander 1
Atlantic Area, U. S. Coast Guard
159E, Navy Yard Annex
Washington, D.C. 20590

Commanding Officer 1
U. S. Coast Guard Oceanographic Unit
Building 159E, Navy Yard Annex
Washington, D. C. 20590

Dr. Robert E. Stevenson 1
Scientific Liaison Office, ONR
Scripps Institution of Oceanography
La Jolla, California 92037

SIO Library 1
University of California, San Diego
P. O. Box 2367
La Jolla, California 92037

University of Washington
Seattle, Washington 98105
Dept. of Oceanography Library 1
Dr. L. K. Coachman 1
Dr. K. Aagaard 1
Dr. S. Martin 1

Library, School of Oceanography 1
Oregon State University
Corvallis, Oregon 97331

CRREL
U. S. Army Corps of Engineers
Hanover, NH 03755
Library 1

Commanding Officer 1
Fleet Numerical Oceanography Center
Monterey, California 93940

Commanding Officer 1
Naval Environmental Prediction Research Facility
Monterey, California 93940

Defense Technical Information Center 1
Cameron Station
Alexandria, Virginia 22314

Commander 1
Oceanographic Systems Pacific
Box 1390
Pearl Harbor, Hawaii 96860

Commander
Naval Oceanography Command
NSTL Station
Bay St. Louis, Mississippi 39522 — 1

Department of Meteorology Library
Naval Postgraduate School, Code 63
Monterey, California 93940 — 1

Commanding Officer
Naval Ocean Research and Development Activity
NSTL Station
Bay St. Louis, MS 39522
Technical Director — 1

Commanding Officer
Naval Polar Oceanography Center, Suitland
Washington, D. C. 20373 — 1

Director
Naval Oceanography Division
Naval Observatory
34th and Massachusetts Avenue, NW
Washington, DC 20390 — 1

Commanding Officer
Naval Oceanographic Office
NSTL Station
Bay St. Louis, MS 39522 — 1

Scott Polar Research Institute
University of Cambridge
Cambridge, England
CB2 1ER
Library — 1
Sea Ice Group — 1

Chairman
Department of Oceanography
U. S. Naval Academy
Annapolis, MD 21402 — 1

Dr. Ola M. Johannessen
Geophysical Institute
University of Bergen
Bergen, Norway — 1

Dr. James Morison
Polar Science Center
4059 Roosevelt Way, NE
Seattle, WA 98105 — 1

Dr. Ken Hunkins 1
Lamont-Doherty Geological Observatory
Palisades, NY 10964

Dr. David Paskowsky, Chief 1
Oceanography Branch
U. S. Department of the Coast Guard
Research and Development Center
Avery Point, CT 06340

Science Applications, Inc.
13400B Northrup Way
Suite 36
Bellevue, WA 98005
Dr. Robin Muench 1
1

Institute of Polar Studies
103 Mendenhall
125 South Oval Mall
Columbus OH 43201
Library 1

Institute of Marine Science
University of Alaska
Fairbanks, AK 99701
Library 1

Dept. of Oceanography
University of British Columbia
Vancouver, B. C. Canada
V6T 1W5
Library 1

Geophysical Institute
University of Alaska
Fairbanks, AK 99701
Dr. J. B. Matthews 1

Bedford Institute of Oceanography
P. O. Box 1006
Dartmouth, Nova Scotia
Canada
B2Y 4A2
Library 1

Carol Pease 1
Pacific Marine Environmental Lab/NOAA
3711 - 15th Ave. N.E.
Seattle, WA 98105

Dept. of Oceanography 1
Dalhousie University
Halifax, Nova Scotia
Canada
B3H 4J1

Lyn McNutt
F.G. Bercha & Associates Limited 1
938-2nd Ave. N.W.
Calgary, Alberta
Canada

Office of Naval Research (Code 480) 1
Naval Ocean Research and Development
Activity
NSTL Station
Bay St. Louis, MS 39522

Library 1
CICESE
P.O. Box 4803
San Ysidro, CA 92073

Dr. E. C. Carmack 1
Canada Centre for Inland Water
4160 Marine Drive
W. Vancouver, B.C., V7V 1N6
Canada

Dr. P. D. Killworth 1
Dept. of Applied Math and Theoretical Physics
Silver Street
Cambridge, England
CB3 9EW

Dr. B. Rudels 1
Geofysikk Institutt
Bergen, Norway


DAT
ILM